

Optimization of the installation sequence of an Offshore Wind Farm Monopile Installation Template

by improving the foundation design

MSc Research Thesis

Marten Bosma

Delft University of Technology

Optimization of the installation
sequence of an Offshore Wind Farm Monopile Installation
Template

by improving the foundation design

by

Marten Bosma

4480813

To obtain the degree of
Master of Science in Offshore & Dredging Engineering
at the Delft University of Technology,

To be defended publicly on 26 January 2023 at 01:00 PM



**MARINE
CONTRACTORS**



Committee:

TU Delft

Prof. dr. A. Metrikine

Ir. J. Hoving

Ir. E. Kementzetzidis

Heerema Marine Contractors

Ir. M. Veldhuizen

Ir. J. ter Braak

Preface

I proudly present to you my master thesis for the completion of the MSc Offshore & Dredging Engineering. Over the past months I have been working in collaboration with Heerema Marine Contractors to execute this project. I have worked on this project with lots of interest and excitement about the potential of the offshore wind industry within Heerema Marine Contractors.

This project would not have been possible without the useful help of my supervisors Maarten Veldhuizen and Jelle ter Braak. I would like to thank you both enormously for all the help and useful feedback I have received. You challenged me to be critical on myself and motivated me throughout the whole process.

Jeroen, I am honoured to have you as my supervisor. Your great enthusiasm during our meetings motivated me and I want to thank you for always being so supportive. I received the best advice whenever I was stuck, including the constructive criticism that I needed.

Vagelis, you have helped me enormously during my research. I would like to thank you for all your feedback and the endless information on soils and foundations.

Besides my supervisors, I would also like to thank all my colleagues at Heerema Marine Contractors. You all have been very supportive and I enjoyed each day coming to the office. I can't wait to go offshore to experience offshore wind farms in real life!

Lastly, I would like to thank my friends and family. They have always been a huge support during this process. Thank you for always being there for me from start to finish.

*Marten Bosma
Leiden, January 2023*

Abstract

This thesis presents an optimization of the installation sequence of the Offshore Wind Farm Monopile Installation Template for the He Dreiht Wind Farm project.

Heerema Marine Contractors is assigned to execute the installation of 64 monopiles for the He Dreiht Offshore Wind Farm project provided by Energie Baden-Württemberg (EnBW). This windfarm is located approximately 90 kilometers of the German North Sea coastline and will have a grid capacity of 900 MW. The installation of the monopiles is done by means of a template structure. This template is specifically designed for this project and is installed on the seabed temporarily. The initial design of the template contains a mudmat foundation to ensure the required stability during the full monopile installation sequence. In order to provide the required stability, the initial designed mudmat foundation concept holds a horizontal surface area of 1210 m². Analysis showed that this designed template obtained a low performance considering the template installation sequence. When lifting the template through the wave zone, the template obtained significant hydrodynamic forces acting on the template in vertical direction due to the large horizontal surface area.

Therefore, the main objective of this thesis is to generate and develop alternative foundation concepts to optimize the template installation sequence. This research considers the design of a mudmat, suction bucket, push-in pile and helical pile foundation concept. A homogeneous sand seabed and clay seabed are considered as soil conditions. The design of the foundation concepts is based on the environmental loads acting on the template during three critical load cases. For the design, the supporting frame and noise mitigation system are assumed to be fixed. The usage of a noise mitigation system is prescribed by the client. The design of the mudmat showed to have a foundation area of 924 m² in order to ensure stability on the seabed, independent of the soil type. The suction bucket foundation concept resulted in a horizontal foundation area of 390 m² for sand, or 117 m² for a clay seabed. The push-in pile and helical pile foundation concepts developed for a sand seabed resulted in an area of 306 m² and 319 m². For a clay seabed this resulted in an area of 75 m² and 88 m².

After the design of the four foundation concepts the operability of each concept is determined by means of a hydrodynamic analysis. The operability states the amount of time the template can be lifted through the wave zone expressed in percentage, based on 24 hours. A simplified method stated by DNV is used to determine the hydrodynamic loads acting on the foundation in heave direction, when lifting the template through the wave zone. The mudmat foundation concept showed an operability of 23%, independent of the considered soil type. For the suction bucket concepts developed for a sand seabed, the operability resulted in 67%. For a clay seabed this resulted in 94%. Considering the push-in pile and helical pile foundations the operability resulted in 78% for the sand developed concepts. The foundations designed for a clay seabed resulted in an operability of 95%. To evaluate which concept has the best performance considering the template installation sequence, a multi-criteria analysis (MCA) is performed. This MCA also takes the installation time, construction costs and the risk of damage into account as criteria. Taking all these criteria into account, it is stated that the mudmat foundation concept provides the best performance when considering the template installation sequence, based on the assumptions stated throughout this thesis. The mudmat foundation concept shows a low performance when lifting the template through the wave zone, however this is compensated by a short installation time on the seabed, low construction costs and low damage risks. The suction bucket foundation concept shows an average score on all criteria. This resulted in the second preferred option. The push-in pile and helical pile foundation concepts show a good operability, however, these concepts score low on the construction costs, installation time and damage sensitivity. As a result, these concepts show the lowest performance considering the template installation sequence.

Contents

Preface	i
Summary	ii
1 Introduction to an Offshore Wind Farm Installation Template	1
1.1 The need for innovation of monopile installation techniques	1
1.2 Heerema Marine Contractors	2
1.3 He Dreiht Offshore Wind Farm Installation Template	2
1.3.1 Template design	3
1.3.2 Template installation sequence	5
1.4 Problem Definition	7
1.4.1 Design statement	7
1.5 Outline of the report	7
2 Foundation concepts within the offshore industry	9
2.1 Offshore foundation techniques	9
2.1.1 Shallow foundation techniques	10
2.1.2 Deep foundation techniques	12
2.2 Soil behavior of sand and clay soils	14
2.3 Soil structure interaction due to loading	17
2.3.1 Shallow foundation theory	17
2.3.2 Deep foundation theory	24
2.4 Environmental wave loading	31
2.5 Lifting through the wave zone	32
2.5.1 Motion response of the structure	33
2.5.2 Characteristic total force when lifting through the wave zone	35
3 Generation of foundation concepts	40
3.1 Boundary conditions and assumptions for the He Dreiht template design	40
3.2 Environmental conditions at the He Dreiht Wind Farm location	42
3.2.1 Weather restricted conditions	42
3.2.2 Soil conditions	43
3.3 Modelling the environmental loads acting on the template	44
3.4 Choosing which foundation concepts to consider	46
4 Development of the foundation concepts	47
4.1 Calculating required dimensions of the foundation concepts	47
4.2 Results of the calculation model	57
4.2.1 Initial stability of the pile foundation concepts	58
4.2.2 Discussion	63
5 Lifting the template through the wave zone	64
5.1 Consideration and assumptions	65
5.1.1 Lifting operation	65
5.1.2 Crane position	65
5.1.3 Template position	66
5.1.4 Shielded and undisturbed waves	66
5.2 Template model	67
5.3 Hydrodynamic forces acting on the template	67
5.4 Limitations and criteria	69
5.5 Software applied	70
5.6 Results	71

5.7 Discussion	77
6 Concept selection by means of a multi-criteria analysis	82
6.1 Criteria for the template installation sequence	82
6.2 Results	86
6.3 Discussion	87
7 Conclusion, discussion and recommendations	89
7.1 Conclusion	89
7.2 Discussion	91
7.3 Recommendations	93
References	94
Nomenclature	99
A Vessel overview	101
B Initial template design properties	104
C Monopile installation sequence	105
D Foundation concept installation sequence - planning	106
E Multi-criteria analysis	109
F Operability	110
G Thialf components overview	112

Introduction to an Offshore Wind Farm Installation Template

1.1. The need for innovation of monopile installation techniques

Since the past few decades the sources of energy supply throughout the world has been changing rapidly. Large interest is directed towards offshore renewable energy sources, resulting in a significant increase for offshore wind farms. With a better understanding on climate change and its effect on human kind, the developments and innovation on offshore wind turbines is growing extensively. This results in governments and energy suppliers shifting their focus from the offshore oil and gas industry to offshore renewables, forcing contractors to comply with these demands. As for the European Union, the ambition is to increase the installed wind energy capacity up to 60 GW by 2030 and up to 450 GW by 2050 [2].

An offshore wind turbine is constructed of multiple components as shown in figure 1.1, and can generally be divided in three components. These are the rotor-nacelle assembly (RNA), the tower and the sub-structure. Three types of foundations related to each sub-structure are displayed. The foundation depicted on the left is a monopile foundation, the middle presents a jacket sub-structure with a pile foundation, and on the right a gravity based foundation is shown. This research considers the installation of a monopile foundation sub-structure. With 80.5%, the monopile foundation are the most used sub-structure for an offshore wind turbine to date [36]. As larger turbines are being developed, the size of monopile foundations are increasing gradually and has doubled within the past decade [13]. Traditional technologies for monopile installation are not always applicable anymore and current installation vessels do not have the required technology to install such large monopiles at all times. One of the main solutions to cope with the increase in larger turbines are new installation and foundation technologies, as this contributes significantly to the total cost-structure of an offshore wind farm [9]. Therefore innovation on current and research for new monopile installation methods is required in order to comply with the increase in size and numbers of monopiles and to propose cost-effective solutions.

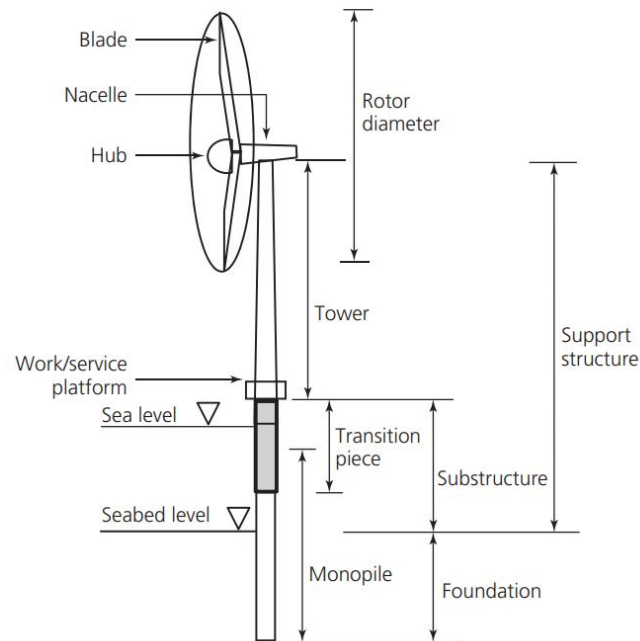


Figure 1.1: Components of an offshore wind turbine with a monopile foundation [5]

This report focuses on the installation of a monopile foundation by means of a template structure. A template structure is placed on the seabed prior to monopile installation, to ensure stability during monopile installation and the monopile to be installed on the required position. After monopile installation, the template is retrieved from the seabed and is used for the installation of the next monopile. Figure 1.3 shows a template structure used for monopile installation.

1.2. Heerema Marine Contractors

This research thesis is done in collaboration with Heerema Marine Contractors (HMC). HMC is a market leader in the offshore industry regarding the installation and decommissioning of oil and gas platforms and is currently shifting their focus to the offshore wind industry. Recently, the usage of HMC vessels have become cost-effective due to the increase in size of monopile foundations for offshore wind farms. This results in innovative projects within the HMC company to comply with the demands for the installation of offshore wind farms. The past few years Heerema has won tenders for the installation of the foundation of multiple wind farms. An overview of the fleet of Heerema can be found in appendix A. This research considers the usage of the Thialf.

1.3. He Dreih Offshore Wind Farm Installation Template

HMC is assigned to execute the installation of 64 monopile foundations for the He Dreih Offshore Wind Farm Project provided by Energie Baden-Württemberg (EnBW), a German company for energy supply. The location of this project is around 90 kilometers of the German North Sea coastline and will have a grid capacity of 900 MW. An overview of the location can be found in figure 1.2 below. The project is planned to be executed in the first quarter of 2024. The installation of the monopile foundations is executed using the Semi-Submersible Crane Vessel (SSCV) Thialf in combination with an Offshore Wind Farm Monopile Installation Template. During offshore operations it is obligated to be in compliance with the German governmental regulations for noise production. Therefore the the monopile installation template includes the usage of a Noise Mitigation System (NMS) prescribed by EnBW.

The template construction will be temporarily installed on the seabed and is specifically designed as a tool for the installation of the monopiles required for the He Dreih Wind Farm Project. After the monopile is installed in the seabed the template will be retracted from the seabed and is used at the next location. In general, the main objective of the template is to support the monopile during installa-

tion and to ensure an accurate position of the monopile foundation.

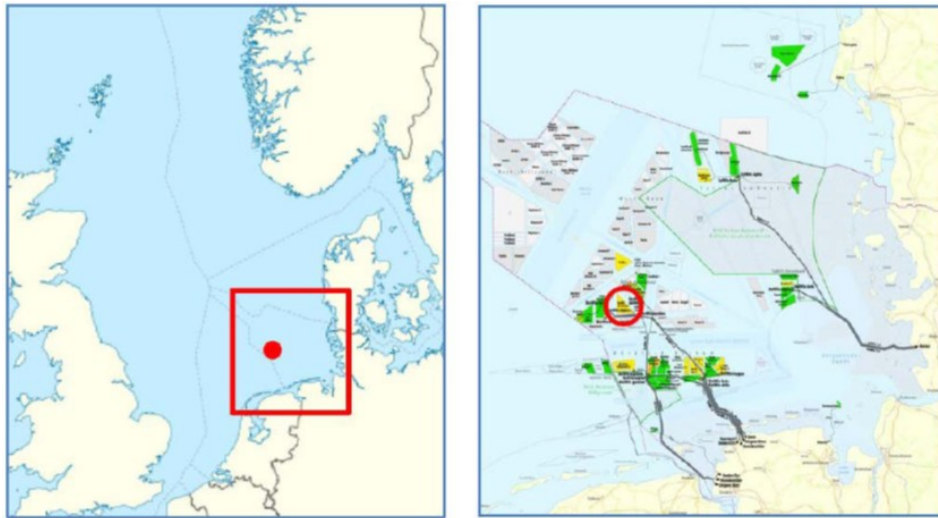


Figure 1.2: Location of the He Dreht Wind Farm

1.3.1. Template design

The template for the EnBW He Dreht Wind Farm Project is designed to install the monopile foundations of the 64 offshore wind turbines. This template is designed to install a monopile foundation with a bottom diameter of 9.5 meter. As mentioned in previously, the tender stated by EnBW prescribed the usage of the Noise Mitigation System (NMS) 10000 Pile Guided provided by IQIP IHC in order to be in compliance with the German governmental regulations for noise production during offshore operations. For the installation of the monopiles a template construction is designed with the NMS incorporated in the frame. The initial concept design of the monopile installation template is depicted in figure 1.3 below. In the figure, it can be obtained that the NMS is incorporated in the design and is attached to the foundation via a six legged steel supporting frame. The template design shown in figure 1.3 is the initial template design for the installation of the monopiles for the He Dreht Wind Farm and is taken as a base case throughout this research. This means that the template design in figure 1.3 is referred to, when the initial template design is mentioned.

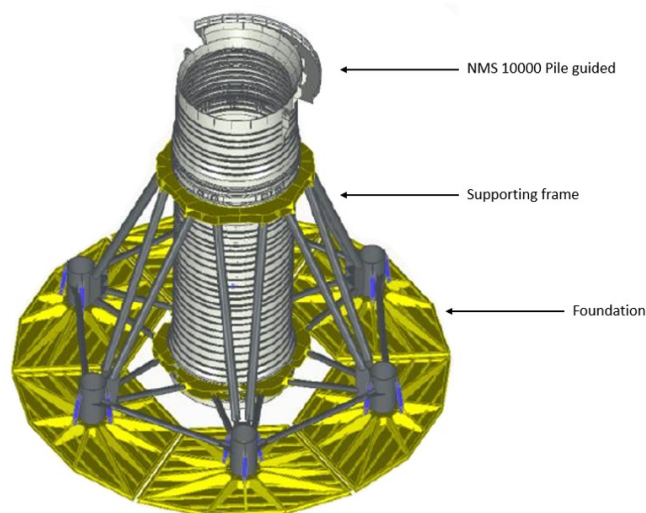


Figure 1.3: Initial template concept design

The template frame can be divided into three segments, being the Noise Mitigation System (NMS)

provided by IHC, secondly a supporting frame that connects the NMS to the foundation and thirdly the foundation that ensures stability on the seabed. The template construction is able to guide and support the monopile during installation, and in combination with the NMS, to reduce the noise produced during installation. The temporary installation of the template on the seabed is done by a single crane lift, resulting in the template being lowered vertically through the wave zone. An overview of the full installation sequence of a monopile foundation by means of the initial designed template can be found in appendix C. The sections below elaborate each of the three segments of the template construction.

Noise Mitigation System 10000 Pile guided

The NMS that is incorporated within the frame is provided by the subcontractor IHC and is referred to as the NMS-10000 Pile guided, meaning that it reduces the noise produced during monopile installation and is able to guide the monopile during pile driving. The NMS is a double-walled noise mitigation system that reduces the noise produced during installation to below 160 dB [26], which is enough to be in compliance with the German governmental noise production regulations during offshore operations[45]. The system has a flexible connection between the inner and outer wall in which an air gap exists that is kept stable by means of overpressure. Centralizers are located inside the NMS at the bottom and the top sections of the NMS in order to guide and centre the monopile during installation to obtain the correct position of the monopile. The centralizers are also used during retraction of the template after monopile installation. These are used in order to prevent the NMS from damaging the monopile due to the hydrodynamic motions induced by wave loading.

Supporting frame

For the initial template design shown in figure 1.3, the NMS is connected to the foundation by means of a six legged jacket supporting frame. This supporting frame is made of steel tubular members with diameters that are small compared to the diameter of the NMS. A top view of the six legged supporting frame can be found in figure 3.2. During the complete installation process of the monopile the supporting frame will be flooded with water when submerged, in order to reduce the buoyancy force acting on the structure.

Foundation

For the base case design, the six legged steel supporting frame is connected to a mudmat foundation that is designed to ensure the required stability, meaning it can take on the horizontal and vertical loads acting on the structure. The foundation of the initial design has a horizontal surface area of 1210 m². Although the template design ensures the required stability when installed on the seabed, large hydrodynamic motions occurred during the analysis when lowering the template through the wave zone. The foundation of the template is designed to ensure the required on-bottom stability of the structure. The failure criteria that are considered for stability are bearing failure, sliding failure and overturning failure.

This report focuses on the design of alternative foundation concepts for a monopile installation template. In order to design alternative foundation concepts for the He Dreiht template, the drivers for the design of the initial designed template should be known. The sections below describe the installation sequence in order to determine the governing phases in terms of environmental loading.

1.3.2. Template installation sequence

The template installation sequence is a section of the full monopile installation sequence. The installation sequence of the monopile can be divided in four main phases that each consists of multiple steps, plus a contingency procedure being the fifth phase. During the contingency case the template is located on the seabed. Installation of a monopile cannot be executed safely due to extreme environmental conditions. The template is to be left alone until the environmental conditions are such that monopile installation can be executed safely. However, during the contingency case the template should ensure stability on the seabed. The installation sequence of the template starts at lifting the template from the deck of the Thialf to above the wave zone, and ends when the template is installed on the seabed. However, the template should ensure stability throughout the full monopile installation sequence. Therefore each phase described below is taken into account for the environmental loads that act on the template. The five main phases are stated below (including the contingency procedure). In appendix C each step of the full monopile installation sequence is stated.

1. Template installation
2. Monopile lowering
3. Monopile driving
4. Template recovery
5. Contingency procedure

Figure 1.4 below shows a monopile installation by means of a template construction. On the left the template construction is being lowered through the wave zone by the Thialf (Phase 1. Template installation) and on the right a monopile foundation is lowered in the template for monopile installation (Phase 2. Monopile installation).

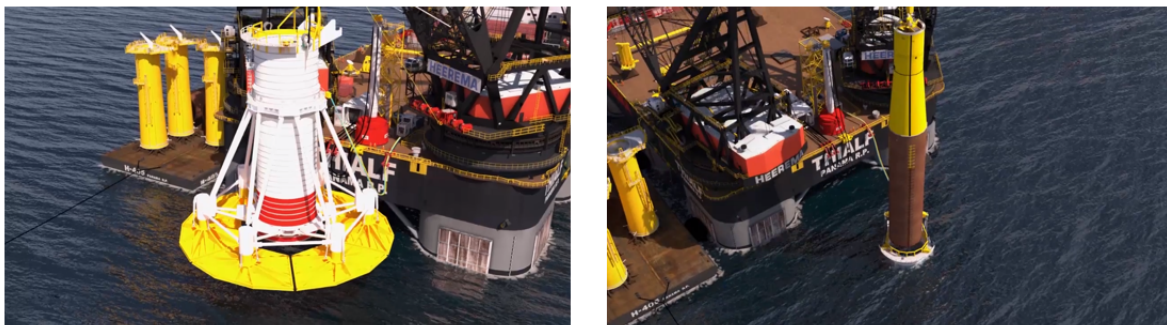


Figure 1.4: Monopile installation by means of a template construction

In general, a mudmat foundation is used for temporary support structures. It obtains its stability due to its large surface area resting on the seabed that distributes the load to the soil. For the design of the mudmat foundation, three cases are considered to be critical in terms of the environmental loading acting on the template. The first case is the template set down on the seabed, the second case is the contingency case. The third case is when lifting the template through the wave zone. Each case is described below.

Template set down on the seabed

This case considers the point in time where the template touches the seabed and initial stability is required in order to avoid instability due to the environmental loads acting on the template. The initial stability is the stability that is to be obtained right after set down of the template, and installation of the template is not yet completed. Initial stability will be discussed in more detail in chapter 4. The environmental conditions during this case are such that after stability is reached, monopile installation can safely be executed. More detail on the environmental conditions that are present during this step is provided in section 3.2.1. This case is referred to as the 'Template set down'.

Contingency procedure - Template left alone

For the contingency case the environmental conditions are above the stated limit for which monopile installation can be executed safely. However, a stable position of the template is to be ensured. This is determined for a maximum significant wave height of 3.0 m. The template will be left alone on the seabed until the environmental conditions have reduced to conditions for which monopile installation can be executed safely. This step is stated to be governing in terms of environmental loads acting on the structure, since the template should provide the required stability. Further detail on the environmental conditions is elaborated later in section 3.2.1. This case is referred to as the 'Contingency procedure'.

As mentioned previously, the initial template design resulted in an outer diameter of 45 meter with a corresponding horizontal surface area of approximately 1210 m², see appendix B. It is observed that this results in large hydrodynamic loads when lifting the template through the wave zone, and therefore having a low operability. The definition of operability throughout this research is stated to be the expected amount of time the template can be installed per day, based on the metocean data at the current site. This value is expressed in percentage. The operation of lifting the template through the wave zone resulted to be critical due to the large foundation area. This is described below.

Lifting the template through the wave zone

After the initial design of the mudmat foundation, a hydrodynamic analysis is performed for lifting the template through the wave zone. This analysis showed large dynamic motions of the template in heave direction, due to the horizontal surface area of the mudmat foundation. Obtaining large motions when lifting through the wave zone is undesirable since this affects the operability of the template. Therefore this installation step is considered to be critical in terms of the hydrodynamic forces acting on the foundation in vertical direction. A dynamic amplification factor (DAF) limit on the crane hoist wire is used to state the maximum allowable hydrodynamic load acting on the template.

Figure 1.5 below shows the template during each critical case as mentioned above.

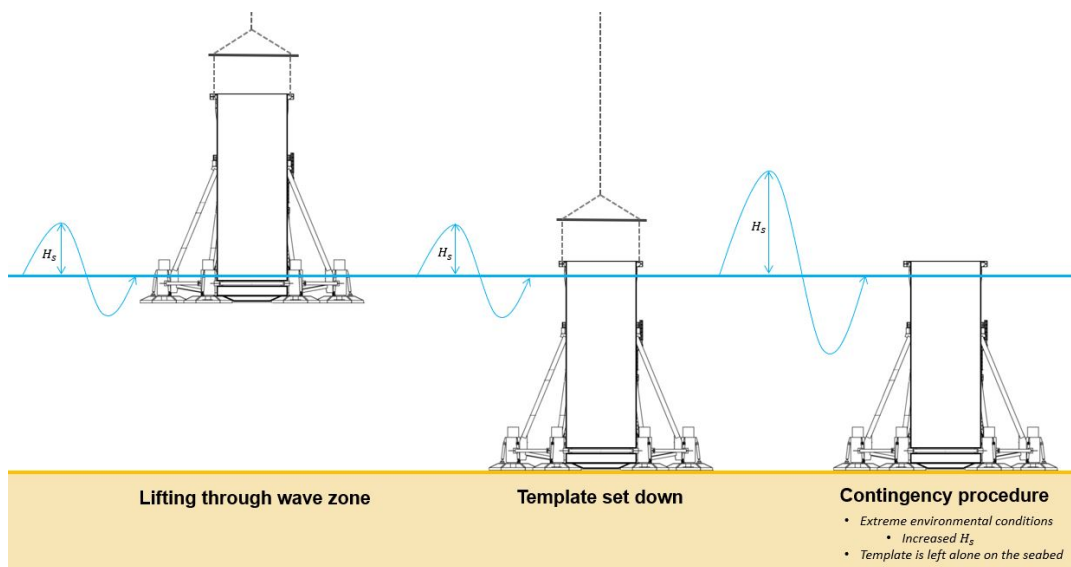


Figure 1.5: Critical cases during template installation in terms of environmental loads

1.4. Problem Definition

Interest has grown in an alternative foundation concept for the monopile installation template, due to the unfavourable performance of the initial design. The objective of an alternative foundation concept is to optimize the template installation sequence. The initial designed template for the installation of the monopiles of the He Dreiht wind farm is supported by means of a mudmat foundation. In order to obtain the required on-bottom stability the design resulted in a large foundation area. The on-bottom stability is determined for the failure criteria considering bearing failure, sliding failure and overturning failure.

As a result of this large foundation area the template construction proved to obtain large heave motions during the hydrodynamic analysis when being lowered through the wave zone. This is caused by the vertical wave forces that act on the horizontal foundation surface area, resulting in large dynamic motions in the slings and crane. An alternative foundation concept should be designed that contains the required on-bottom stability and optimizes the template installation sequence.

1.4.1. Design statement

The overarching design statement of this thesis is as follows:

"Optimization of the installation sequence of the He Dreiht Monopile Installation Template by improving the template foundation design."

The design statement is supported by the following research questions:

- **Research question 1:** What is the effect of the critical cases obtained during the template installation sequence in terms of environmental loading?
- **Research question 2:** What are the effects of the considered seabed characteristics on the design of the template?
- **Research question 3:** What are the advantages and disadvantages of the considered method used for the hydrodynamic analysis?
- **Research question 4:** What are the advantages and disadvantages of the alternative foundation concepts compared to the considered conventional foundation concepts?
- **Research question 5:** Which foundation concept is preferred for optimization of the monopile template installation sequence, based on the assumptions and limitations stated throughout this thesis?

1.5. Outline of the report

Chapter 2 will describe state-of-the-art foundation techniques that are used within the offshore industry. Besides the traditional techniques there are also new concepts under development within Heerema that will be taken into account. This chapter will explain various foundation techniques that can be considered for the design of the template. State-of-the-art foundations that are considered are for instance Gravity Based Structures (GBS), suction buckets and mudmat foundations. This chapter also describes the theory that is to be used for the design of shallow and deep foundations under vertical and lateral loading. The considered theory is stated by API standards and is generally used in a preliminary design phase [20]. Chapter 2 also describes literature on soil conditions and soil characteristics that are of importance for this research. Thereafter the theory used to calculate the environmental loads acting on the structure due to current and wave forces is stated. This is done by simplifying the template to a slender cylinder and to apply Morison's equation. Lastly, the theory considered for calculating the total characteristic forces acting on the foundation when lifting the template through the wave zone is stated. This theory is then used in Chapter 5 for the hydrodynamic analysis.

In chapter 3 the boundary conditions, limitations and assumptions that are made for this research are considered. This will include any limitations on the design of the template provided by Heerema, the environmental conditions and soil conditions at the considered location. In this chapter a selection is made of the foundation techniques that will be developed throughout this research. The selection of the chosen concepts are based on boundary conditions, assumptions made and limitations that are

applicable for the design of the template. This chapter also states the results of the environmental loads acting on the template during the set down case and contingency case, based on Morison equation.

The theory stated in chapter 2 is used for the calculation model developed in chapter 4. The environmental loads determined in chapter 3 are used as input in the calculation model, as well as the soil conditions considered throughout this thesis. The model calculates the minimum required dimensions in terms of diameter, pile length and wall thickness to ensure stability on the seabed for each of the considered foundation technique.

Chapter 5 states the limitations and assumptions that are considered during the hydrodynamic analysis. The hydrodynamic analysis determines the operability of each developed foundation concept. This is obtained by calculating the total hydrodynamic force acting on the structure during the wave zone transition. This is done by the theory stated in chapter 2 that considers the simplified method stated by DNV [18]. By means of this method the mass force, buoyancy force, slamming impact force and drag force are determined at two stages. A stage when the foundation concept is partly submerged and a stage when fully submerged. The theory stated in chapter 2 is used in a model in chapter 5 to perform a hydrodynamic analysis of each considered foundation concept. Based on a stated dynamic amplification factor limit, the operability of each foundation concept is determined. A short discussion is written on the applied DNV method for the hydrodynamic analysis.

This leads to chapter 6 where the concepts are compared in a multi-criteria analysis (MCA) by means of the Weighted Product Method (WPM). This MCA considers the results of previous chapters and includes a first estimate on the installation time, structural costs and damage sensitivity of each considered foundation concept. This results in the selection of the most preferable foundation concept based on the assumptions stated throughout this thesis.

Chapter 7 presents a conclusion of the results obtained throughout this thesis. Answers on the research questions stated in section 1.4.1 will be provided in the discussion. Also the recommendations for this thesis will be stated.

Foundation concepts within the offshore industry

This chapter describes foundation techniques that can considerably be used as an alternative foundation technique for the template. Foundation techniques that are state-of-the-art and techniques that are under development within Heerema are considered. Then the relevant theory on soil conditions is stated that is to be used for the design of the foundation concepts. The design of the foundation concepts is done by means of the theory stated by the API standards, and is elaborated in section 2.3. Thereafter the approach for the calculation of the environmental loads acting on the template for the set down case and contingency case is mentioned. Lastly, this chapter describes the theory stated by DNV [18] that is used in order to determine the hydrodynamic forces acting on the structure when lowering through the wave zone.

2.1. Offshore foundation techniques

The type of foundation techniques that are considered can be divided in shallow and deep foundation techniques. Deep foundations are considered to be pile foundations. Shallow foundations are usually a flat plate with a large area resting on the seabed, or when skirts are added that penetrate into the seabed to a limited depth. A shallow foundation is defined as having an embedment depth to foundation diameter ratio being less than one [10]. This section describes state-of-the-art foundation concepts that are currently used in the offshore industry, or are currently under investigation at HMC. In this research, the following shallow and deep foundation techniques are discussed in order to determine which foundation concepts will be considered for further development.

- **Shallow foundations**
 - Gravity Based Structures
 - Suction bucket
- **Deep foundations**
 - Pile foundations

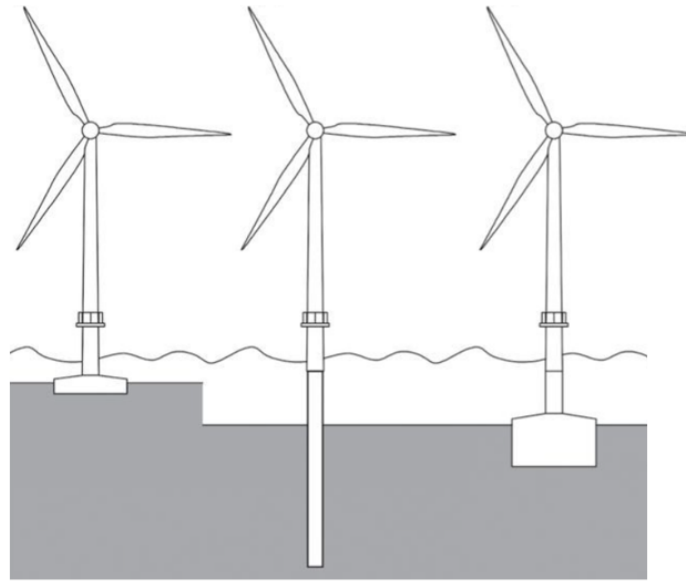


Figure 2.1: Left: Gravity Based; Middle: Monopile foundation; Right: Suction bucket [29]

2.1.1. Shallow foundation techniques

Gravity Based Structures

Gravity Based Structures (GBS) are foundation structures for which stability is reached due to the horizontal surface area and its self-weight. This often result in structures with a large footprint size on the seabed and are generally used for the support of large fixed sub-structures [37]. When softer soils are present the foundation can be provided with skirts in order to gain more transient sliding capacity against environmental loads. Gravity based structures are generally made of large concrete structures in order to obtain the required weight and stability.



Figure 2.2: Concrete Gravity Based Structure (Troll A platform) [17]

Mudmat

A mudmat can also be considered as a gravity based structure. This foundation technique is a steel frame and is generally used as a temporary support for pile jacket structures prior to the installation of the piles [37]. This technique consists of a large horizontal surface area in order to provide enough on-bottom stability due to load distribution to the soil and its self weight. As a result, mudmats can become relatively large in foundation area to provide enough resistance against sliding and overturning. This can be improved by the addition of skirts that penetrate into the soil.



Figure 2.3: Mudmat foundation [1]

Suction bucket

A suction bucket consists of a thin steel cylinder (skirt), which is closed at the top side of the cylinder by a steel plate, a so-called lid. A suction bucket obtains its capacity from the soil due to penetration of the skirts (see figure 2.4). When adding skirts to a mudmat foundation, the geometry will become like a suction bucket. However, the main difference between the two lies in the method of installation. The installation method of a suction bucket consists of two parts and emphasizes the difference between a suction bucket and a mudmat with skirts. The first part is penetration into the seabed due to the effective self-weight of the suction bucket and the soil resistance. Secondly, further penetration can be reached due to suction which is done by creating a differential pressure on the bucket by pumping water out of the bucket. Due to this differential pressure, the bucket pulls itself into the seabed.

For the design of suction buckets, the foundation embedment ratio λ should be taken into account and is dependent on the type of soil. The foundation embedment ratio is the ratio between the skirt penetration depth and the bucket diameter as follows [11]:

$$\lambda = \frac{L_{depth}}{D_{bucket}} \quad (2.1)$$

$$\begin{aligned} 0.5 \leq \lambda_{sand} \leq 1; D_{bucket,max} = 15m \\ 1 \leq \lambda_{clay} \leq 3; D_{bucket,max} = 5m \end{aligned} \quad (2.2)$$

The embedment ratio is required in order to avoid fluidization of the soil during installation. If fluidization occurs the suction bucket is not able to penetrate to the required depth. This is due to loss of pressure inside the bucket. Houlsby and Byrne (2005) determined a method to calculate the maximum installation depth for a clay seabed. This resulted in a maximum installation depth varying from $3D$ for stiff clays and $1D$ for stiff sand. The wall thickness is typically in a range between $D/75$ and $D/200$ [22]. Over the past few years suction buckets have been used as a foundation of jacket structures for windfarm applications. A great advantage of suction buckets as a foundation technique are the low environmental issues regarding the disturbance of marine life. On top of that, suction buckets can easily be removed by pumping water inside the bucket. This results in an overpressure inside the bucket that extracts the bucket from the soil.

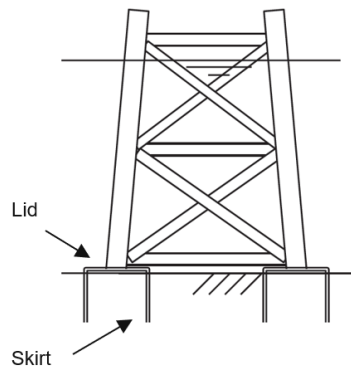


Figure 2.4: Jacket structure with a suction bucket foundation [42]

2.1.2. Deep foundation techniques

Pile foundations

In contrast to shallow foundations, deep pile foundations are favoured when a soft soil is present at the surface and high horizontal loads act on the structure. This could cause the surface foundation to slide. The dimensions of the pile foundations are constructed depending on the geotechnical conditions at the site. Offshore pile foundations can have a diameter ranging from 0.76 m for wellhead conductors to a diameter of 11 meter for large monopile foundations [43]. These piles generally have a diameter to wall thickness ratio of 25-100 [37]. There are in general two types of pile foundations that can be distinguished, namely grouted piles and driven piles. Grouted piles are usually a steel tubular pile inserted into an oversize drilled hole which is filled with grout. These piles are costly to install and are often used as an alternative to driven piles in rock where driving is not possible. Driven steel piles are most commonly used as a foundation technique for an offshore platform [37]. Driven piles are installed by using a hydraulic hammer to drive the pile into the soil. At Heerema, research is done on various types of installation techniques of driven steel piles, such as push-in piles and helical piles. Determining the capacity of these piles is based on the same theory used for conventional piles, being the skin friction and bearing capacity of the pile. Both techniques are described in the sections below.

It should be noted that the installation of the pile foundations can only be performed after the template is set down on the seabed. However, stability should also be ensured during the template set down case. The stability during the set down case is referred to as initial stability. Hence, an additional foundation concept is required for the pile foundation concepts to ensure the required initial stability.

Push-in pile

Push-in pile foundations are considered as silent foundation techniques, since no hammering is required during installation which results in no underwater noise production. Push-in pile foundation is a relatively new foundation method which is still under development, mainly concerning the installation method of these piles. Push-in pile foundations consist of four piles at each leg. The installation of these piles is done by means of a hydraulic lifting tool and using the weight of the piles to push them self into the seabed, see figure 2.5. By alternating this between the piles, the piles can use each other to penetrate into the soil. When focusing on the installation method it is required to consider four piles at each leg. For a conservative first estimation on the dimensions, the push-in pile concept is simplified to one overarching pile that represents the four piles at each leg.



Figure 2.5: Push-in pile foundation including hydraulic installation tool

Helical pile

Helical pile foundations are considered as silent pile foundations, since no hammer is required for installation. The piles can be screwed into the soil for which no underwater noise is produced. Helical pile foundations are characterized by a high bearing and uplift capacity, resulting in a relatively shallow penetration depth to obtain the required stability. The current design consists of a dual diameter tubular pile with a double helix. The lower pile section has a smaller diameter with a single helix near the pile tip. The upper section has a diameter twice the diameter of the lower shaft and a second helix. Both helices have the same pitch and diameter. The upper section consists of a larger diameter in order to cope with the large bending moments at the upper part of the pile. The lower part of the pile consists of a smaller diameter, since the bending moments at the bottom of the pile will be significantly reduced. This smaller diameter will reduce friction during installation and also result in a lower pile weight and material costs [23]. The installation is done by means of a torque tool connected to the vessel to provide the required torque. The Dynamic Position (DP) station keeping system should be assessed on the ability to keep the vessel in place as well as generating sufficient thrust to work against the reaction force in the connecting tool.

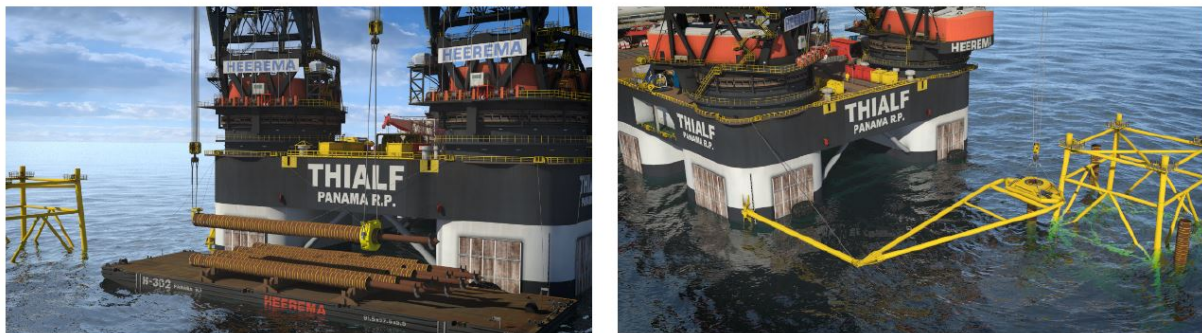


Figure 2.6: Artist impression of the helical pile (left) and torque tool (right)

2.2. Soil behavior of sand and clay soils

General soil behaviour

In the North Sea the seabed predominantly consists of sand and clay seabeds [6]. This research will consider a homogeneous sand and clay seabed. Since all considered soils in this research thesis are below sea level, the soils are assumed to be saturated. Saturated soil means that the pores and voids are filled with a fluid, in this case sea water. Its degree of saturation S is estimated as follows:

$$S = \frac{V_w}{V_p} \quad (2.3)$$

Where V_w is the volume of water, and V_p is the volume of pore space. When the soils are completely saturated, $S = 1$, and when the soil is completely dry, $S = 0$. From an engineering point of view, important characteristics of the soil are its strength, compressibility, permeability and volume change [41]. These characteristics are different for each type of soil and are dependent on its environment and time. On top of that, the depth of a soil, grain-size distribution, drainage and water holding capacity are also important parameters that could affect the behaviour of a soil [44].

An important property of a soil is its non-linear elastic behaviour when linearly increasing the pressure on a soil, shown in figure 2.7. This leads to a non-linear increase in soil strength, due to a decrease in pore size between the particles.

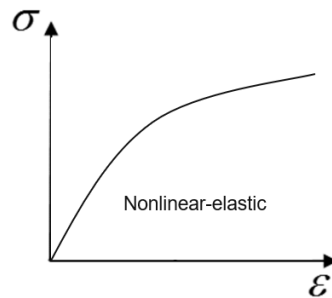


Figure 2.7: Non-linear elastic stress-strain relation under linear increased loading

Classification

Soils can be classified in various types based on its mechanical properties. A classification that is often made is based on the grain size that constitutes the soil. Coarse granular material, referred to as gravel, have a grain diameter of than 2 mm, whereas fine granular material is denoted as sand and have grain sizes that are between 0.063 mm and 2 mm. Grain sizes smaller than 0.002 are referred to as clay particles [41].

Cohesive and non-cohesive soils

A different classification in soils can be made between the cohesion of soil particles, which is formed by bonding forces. These bonding forces keep the soil particles together and cause friction between them when the soil is deformed. Sand is a non-cohesive soil, since there is no intergranular bonding. It will therefore fall apart when there is no external supporting force to keep the grains together [41]. For non-cohesive soils, the angle of internal friction (ϕ) describes the mechanical behaviour of non-cohesive soils. This angle will increase when the grains are more angular and decrease when the grains are more round. Non-cohesive soils are well permeable and quite stiff when pre-loaded by compression. Clay does contain intergranular bondings. Therefore it acts as a cohesive soil and is less permeable.

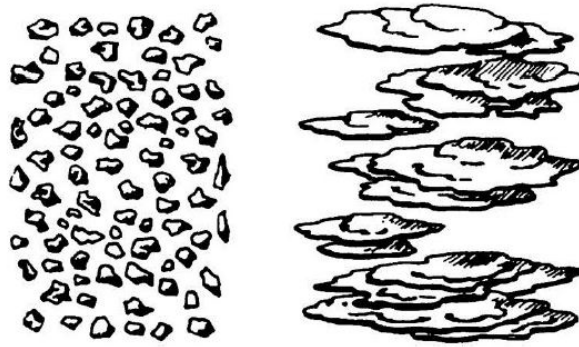


Figure 2.8: Example of a non-cohesive soil structure (left) and a cohesive soil structure (right)

Drained and undrained condition

The pore water inside a soil can flow away under the pressure gradient due to an imposed load, meaning there is a transfer from the pore water to the grains of the soil. The rate of this load transfer is dependent on the permeability coefficient k . The permeability coefficient is the drainage condition of the soil and the rate at which the load is applied. A drained condition is defined as when the pore water is free to flow away. An undrained condition is reached when the water stays inside the pores.

Sand characteristics

Fine granular soils, such as sand, can not transfer tensile stresses and therefore show a non-cohesive behavior. This results in only compression forces that can be transferred throughout the soil. An exception can be made when the particles are very small and saturated with water. Tensile stresses can then be transmitted via the capillary forces within the contact points [41]. Friction stresses between the granular particles and the fluid can occur, due to the fact that the fluid can flow with respect to the granular material. When loading is applied on the soil, the fluid inside the pores can flow out of the granular material and settlement will occur. This leads to an increase in stiffness. When loading is applied on a sandy type of soil, the soil will deform immediately and will remain at rest if the load remains constant. The behaviour of sand can therefore be classified as drained or undrained, depending on the loading period on the soil layer. Sand will behave as a drained soil after a relatively short loading period. Therefore the sand seabed is only considered as a drained material. The shape of sand particles affects the mechanical properties, even when having the same grain size. Round shaped sand particles can have a much smaller strength than sharp pointed particles. This is due to a difference in the packing of grains, which affects the friction and strength of the granular material.

From literature it can be assumed that an increase in friction angle ϕ will result in an increase in bearing capacity of the sand layer [3]. The friction angle generally varies between $\phi = 30^\circ$ for a soft layer, and up to $\phi = 42^\circ$ for a dense sand layer. When considering sand seabeds that are present in the North Sea, the common types of sand seabeds consist of a top layer of silty fine sand with an angle of internal friction of 40° [30]. Therefore a sand seabed with an internal friction angle of $\phi = 40^\circ$ is considered in this research. This sand layer has a dry unit weight of soil of $\gamma_{sand} = 17.60 \text{ kN/m}^3$ with a shear strength that linearly increases over depth.

Clay characteristics

Clay is stated to be a fine grained cohesive material and have particle sizes with a maximum of 0.002 mm [41]. Due to this cohesion between particles a clay soil can take on shear and tensile strengths. This is expressed as the undrained shear strength. Clay is a less permeable soil for water than sand due to the small size of the grains. It will therefore act as an undrained soil under a much longer period of loading time [41]. The cause of the long consolidation time for clay is due to the geometry of the structure, which is formed of thin plates stacked upon each other. The geometry causes clay to be an anisotropic material, meaning to have different characteristics in the vertical and horizontal plane.

As mentioned previously it is stated that clay layers are common in the North Sea. This research considers an uniform clay seabed. The outliers for the undrained shear strength of clay soils lie between

$s_u = 50kPa$ for soft clay and a shear strength of $s_u = 200kPa$ for hard clay. The common seabeds in the North Sea consist mainly of hard silty clay as a top layer, when considering clay seabeds [6]. This clay has an undrained shear strength often between 100 and 200 kN/m². In this research thesis an average undrained shear strength of 150 kN/m² for the clay seabed is considered and is assumed to be constant over depth. This clay seabed corresponds with a saturated soil unit weight of 20 kN/m³ [30].

Failure criteria

The foundation shall be designed such that the template remains in a stable position on the seabed during the full monopile installation sequence. This sequence includes installing the template construction onto the seabed until retracting the template from the seabed. The failure criteria for which the template is designed on considers bearing failure, sliding failure and failure due to overturning. These criteria are caused due to the vertical load and horizontal load that result in a base shear and an overturning moment on the template. The construction has lost its stability if it displaces in any x,y,z-direction. Each failure criteria is shown in figure 2.9 below.

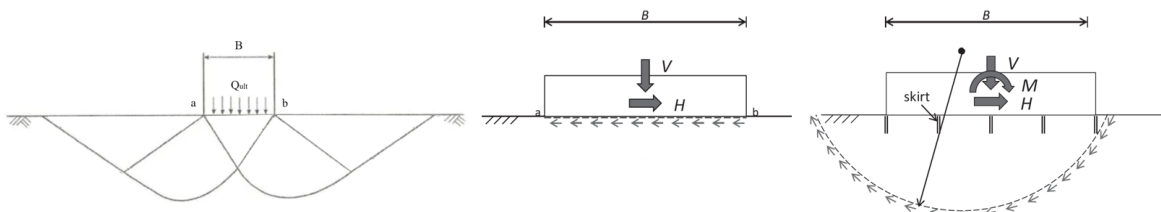


Figure 2.9: Left: bearing failure; middle: sliding failure; right: overturning failure [42]

Effective Stress

Since only saturated soils are considered here, which means that the pores are filled with sea water, the principle of effective stress plays a role. The effective stress is a principle introduced by Karl Terzaghi, which is often quoted as the "total stress equals effective stress plus pore pressure" [41]. This means that the stresses that are present in the particles are partly generated by the pressure in the water that is present inside the pores, and partly by the contact forces in the particles. This shows that a part of the stress in a saturated soil is transferred by water. The effective stress is calculated by means of the total stress σ acting on the soil and the pore pressure p inside a void filled with water, resulting in [41]:

$$\sigma' = \sigma - p \quad (2.4)$$

It is important to note that the principle of effective stress is only relevant for normal stresses. Shear stresses can be transferred via the grain skeleton only [41]. The principle of effective stress by Terzaghi is in full agreement with the Archimedes principle considering the upward force on a submerged body.

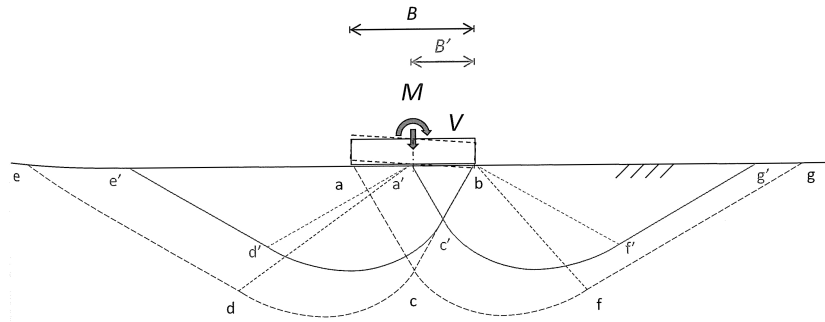


Figure 2.11: Shear failure of a shallow foundation due to overturning loading

A general equation is developed for the vertical soil resistance by Brinch Hansen combining multiple effects of vertical loads acting on a soil [19]. This general equation for the ultimate vertical soil resistance is referred by API [4] and ISO [27], and is stated as follows:

$$q_v = c * N_c * s_c * d_c * i_c * g_c * b_c + q * N_q * s_q * d_q * i_q * g_q * b_q + \frac{1}{2} \gamma'_s * B * N_\gamma * s_\gamma * d_\gamma * i_\gamma * g_\gamma * b_\gamma \quad (2.5)$$

When considering undrained conditions the internal friction angle reduces to $\varphi = 0$. Then the equation reduces to:

$$q_v = 5.14 * c_u * (1 + s'_c + d'_c - i'_c - b'_c - g'_c) + q \quad (2.6)$$

The vertical foundation resistance Q_v can then be calculated by multiplying the ultimate vertical soil resistance by the effective area, resulting in:

$$Q_v = q_v * A' \quad (2.7)$$

The parameters of the Equations 2.5 to 2.7 are listed in the table below:

Q_v	is the vertical foundation resistance [kN]
q_v	is the ultimate unit vertical soil resistance [kPa]
c	is the average cohesive shear strength over depth B below the foundation [kPa]
c_u	is the average undrained cohesive shear strength over depth B below the foundation [kPa]
q	is the overburden pressure $q = \gamma'_s * D$ [kPa]
γ'_s	is the soil submerged unit weight [kN/m ³]
D	is the depth of the foundation base [m]
B	is the width of the foundation base [m]
A	is the area of the foundation base [m ²]
N_c, N_q, N_γ	are the bearing resistance factors [-]
s_c, s_q, s_γ, s'_c	are the shape factors [-]
d_c, d_q, d_γ, d'_c	are the depth factors [-]
i_c, i_q, i_γ, i'_c	are the inclination factors [-]
g_c, g_q, g_γ, g'_c	are the ground factors [-]
b_c, b_q, b_γ, b'_c	are the base factors [-]

The shape, depth and inclination factors that are stated in equations 2.5 to 2.7 are determined via the equations given in Table 2.1 below.

Shape factors	Depth factors	Inclination factors
$s_c = 1 + \frac{N_q * B}{N_c * L}$	$d_c = 1 + 0.4 * \tan^{-1}(\frac{D}{B})$ for $D > B$	$i_c = i_q - \frac{1 - i_q}{N_q - 1}$
$s_q = 1 + \frac{B}{L} * \tan \varphi$	$d_q = 1 + 2 * \tan \varphi (1 - \sin \varphi)^2 * \frac{D}{B}$ for $D < B$ $d_q = 1 + 2 * \tan \varphi (1 - \sin \varphi)^2 * \tan^{-1}(\frac{D}{B})$ for $D > B$	$i_q = (1 - \frac{0.5 * H}{V + A' * c * \cot \varphi})^5$
$s_\gamma = 1 - 0.4 * \frac{B}{L}$	$d_\gamma = 1.0$ for all φ	$i_\gamma = (1 - \frac{0.5 * H}{V + A' * c * \cot \varphi})^5$
$s'_c = 0.2 * \frac{B}{L}$	$d'_c = 0.4 * \frac{D}{B}$ for $D \leq B$ $d'_c = 0.4 * \tan^{-1}(\frac{D}{B})$ for $D \leq B$	$i'_c = 0.5 - 0.5 \sqrt{1 - \frac{H}{A'} * c}$

Table 2.1: Shape, depth and inclination factors [42]

For this research a horizontal foundation base and seabed is assumed, resulting in the parameters g_c , g_q , g_γ and b_c , b_q , b_γ are reduced to 1, and $g'_c = b'_c = 0$. The bearing resistance factors are calculated as follows [42]:

$$N_q = \tan^2(45 + \frac{\varphi}{2}) * e^{\pi * \tan \varphi} \quad (2.8)$$

$$N_c = (N_q - 1) * \cot \varphi \quad (2.9)$$

$$N_\gamma = 1.5 * (N_q - 1) * \tan \varphi \quad (2.10)$$

Horizontal resistance

In order to calculate the horizontal foundation resistance Q_h , the following general equation can be assumed:

$$Q_h = V * \tan \delta + c * A' \quad (2.11)$$

where

Q_h is the horizontal foundation resistance [kN]

V is the vertical action on the foundation [kN]

δ is the friction angle between soil and foundation base [deg]

c is the cohesive shear strength at the level of a shear plane [kPa]

A' is the effective foundation area [m²]

For a shallow foundation on the seabed under predominant horizontal loading, a shear plane is formed between a-b (figure 2.12, left side) and shear resistance is generated by the friction between the foundation base and the soil. The horizontal resistance of the foundation can be improved by the addition of skirts onto the shallow foundation. Considering the failure criteria of sliding, the skirts will move the failure plane to a deeper location into the soil, at the tip of the skirts. This results in soil-to-soil friction for sliding to occur. If the shear strength strength of a soil increases with depth, the addition of vertical skirts result in an increased horizontal resistance. Figure 2.12 below shows a shallow foundation without skirts (left) and with the addition of skirts (right). The points a-d-e represent the active soil wedge. Points b-c-f represent the passive soil wedge for the foundation with skirts [42].

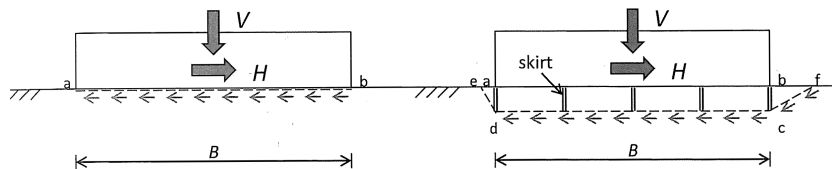


Figure 2.12: Failure modes due to sliding

It has to be noted that due to the addition of skirts on shallow foundations the horizontal resistance can be increased. This results in the following advantages of skirts [42]:

- the soil-to-soil friction is mobilized because the failure plane runs through the soil, instead of through the interface of the soil-to-structure; therefore this friction is often higher;
- when considering sand, the soil strength increases with depth; therefore it can be assumed that at the depth of the skirt tips the soil strength for horizontal resistance to the foundation will be better.
- due to the difference in the active and the passive soil wedge, extra horizontal resistance can be achieved;
- when a surcharge is available in a sand soil, the horizontal resistance will increase substantially. This overburden pressure is equal to $q = \gamma' * D$, where γ' is the submerged weight of the soil and D the depth of the skirt.

Undrained bearing capacity - constant shear strength with depth

A constant shear strength with depth can be considered when the strength is constant to a depth equal to two-third of the foundation width [4]. Since this research thesis only considers an uniform clay seabed, the shear strength is assumed to be constant over depth. For this case a simplification of constant soil strength can be used. If the seabed consists of multiple soil layers, the impact of lower soil strength below this depth on foundation capacity should also be considered. The maximum total vertical load capacity can be determined as:

$$Q_c = (s_u N_c K_c) * A' \quad (2.12)$$

where s_u is the undrained shear strength, N_c is a dimensionless constant equal to 5.14. K_c is the correction factor accounting for inclination and footing shape and A' is the effective area of the foundation. The determination of the correction factor K_c is stated as a standard by API [4]. However, since a horizontal seabed and foundation base is assumed the correction factor K_c can be assumed to be 1.

When considering a circular or square footing, a simplification can be made for the correction factor and the effective area. This is stated in equation 2.13 below.

For a circular or square footing:

$$Q_c = 6.05 s_u A \quad (2.13)$$

where Q_c is the vertical load capacity and A is the actual foundation area.

Ultimate capacity envelope

An envelope can be derived that captures the ultimate capacity of the foundation under certain loading conditions. Safety factors should be applied to these envelopes to obtain the envelopes of the allowable loads for undrained conditions. This envelope demonstrates the ultimate capacity for the vertical load Q_d and the horizontal load H_d , considering a safety factor of 1.5. This results in a large decrease of the allowable load envelope for vertical and horizontal loads. The ultimate capacity envelope stated by API [4] is shown in Figure 2.13 below.

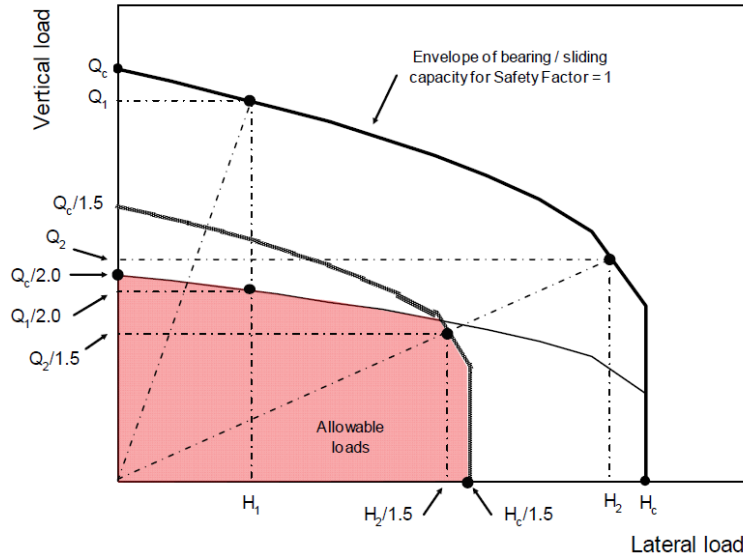


Figure 2.13: Envelope of the ultimate capacity under undrained conditions [4]

Q_c and H_c are the vertical and horizontal load capacities determined based on the foundation geometry. Safety factors are required to determine the foundation design capacities, denoted as Q_d and H_d , being the ultimate vertical load capacity and ultimate horizontal load capacity. These are determined as follows:

$$Q_d = \frac{Q_c}{1.5}; H_d = \frac{H_c}{1.5} \quad (2.14)$$

Drained bearing capacity

This method can be used when considering surface foundations on a sand seabed. This method also holds when skirted foundations are considered, for which the weight of the soil plug is balanced by the weight of the soil overburden outside of the skirts. Under drained conditions, the maximum total vertical load, Q'_c , can be calculated as follows [4]:

$$Q'_c = (p'_o(N_q - 1)K_q + 0.5\gamma'B'N_\gamma K_\gamma)A' \quad (2.15)$$

where

- Q'_c is the maximum total vertical load applied to the base of the footing at failure (excluding weight of soil plug inside skirts) under drained conditions [kN]
- N_q is $\exp[\pi \tan \phi'](\tan^2(45^\circ + \phi' / 2))$, a dimensionless function of ϕ' [deg]
- N_γ is an empirical dimensionless function of ϕ' that can be approximated by $1.5(N_q - 1)\tan\phi'$;
- ϕ' is the effective friction angle of Mohr envelope [deg]
- γ' is the effective unit weight of soil [kN/m^3]
- p'_o is the vertical effective stress at base level (skirt tip level when skirts are used) [kPa]
- B' is the minimum effective lateral foundation dimension [m]
- A' is the effective area of the foundation depending on the load eccentricity [m]
- K_q, K_γ is the correction factors which account for load inclination, footing shape, depth of embedment, inclination of base, and inclination of seafloor. The subscripts q and γ refer to the particular term in the equation.

However, equation 4.6 can be reduced by the assumption of a horizontal foundation base and a horizontal seafloor. This results in the following equation for a circular or square footing:

Circular or square footing:

$$Q_c = 0.3\gamma'BN_\gamma A \quad (2.16)$$

where

B is the minimum lateral foundation dimension.

An envelope can be derived that captures the ultimate capacity of the foundation under certain loading conditions. Safety factors should be applied to these envelopes to obtain the envelopes of the allowable loads for drained conditions. This envelope demonstrates the ultimate capacity for the vertical load Q and the horizontal load H . The envelope of the sliding capacity under drained conditions shows a linear increase under increasing vertical and horizontal loads. This is due to an increase in shear friction on the seabed with an increase in vertical loading.

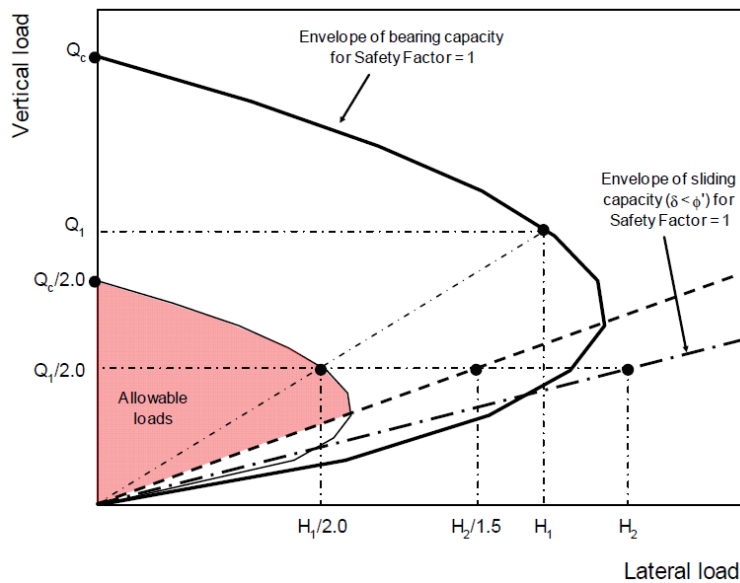


Figure 2.14: Envelope of the ultimate capacity under drained conditions [4]

Q_c and H_c are the vertical and horizontal load capacities determined based on the foundation geometry. Safety factors are required to determine the foundation design capacities, denoted as Q_d and H_d . These are the ultimate vertical load capacity and ultimate horizontal load capacity, determined as follows:

$$Q_d = \frac{Q_c}{2.0}; H_d = \frac{H_c}{1.5} \quad (2.17)$$

Since a homogeneous seabed is considered throughout this research, the theory for the calculation of the bearing capacity for undrained and drained conditions stated above can be used. This theory does not hold when considering layered seabeds [4].

Sliding stability

Shallow foundations should be assessed on instability due to sliding. The maximum horizontal load has to be limited to the lateral capacity determined for sliding in its extreme condition. This means only a horizontal load acts on the foundation. This can be determined for drained and undrained soils as follows:

Undrained case:

$$H_c = \alpha s_{uo}A \quad (2.18)$$

Drained case:

$$H'_c = Q \tan(\phi') \quad (2.19)$$

where:

- H_c is the maximum total horizontal load applied to the base of the foundation at failure under undrained conditions [kN]
- α is the soil adhesion coefficient [-]
- s_{uo} is the shear strength at base level [kPa]
- H'_c is the maximum total horizontal load applied to the base of the foundation at failure under drained conditions [kN]
- Q is the actual vertical load acting during the relevant loading condition, also including the self weight of the structure [kN]

Equations 2.18 and 4.7 assume that full soil resistance occurs due to complete interaction between the interface of the foundation and the soil [4].

2.3.2. Deep foundation theory

This section describes the theory used to determine the capacity of deep foundations, stated by API standards [4]. Pile foundations are usually considered as deep foundations. The capacity is determined by two components, namely the axial and lateral capacity. The axial capacity is determined by the skin friction along the pile shaft and the end bearing capacity at the tip of the pile. The lateral capacity consists of the strength of the pile and the interaction between the lateral soil resistance induced due to displacements in lateral direction. Pile foundations are often steel cylinders that can have an open ending or a closed-ending section.

Axial resistance

A deep foundation pile can take on loads in compression and tension in the axial direction. The resistance can be calculated for both open-ended and closed-ended pile foundations. This is determined by the sum of the outside skin friction, the end bearing capacity on the pile tip, and the total internal skin friction or end bearing capacity of the plug, whichever is less [4]. The components of the axial capacity resistance in compression and tension is shown in figure 2.15 below.

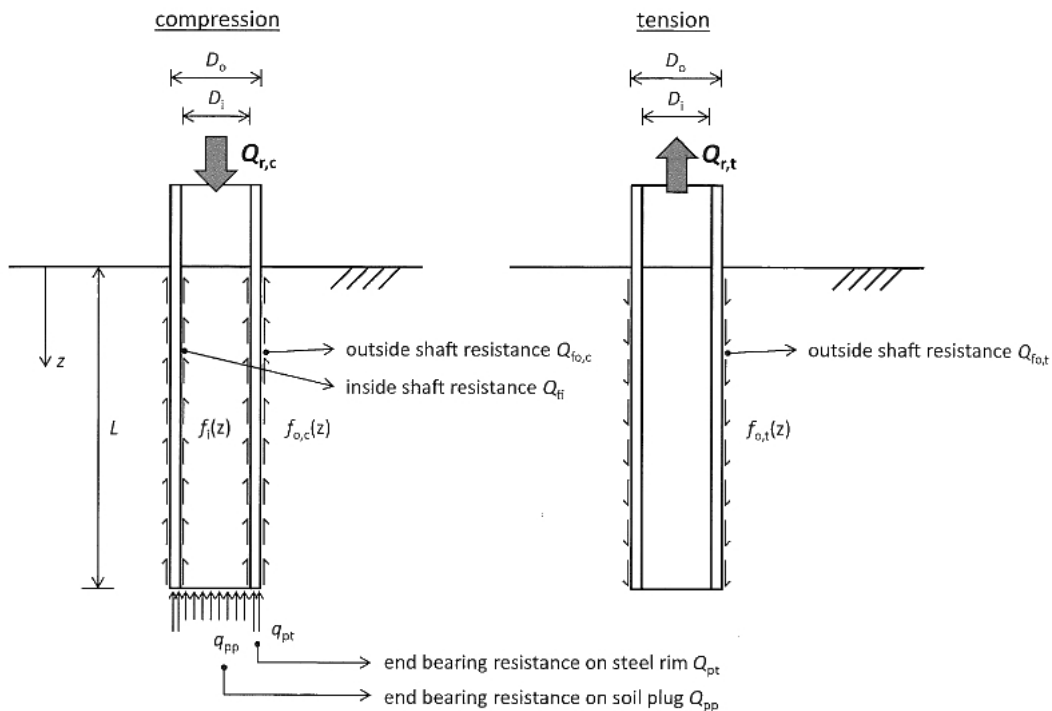


Figure 2.15: Resistance components of axial capacity in compression (left) and tension (right) [4]

The ultimate pile capacity under axial compression consists of the summation of the outside shaft resistance and the end bearing capacity, as follows:

$$Q_c = Q_{f,c} + Q_p = f(z)A_s + qA_p \quad (2.20)$$

where

- $Q_{f,c}$ is the skin friction capacity in compression, in force units [kN]
- Q_p is the end bearing capacity, in force units [kN]
- $f(z)$ is the unit skin friction, in stress units [kPa]
- A_s is the side surface area of the pile [m²]
- q is the unit end bearing at the pile tip or plug, in stress units [kPa]
- A_p is the gross end area of the pile [m²]
- z is the depth below the original seafloor [m]

The ultimate pile capacity under axial tension Q_t is less than or equal to $Q_{f,c}$ but shall not exceed the total skin friction capacity in compression. When determining the tension capacity of the pile, also the weight of the pile shall be taken into account. This also includes the weight of the plug if relevant. The tension capacity is generally determined by the outside skin friction of the pile. The weight of the pile should also be taken into account.

$$Q_t = Q_{f,c} + F_{pile} = f(z)A_s + M_{pile}g \quad (2.21)$$

where M_{pile} is the mass of the pile.

Corresponding to the figure 2.15 above, the determination of the outside and inside skin friction is determined with the equations shown below.

$$\text{Outside skin friction (compression):} \quad Q_{f_o,c} = \pi D_o * \int_0^L f_{o,c}(z) dz \quad (2.22)$$

$$\text{Outside skin friction (tension):} \quad Q_{f_o,t} = \pi D_o * \int_0^L f_{o,t}(z) dz \quad (2.23)$$

$$\text{Inside skin friction:} \quad Q_{f_i} = \pi D_i * \int_0^L f_i(z) dz \quad (2.24)$$

$$\text{End bearing resistance on tubular (open ended):} \quad Q_{pt} = q_{pt} * \pi (D_o^2 - D_i^2) \quad (2.25)$$

$$\text{End bearing resistance on soil plug:} \quad Q_{pp} = q_{pp} * \pi D_i^2 \quad (2.26)$$

with the following parameters:

D_o	is the outside diameter [m]
D_i	is the inside diameter [m]
L	is the pile penetration into the seabed [m]
z	is the depth in [m]
$Q_{f_o,c}$	is the outside skin friction in compression [kN]
$Q_{f_o,t}$	is the outside skin friction in tension [kN]
Q_{f_i}	is the inside skin friction [kN]
Q_{pt}	is the end bearing capacity on tubular [kN]
Q_{pp}	is the end bearing capacity on soil plug [kN]
$f_{o,c}(z)$	is the outside unit skin friction in compression as function of depth z [kPa]
$f_{o,t}(z)$	is the outside unit skin friction in tension as function of depth z [kPa]
$f_i(z)$	is the inside unit skin friction as function of depth z [kPa]
q_{pt}	is the unit end bearing resistance on tubular [kPa]
q_{pp}	is the unit end bearing resistance on soil plug [kPa]

Plugged and unplugged

If piles are considered to show plugged behavior, the bearing capacity is assumed to act over the entire cross-section of the pile. For unplugged piles the bearing capacity is only obtained by the pile tip. The inside skin friction contributes to the total skin friction of the pile. For conservative reasons, the pile is considered to be plugged or unplugged based on which behavior shows the most conservative capacity. Experience within Heerema showed that pile foundations generally show unplugged behavior.

Skin friction resistance

The determination of the skin friction resistance is dependent on the type of soil, for which a distinction can be made between cohesive (clay) and non-cohesive (sand) soils. The equations stated below are used to determine the skin friction resistance. These are used in the API [4], DNV [40] and ISO [27] standards.

Skin friction in cohesive soils

$$f(z) = \alpha * c_u(z) \quad (2.27)$$

where:

- $f(z)$ is the unit skin friction at depth z [kPa]
- $c_u(z)$ is the undrained shear strength at depth z [kPa]
- α is the adhesion factor [-]

The adhesion factor is specific for each type of clay, and is recommended by API, DNV and ISO to calculate as follows:

$$\alpha = 0.5\Psi^{-0.5}; \Psi \leq 1.0 \quad (2.28)$$

$$\alpha = 0.5\Psi^{-0.25}; \Psi > 1.0; \alpha \leq 1.0 \quad (2.29)$$

where:

- Ψ is the consolidation factor, where $\Psi = \frac{c_u(z)}{\sigma'_v(z)}$ [-]
- $\sigma'_v(z)$ is the effective vertical stress, where $\sigma'_v(z) = \gamma'_s * z$ [kPa]
- γ'_s is the soil submerged weight [kN/m³]
- z is the depth below the seabed in [m]

In cohesive soils the unit skin friction is stated to be the same for the inside and outside of the pile, both in compression and in tension [4].

Skin friction in non-cohesive soils

When considering the skin friction in non-cohesive soils, the API, DNV and ISO standards determine the skin friction resistance with the following equation below.

$$f(z) = \beta * p'_0(z) \leq f_{lim} \quad (2.30)$$

where:

- $f(z)$ is the unit skin friction at depth z [kPa]
- β is the dimensionless skin friction factor, for sands [-]
- $p'_0(z)$ is the effective vertical stress at depth z [kPa]

Since a dense sand seabed is considered, the dimensionless skin friction factor is set at $\beta = 0.46$ [4].

End bearing resistance

When the limit of the end bearing capacity is exceeded, a failure mechanism occurs. This is represented by an axisymmetric failure body where the failure planes follow a logarithmic spiral, shown in figure 2.16 below. The area underneath the pile tip is pushed downwards when the pile tip fails, resulting in a rotation of the soil volume area II (see figure 2.16) to make room for the pile. As well as for the skin friction, a distinction can be made between cohesive and non-cohesive soils. For cohesive soils the failure plane has the shape of a circle. The curve does not reach the soil surface for deep foundation piles, but are assumed to extend above the pile tip to the point where they reach the outer wall of the pile. For non-cohesive soils the failure plane takes on the shape of a logarithmic spiral. This is shown in figure 2.16 below.

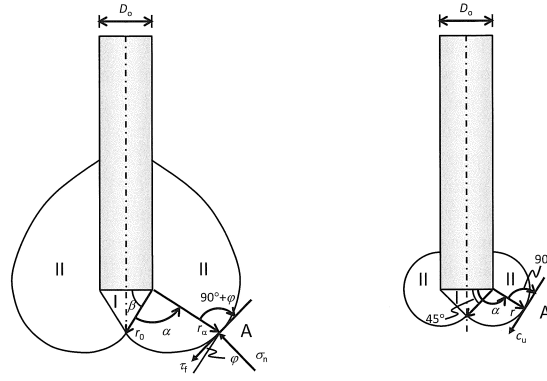


Figure 2.16: Failure shapes of deep foundation under vertical action for non-cohesive (left) and cohesive soils (right) [42]

The end bearing capacity in cohesive soils uses the equation stated in the API, DNV and ISO standards [42], which is defined as:

$$q_p = 9c_u(L) \quad (2.31)$$

where q_p is the unit end bearing resistance in kPa and $c_u(L)$ represents the undrained shear strength at penetration L in kPa. It has to be noted that equation 2.31 can only be used when considering a homogeneous seabed, or when the pile tip has penetrated to a minimum distance of 2 to 3 times the diameter into a clay layer and is at least 3 diameters above the bottom of the clay layer. Modifications to the equation have to be made when these boundaries are not met [4].

For determining the unit end bearing capacity in non-cohesive soils, in stress units, the following equation stated from the API, DNV and ISO standards has to be used:

$$q = N_q p'_{o,tip} \leq q_{lim} \quad (2.32)$$

$p'_{o,tip}$ is the effective vertical stress at the pile tip and N_q is the dimensionless bearing capacity factor. q_{lim} is the limit unit end bearing resistance taken in kPa, depending on the type of sand. It has to be noted that equation 2.32 can only be used when considering a homogeneous seabed, or when the pile tip has penetrated to a minimum distance of 2 to 3 times the diameter into a clay layer and is at least 3 diameters above the bottom of the clay layer. Modifications to the equation have to be made when these boundaries are not met.

Lateral capacity for sand

Considering a sand layered seabed, the ultimate lateral bearing capacity varies throughout the depth of the soil. Therefore, two equations are provided. The integral over the depth should be taken in order to obtain the lateral capacity at the required depth. Equation 2.33 is to be used at shallow depths and equation 2.34 is to be used at deep depths. It should be noted that at a given depth the smallest calculated value of p_u should be taken as ultimate lateral bearing capacity.

$$H_{us} = \int_0^L (C_1 z + C_2 D) \gamma' z dz \quad (2.33)$$

$$H_{ud} = \int_0^L C_3 D \gamma' z dz \quad (2.34)$$

where:

$$C_1 = \frac{(\tan\beta)^2 \tan\alpha}{\tan(\beta - \phi')} + K_0 * \left[\frac{\tan\phi' * \sin\beta}{\cos\alpha * \tan(\beta - \phi')} + \tan\beta * (\tan\phi' * \sin\beta - \tan\alpha) \right]$$

$$C_2 = \frac{\tan\beta}{\tan(\beta - \phi')} - K_a \quad (2.35)$$

$$C_3 = K_a * [(\tan\beta^8) - 1] + K_0 * \tan\phi' * (\tan\beta)^4$$

$$\alpha = \frac{\phi'}{2}; \beta = 45 + \frac{\phi'}{2}$$

where:

p_u	is the ultimate resistance, (s = shallow; d = deep) [kN/m ²]
γ'	is the submerged soil unit weight [kN/m ³]
z	is the depth below the original seafloor [m]
ϕ'	is the angle of internal friction of sand [-]
D	is the pile outside diameter [m]
C_1, C_2, C_3	are the coefficients determined as follows as function of ϕ' [-]
K_0	= 0.4
K_a	= $\frac{1-\sin\phi'}{1+\sin\phi'}$

The value of the coefficients C_1, C_2, C_3 as a function of the internal friction angle ϕ' can be obtained from figure 2.17 below.

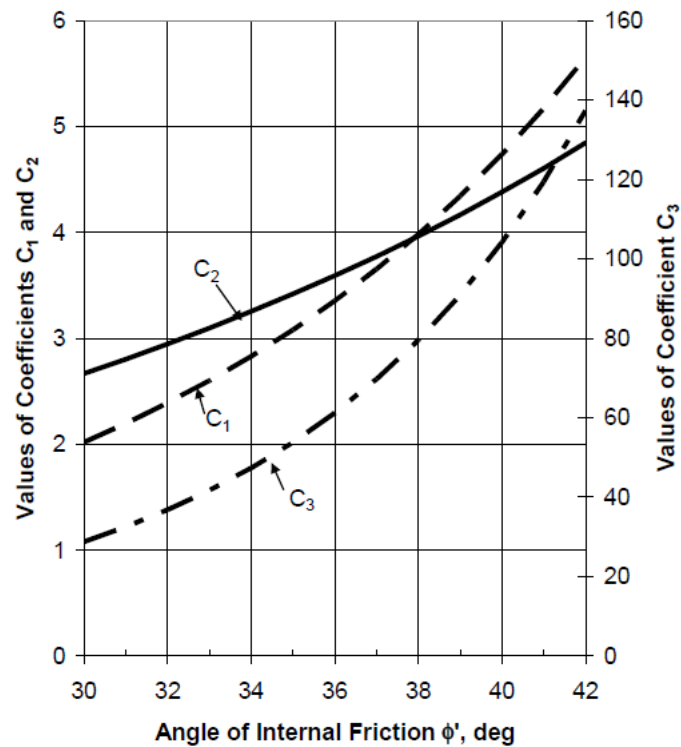


Figure 2.17: Coefficients C_1, C_2 and C_3 as a function of the internal friction ϕ' [4]

Lateral capacity for clay

When determining the ultimate lateral capacity $p_u D$ in force per unit length, there is a difference between static lateral loads and cyclic lateral loads. Considering static lateral loads the capacity is found to be between $8s_u D$ and $12s_u D$. There is an exception for shallow depths where failure can occur in a different mode due to a low overburden stress [4]. Considering cyclic loads a lower limit and an upper limit is stated that is determined by the following equations. The integral over the depth should be taken in order to obtain the lateral capacity at the required depth.:

Lower limit:

$$H_{u,lower} = \int_0^L 3s_u D + \gamma' z D + J s_u z dz \quad (2.36)$$

Upper limit:

$$H_{u,upper} = \int_0^L 9s_u D dz; z \geq z_R \quad (2.37)$$

where:

- p_u is the ultimate resistance, units of pressure [kPa]
- s_u is the undrained shear strength of the soil at the point in question, in stress units [kPa]
- D is the pile outside diameter [m]
- γ' is the submerged soil unit weight [kN/m³]
- J is the dimensionless empirical constant with values ranging from 0.25 to 0.5 [-]
- z is the depth below the original seafloor [m]
- z_R is the depth below soil surface to bottom of reduced resistance zone [m]

However, when constant strength with depth can be assumed, the following equation can be used to calculate z_R :

$$z_R = \frac{6D}{\frac{\gamma' D}{s_u} + J} \quad (2.38)$$

Working Stress Design Method

Based on the theory stated in section 2.3 the maximum bearing (Q_c) and lateral (H_c) capacity can be determined. API standards stated that safety factors are required to apply when determining the ultimate bearing and lateral design capacity. These safety factors are stated in figures 2.13 and 2.14 and convert the capacity values to a design capacity value, based on the Working Stress Design (WSD) method. Calculating the ultimate bearing (Q_d) and lateral (H_d) design capacity is done by applying a safety factor to the maximum bearing (Q_c) and lateral (H_c) capacity. Considering lateral capacity the safety factor for undrained conditions is 1.5 and 2.0 for drained conditions. For the design bearing capacity the safety factor is 2.0 for both undrained and drained conditions.

	Lateral capacity	Bearing capacity
Drained conditions	2	2
Undrained conditions	1.5	2

Table 2.2: Considered safety factors based on the WSD method [4]

Cyclic axial behavior of piles

Cyclic loads can significantly reduce the axial capacity of the foundation pile permanently or periodically. Such loads can be induced due to environmental conditions such as storm waves and earthquakes. This can have counteractive effects on the static axial capacity of a foundation pile. Repetitive loads can result in a temporary or permanent decrease in resistance and/or an accumulation of deformation. A distinction is made between rapidly applied loads and slowly applied loads. Rapidly applied loads cause an increase in resistance and/or stiffness of the pile, where very slowly applied loads cause a decrease in resistance and/or stiffness of the pile [4]. The resulting effect of cyclic loads is a function of the combined effects of the magnitude, rates of change of applied loads, cycles, structural characteristics of the pile and the type of soil. Therefore, modelling of cyclic effects is rather done implicitly than explicitly [4]. Experience has proven that determining the pile penetration based on static capacity by

means of static design loads in combination with working stress design (WSD), safety factors account in part for the cyclic effects [12]. Therefore the WSD method will be considered for determining the required foundation capacity. However, cyclic are not widely discussed since the template is installed on the seabed temporarily (in the order of days). On top of that the template is assumed to be installed only during operational months, ranging from March until October. Therefore cyclic loads due to environmental conditions such as storm waves will be limited compared to permanent structures, that are subjected to the environmental conditions during winter months. However, since the template is to be installed and retrieved at least 64 times (for each monopile installation), this process also induces a certain cyclic behavior on the foundation. This effect of cyclic behavior is not considered within the scope of this research, but should be taken into account in a more detailed design phase.

2.4. Environmental wave loading

This section describes the theory used to determine the hydrodynamic loads that act on the structure. The first part describe approach for the hydrodynamic loads in horizontal direction. This is relevant to determine the load during the set down case and contingency case. The second part, determines the hydrodynamic loads in vertical direction. This is relevant for the dynamic motion of the structure when lifting the template through the wave zone. A full section (section 2.5) is dedicated to describe the approach of the loads in vertical direction that is used throughout this research.

Hydrodynamic loads

When the template is set down on the seabed, the hydrodynamic loads acting on the template are estimated by Morison's equation. Morison's equation describes the resultant force acting on a structure by the superposition of the linear inertia force and the quadratic drag force [28]. Morison's approach assumes a slender fixed structure on the seabed that extends through the free surface, present in an oscillatory flow. A cylinder can be considered as slender when the cylinder diameter compared to the wave length is $5D \leq \lambda$. This assumption ignores the effect of the presence of the structure on the waves [39]. Morison's equation is stated by the following formula [14]:

$$F(t) = F_{inertia}(t) + F_{drag}(t) \quad (2.39)$$

$$F(t) = \rho(1 + C_A) \frac{\pi}{4} D^2 \dot{v}(t) + \frac{1}{2} \rho C_D D v(t) |v(t)|$$

where:

- $F(t)$ is the total force on the object [kN]
- D is the diameter of the cylinder [m]
- $v(t)$ is the flow velocity [m/s]
- $\dot{v}(t)$ is the flow acceleration, as a time derivative of the flow velocity [m/s²]
- C_A is the added mass coefficient [-]
- C_D is the drag coefficient [-]

The first segment of the two terms represents the inertia force and is induced by the water particle acceleration. The non-dimensional added mass coefficient C_A accounts for the inertia that is added to the system. This is caused by the displaced volume due to an accelerating (or decelerating) body that moves through the fluid. The second segment represents the drag force induced by the water particle velocity. The non-dimensional drag coefficient C_D accounts for the drag an object experiences when flowing through a fluid. For large-diameter structures, the application of Morison result in an overestimation of the hydrodynamic loads and can therefore be considered as conservative. The effect of the structure on the incoming wave field is called diffraction, and reduces the magnitude of the inertia force.

Load calculation

This section describes the loads acting on the template when the template is installed on the seabed. The template will be designed on loads induced by the environmental conditions, such as the hydrodynamic load distribution ($q_{hydrodynamic}$) and the wind load distribution (q_{wind}). The hydrodynamic load distribution consists of a current load distribution ($q_{current}$) and a wave load distribution (q_{wave}). The environmental loads act horizontally on the template and result by the integration of the distributed load over the depth. The self-weight of the template results in a vertical static load (F_{TP}). Figure 2.18 below shows an overview of the environmental load distributions acting on the template.

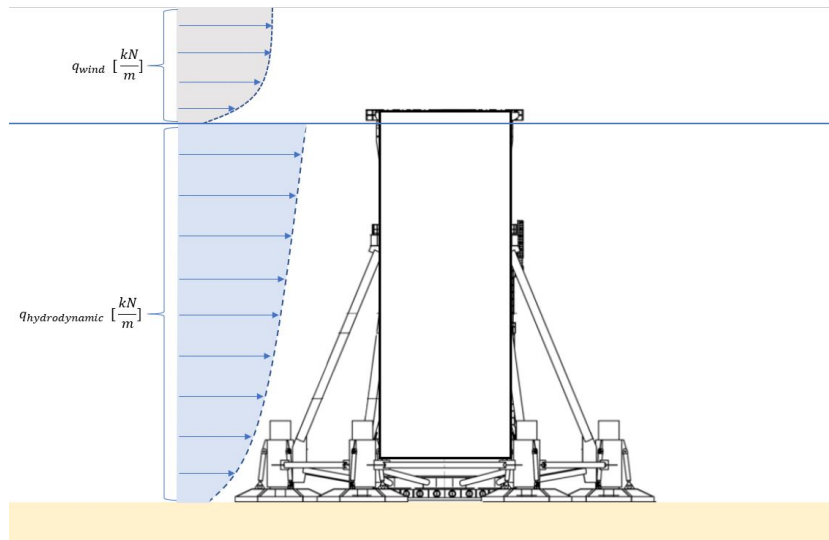


Figure 2.18: Environmental load distribution acting on the template

The on-bottom stability of the template is designed on bearing failure, sliding failure and instability due to overturning as shown in figure 2.9. The minimum required dimensions of each foundation concept to ensure stability are determined. This is done by means of the API theory stated in section 2.3 and the environmental loads acting on the template determined by Morison.

2.5. Lifting through the wave zone

A hydrodynamic analysis is performed for the initial designed template, to determine the behavior when lifting through the wave zone. This analysis showed large motions in heave direction due to the hydrodynamic forces in vertical direction. The Dynamic Amplification Factor of the system is believed to play a governing role for the performance of the initial designed template when lifting through the wave zone.

Dynamic Amplification Factor

The Dynamic Amplification Factor (DAF) is defined as the ratio of the amplitude of the dynamic response to the static response [7]. The DAF limit is used to determine the maximum allowable dynamic loading on the structure during the lowering sequence. The DAF is calculated as follows:

$$DAF = \frac{|F_{dyn}(t)|}{Mg} \quad (2.40)$$

$$F_{dyn}(t) = Mg + F_{hydrodynamic,vertical}(t)$$

Since the structure undergoes significant hydrodynamic loading when lifting through the wave zone, the slings obtain alternating tension and loosening. By the application of a DAF limit in the lifting system, a limit for the hydrodynamic loading is stated to avoid failure. The total force acting on the structure is determined by the simplified method stated by the DNVGL-RP-N103 [18]. This method is used since it provides conservative estimates of the static and hydrodynamic forces acting in vertical direction on the object. In order to estimate the forces acting on the structure, the motion response of the structure excited to a known wave spectrum should be determined first.

2.5.1. Motion response of the structure

In order to determine the behavior of a floating structure, the energy distribution of a known incoming wave spectrum is considered. The behavior of the structure is determined by its frequency characteristics. These frequency characteristics, the so-called Response Amplitude Operator (RAO), can be determined via model experiments or computations. Motions of the incoming wave spectrum are considered to be in the frequency domain [28]. In figure 2.19 an overview of this principle is shown. The sections below elaborate on the wave spectrum and the approach to determine the RAO of the structure.

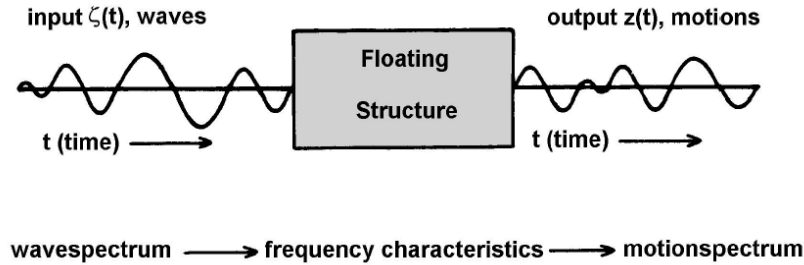


Figure 2.19: Relation between motions and waves [28]

Wave spectrum

When considering a wave spectrum there are different types of spectra that have been developed to describe the energy density spectrum of an irregular sea state. The two most frequently applied spectra for wind developed seas are the Pierson-Moskovitz (PM) and JONSWAP spectra [18]. The PM-spectrum is used for fully developed seastates, whereas the JONSWAP spectrum is used for seastates that include a fetch limit. Therefore this seastate never reaches a fully developed seastate due to non-linear wave-wave interactions [18]. The JONSWAP spectrum shows a good representation of North Sea wave conditions. Therefore this research considers a JONSWAP spectrum seastate to determine the response spectrum of the vessel.

The Pierson-Moskovitz (PM) spectrum $S_{PM}(\omega)$ is stated as follows:

$$S_{PM}(\omega) = \frac{5}{16} * H_s^2 \omega_p^4 * \omega^{-5} \exp\left(-\frac{5}{4} \left(\frac{\omega}{\omega_p}\right)^{-4}\right) \quad (2.41)$$

where $\omega_p = \frac{2\pi}{T_p}$ is the angular spectral peak frequency.

The JONSWAP spectrum $S_j(\omega)$ is a modification of the PM-spectrum for a developing sea state in a fetch limited situation:

$$S_j(\omega) = A_\gamma S_{PM}(\omega) \gamma^{\exp\left(-0.5 \left(\frac{\omega - \omega_p}{\sigma \omega_p}\right)^2\right)} \quad (2.42)$$

where:

- $S_{PM}(\omega)$ is the Pierson-Moskovitz spectrum
- γ is the non-dimensional peak shape parameter, stated at 3.3 for a JONSWAP spectrum
- σ is the spectral width parameter
 - $\sigma = 0.07$ for $\omega \leq \omega_p$
 - $\sigma = 0.09$ for $\omega > \omega_p$
- A_γ is a normalizing factor as $1 - 0.287 \ln(\gamma)$

The figure below shows the difference between a PM and a JONSWAP energy density spectrum based on a significant wave height $H_s = 1m$ and a corresponding peak period of $T_p = 6s$.

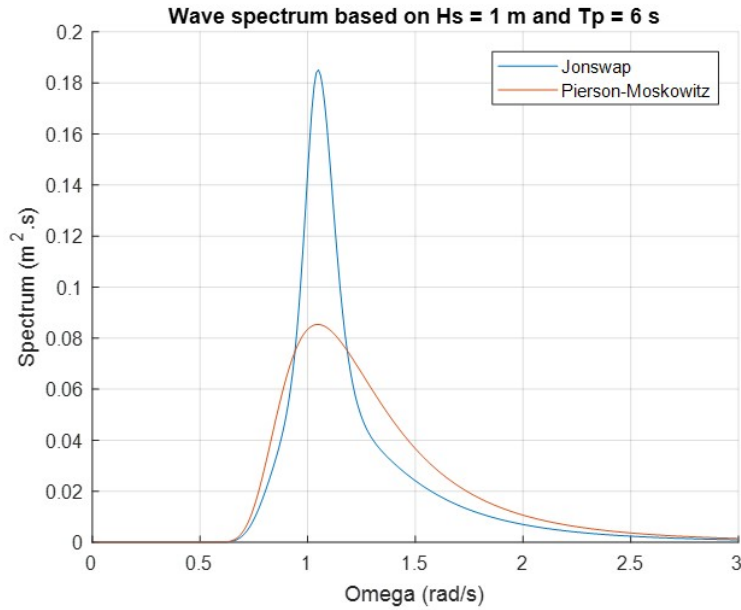


Figure 2.20: JONSWAP and Pierson-Moskowitz wave spectrum

Wave particle motion

The wave particle motions are of importance due to the hydrodynamic forces that act on the structure. These are a function of the wave particle amplitude, velocity and acceleration. In order to determine the wave particle velocity and acceleration the theory of deep water waves can be used, which is determined as follows [21]:

$$\begin{aligned} z_w &= \zeta_a e^{kz} \cos(\omega t - kx) \\ \dot{z}_w &= v_w = \zeta_a e^{kz} \omega \sin(\omega t - kx) \\ \ddot{z}_w &= a_w = -\zeta_a e^{kz} \omega^2 \cos(\omega t - kx) \end{aligned} \quad (2.43)$$

where

- ζ_a is the characteristic wave amplitude [m]
- k is the wave number [-]
- z is the relative distance from the CoG of the characteristic wave particle to the still water level [m]

Assuming that the lifting operation takes less than 30 minutes, the characteristic wave amplitude can be taken as:

$$\zeta_a = 0.9 * H_s \quad (2.44)$$

However, for lifting operations that exceed the 30 minutes limit, the significant wave height H_s should be multiplied with a factor of 1.1 [18].

The wave number k is determined as follows:

$$k = \frac{\omega^2}{g * \tanh(kd)} \quad (2.45)$$

this can be simplified for deep water as follows:

$$k = \frac{\omega^2}{g} \quad (2.46)$$

Response Amplitude Operator

The Response Amplitude Operator (RAO) is used to describe the motion of the vessel due to an incoming wave spectrum. The wave energy excited on the vessel due to the incoming JONSWAP wave spectrum is transferred to vessel motions by means of the RAO's. The RAO is therefore a transfer function that describes the motion for all 6 degrees of freedom (DoF) as a result of an incoming wave amplitude and frequency. The RAO of the crane tip at a certain wave frequency is obtained by means of the crane tip elevation and wave amplitude at that particular frequency in [m/m], as follows:

$$RAO(\omega) = \frac{z_{ct}}{\zeta_a}(\omega) \quad (2.47)$$

The response spectrum of the crane tip S_{ct} can be determined by means of the RAO transfer function at the crane tip and the considered JONSWAP spectrum, stated as follows:

$$S_{ct}(\omega) = \left| \frac{z_{ct}}{\zeta_a}(\omega) \right|^2 S_{JONSWAP}(\omega) \quad (2.48)$$

The assumption is made that the vertical motion of the lifted object follows the vertical motion of the crane tip. Therefore the most probable largest vertical single amplitude crane tip motion can be determined from the response spectrum:

$$\eta_a = \begin{cases} 3.6\sigma_\eta & \text{for lifting operations} \leq 30 \text{ minutes} \\ 4.4\sigma_\eta & \text{for lifting operations} > 30 \text{ minutes} \end{cases} \quad (2.49)$$

where the standard deviation σ_η is defined as:

$$\sigma_\eta = \sqrt{\int_0^\infty S_{ct}(\omega) d\omega} \quad (2.50)$$

From the most probable largest vertical single amplitude crane tip motion η_a the vertical motion, velocity and acceleration of the lifted object can be computed by:

$$\begin{aligned} \eta &= \eta_a \sin(\omega_\eta t + \epsilon) \\ \dot{\eta} &= \eta_a \omega_\eta \cos(\omega_\eta t + \epsilon) \\ \ddot{\eta} &= -\eta_a \omega_\eta^2 \sin(\omega_\eta t + \epsilon) \end{aligned} \quad (2.51)$$

where:

- η is the vertical motion of the lifted object [m]
- $\dot{\eta}$ is the vertical velocity of the lifted object [m/s]
- $\ddot{\eta}$ is the vertical acceleration of the lifted object [m/s²]
- η_a is the vertical single amplitude motion of the lifted object [m]
- ω_η is the circular frequency of the vertical motion of the lifted object [rad/s]
- ϵ is the phase angle between the wave and crane tip motion [rad]

2.5.2. Characteristic total force when lifting through the wave zone

For the characteristic total force acting on the template when lifting through the wave zone, the largest force of the following should be taken:

$$F_{total} = \max \begin{cases} F_{static} + F_{hydrodynamic} \\ F_{static} + F_{snap} \end{cases} \quad (2.52)$$

The forces that act on the structure during lifting through the wave zone consist of a static force and a characteristic hydrodynamic force. The static force is induced by the weight of the object. A characteristic hydrodynamic force is induced by the impact of the wave zone on the structure. This results in a characteristic hydrodynamic force on the template or a characteristic snap force in the hoisting line. The largest value of both loads yields the characteristic total force on an object when lifted through the

wave zone at a certain point. However, due to the weight of the template and the stiffness of the crane hoist, it can be considered that the characteristic snap force will not be governing. The snap force will therefore not be considered. The characteristic total force should be determined at several stages of the lifting procedure to determine the governing load acting on the object when lowered through the wave zone.

The static force is dependent on the volume of displaced water due to the structure, and is determined as follows:

$$F_{static} = Mg - \rho V(z)g \quad (2.53)$$

where:

M is the mass of the object in air [kg]

V is the displaced water volume during each stage when passing through the water surface [m³]

Hydrodynamic forces

The total characteristic hydrodynamic force on an object is a time dependent function of the slamming impact force, varying buoyancy force, hydrodynamic mass force and drag force. The equation used to determine the total hydrodynamic force is shown below. Each individual force is described in the next sections.

$$F_{hyd} = \sqrt{(F_D + F_{slam})^2 + (F_M - F_\rho)^2} \quad (2.54)$$

where:

F_D is the characteristic hydrodynamic drag force

F_{slam} is the characteristic slamming impact force

F_M is the characteristic hydrodynamic mass force

F_ρ is the characteristic varying buoyancy force

Slamming impact force

The slamming impact force on the foundation can be determined by the following formula:

$$F_{slam} = 0.5\rho C_s A_s v_s^2 \quad (2.55)$$

where:

C_s is the slamming coefficient taken as 2π [46]

A_s is the slamming area; part of structure subjected on a horizontal plane that will be subjected to slamming loads [m²]

v_s is the slamming impact velocity [m/s]

The slamming impact velocity is calculated as:

$$v_s = v_c + \sqrt{v_{ct}^2 + v_w^2 * \kappa^2} \quad (2.56)$$

where:

v_c is the hook lowering velocity, stated at 0.1 m/s

v_{ct} is the characteristic single amplitude vertical velocity of the crane tip [m/s]

v_w is the characteristic vertical water particle velocity [m/s]

κ is the amplification factor, typically $1.0 \leq \kappa \leq 2.0$ [-]

The amplification factor κ is only of interest when bucket foundations are considered. The water that is entrapped in the bucket results in an increased slamming impact velocity due to the excitation of water

inside the buckets [18].

The characteristic vertical water particle velocity and acceleration can analytically be determined as follows:

$$\begin{aligned} v_w &= \zeta_a \left(\frac{2\pi}{T_z} \right) * e^{-\frac{4\pi^2 d}{T_z^2 g}} \\ a_w &= \zeta_a \left(\frac{2\pi}{T_z} \right)^2 * e^{-\frac{4\pi^2 d}{T_z^2 g}} \\ \zeta_a &= 0.9 * H_s \end{aligned} \quad (2.57)$$

where:

- ζ_a is the characteristic wave amplitude [m]
- d is the distance from water plane to centre of gravity of submerged part of the object [m]
- H_s is the significant wave height of the design state [m]
- T_z is the zero-up-crossing wave periods [s]

Varying buoyancy force

The change in buoyancy when the foundation is lowered through the wave zone is determined as:

$$\begin{aligned} F_p &= \rho * \delta V * g \\ \delta V &= \tilde{A}_w \sqrt{\zeta_a^2 + \eta_{ct}^2} \end{aligned} \quad (2.58)$$

where:

- δV is the change in volume of displaced water from MSL to wave crest or trough [m³]
- \tilde{A}_w is the mean water line area in the wave surface zone [m²]
- η_{ct} is the characteristic single amplitude in vertical motion [m]

Mass force

The characteristic mass force acting on a structure is a combination of the kinetic mass force and the inertia force that is added to the system. The total mass force is dependent on the crane tip acceleration and the acceleration of the wave particles. This is calculated as:

$$F_M = \sqrt{[(M + A_{33i}) * a_{ct}]^2 + [(\rho V_i + A_{33i}) * a_w]^2} \quad (2.59)$$

where:

- M is the mass of the template [kg]
- A_{33i} is the heave added mass of the considered foundation [kg]
- a_{ct} is the characteristic single amplitude vertical acceleration of crane tip [m/s²]
- V_i is the volume of displaced water of the foundation relative to the MSL [m³]
- a_w is the characteristic vertical water particle acceleration from Equation 2.57 [m/s²]

Drag force

The characteristic drag force on the foundation can be calculated as:

$$\begin{aligned} F_D &= 0.5 \rho C_D A_p v_r^2 \\ v_r &= v_c + \sqrt{v_{ct}^2 + v_w^2 * \kappa^2} \end{aligned} \quad (2.60)$$

where:

- C_D is the drag coefficient, taken as 2.5 [-]
- A_p is the area of the submerged part of the foundation projected on a horizontal plane [m²]
- v_r is the characteristic vertical relative velocity between the foundation and water particles [m/s] and is equal to the slamming impact velocity stated in Equation 2.56

Stiffness of hoisting system

The stiffness K of the hoisting system is calculated by the sum of the stiffness of each individual segment, stated as follows:

$$\frac{1}{K} = \frac{1}{k_{rigging}} + \frac{1}{k_{line}} + \frac{1}{k_{block}} + \frac{1}{k_{boom}} + \frac{1}{k_{other}} \quad (2.61)$$

The line stiffness is calculated by:

$$k_{line} = \frac{EA}{L} \quad (2.62)$$

where:

- E is the modulus of rope elasticity [N/m²]
- A is the effective cross section area of the lines [m²]
- L length of the lines [m]

Hydrodynamic parameters

Drag coefficient

In general the drag coefficient depends on the oscillation amplitude induced by the oscillating flow the object is in. This oscillation amplitude is stated by means of the Keulegan-Carpenter (KC) number, which is a relation of the oscillation amplitude to the dimension of the object. This describes the relative importance of the drag forces over the inertia forces. The simplified method determines a conservative approach for determining the hydrodynamic loads on an object. Therefore the drag coefficient C_D considered for the foundation concepts in this thesis follows the guideline for drag coefficients on typical subsea structures in an oscillatory flow stated by DNV [18], resulting in:

$$C_D \geq 2.5 \quad (2.63)$$

However, in a more detailed design stage more detail should be given to the drag coefficient in order to determine the correct behavior of the object in an oscillatory flow due to the drag force. This can be obtained by the performance of CFD analysis or by means of model scaled tests.

Added mass coefficient

The added mass of an object is the mass that is added to the system due to the volume that the body displaces when it accelerates or decelerates through a medium. The added mass is dependent on the geometry of the structure. It can be reduced by adding perforations on the horizontal projected surface area. Since the foundation concepts all have a circular geometry in the horizontal plane, the heave added mass of a three dimensional circular disc can be calculated as follows [18]:

$$A_{33o} = \rho C_A V_R \quad (2.64)$$

where:

$$\begin{aligned} C_A &= \frac{2}{3} \\ V_R &= \frac{4}{3}\pi a^3 \end{aligned}$$

Circular disc



Figure 2.21: Added mass of a three-dimensional circular disc

The added mass is approximated based on the high frequency limit and is taken as frequency independent. It assumes that the radiated surface waves due to the presence of the structure are negligible

[18]. For the foundation concepts that consider the application of skirts the following approximation of the added mass in heave direction can be applied, stated by DNV:

$$A_{33} = \left[1 + \sqrt{\frac{1 - \lambda^2}{2(1 + \lambda^2)}} \right] * A_{33o} \quad (2.65)$$

$$\lambda = \frac{\sqrt{A_p}}{h + \sqrt{A_p}}$$

where:

h is the height of the skirt [m]

A_p is the area of the submerged part of the foundation projected on a horizontal plane [m²]

A_{33o} is the added mass for a flat plate with a shape equal to the horizontal projected area of the object [kg]

It should be noted that the water volume entrapped inside the water bucket should be taken into account when determining the added mass of the suction bucket.

Slamming coefficient

The slamming coefficient used in this thesis is stated by the DNV [14] and is dependent on the geometry of the object. The slamming coefficient is determined based on the horizontal projected area of the object and the rate of change of added mass with the submergence relative to the surface elevation. DNV stated that the slamming coefficient for smooth circular cylinders $C_s \geq 3.0$ and for non-circular shapes the slamming coefficient $C_s \geq 5.0$.

Generation of foundation concepts

A generation of the foundation concepts is required in order to determine which concepts are interesting to develop further throughout this research. In order to do so the limitations of the template design that are considered throughout this thesis are stated. To determine the environmental loads that act on the template, the environmental conditions based on metocean data of the location of the He Dreiht Wind Farm are considered. After stating the limitations and the environmental conditions, the foundation concepts that will be developed further throughout this research are discussed.

3.1. Boundary conditions and assumptions for the He Dreiht template design

Figure 3.1 stated below shows a figure of the initial template design and the corresponding properties. It shows the crucial dimensions of the template. Additionally the weight of the template when being in air, during operation and during the survival case are stated. Note that when referred to template in figure 3.1, the template excluding the NMS is meant. The weight of the NMS is stated separately.

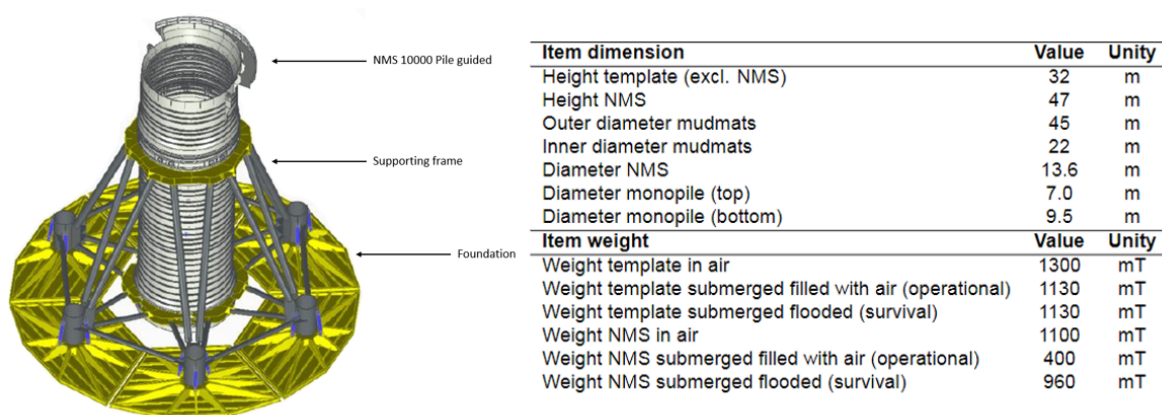


Figure 3.1: Template construction and properties

Noise Mitigation System

The NMS that is incorporated in the template will be the same as was prescribed for the base case template design, being the Noise Mitigation System 10000 Pile Guided. Figure 3.1 above presents the information on dimensions and weight of the NMS. More information on the NMS can be found in section 1.3.1.

Supporting frame

As stated in section 1.3.1 the design of the template foundation considers a foundation with six legs. The wave load direction acting on the template are stated in figure 3.4. This figure represents the loads acting on the horizontal and diagonal of the template, considering a top view. For both situations it is assumed that all wave and current loads come from the same direction. The largest member of the

supporting frame in terms of diameter is 0.90 m.

Foundation

Each foundation concept of the template consists of six identical individual foundations, where each individual foundation is connected to a leg of the supporting frame. In this research each type of foundation will be designed to have a circular top-view geometry. Figure 3.2 below shows a drawing of the top and side view of the template. The maximum distance between the two outer points of the template construction is limited at 45 meter. This is due to the available deck space on the Thialf and other equipment that is required to be present during installation.

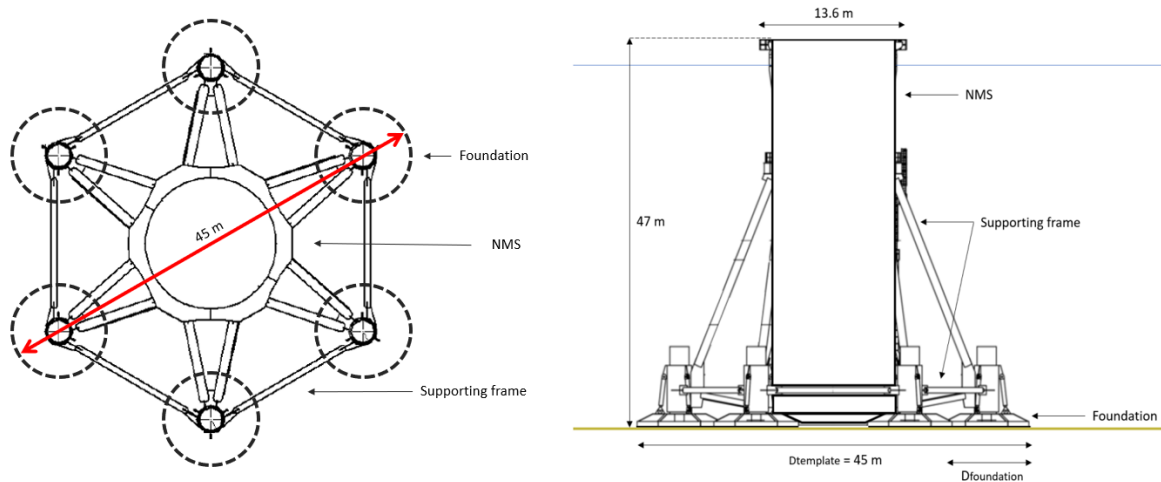


Figure 3.2: Template configuration case study showing top view (left) and side view (right)

Weight of the template

The total weight of the template varies throughout the installation process due to the present buoyancy force. The template in air weight is designed to have a maximum of 2400 mT. Since the assumption is made that the supporting frame is fixed, this weight cannot be exceeded due to various reasons. The supporting frame is designed on a template weight of 2400 mT considering the strength of the fastening between the tubular members of the supporting frame and the attachment of the supporting frame to the foundation. Due to the buoyancy, the total weight of the template when submerged and lowered to the seabed is 2090 mT. The same weight is considered for the survival case of the template. During operation the template is filled with air, resulting in a total weight of 1530 mT. The weight and dimensions of the template when being in air, submerged and during operation are stated in the table shown in figure 3.1.

The weight of each template segment is stated in table 3.1 below, resulting in a maximum in air weight of 800 mT for each foundation concept.

Item	Weight [mT]
Noise Mitigation System	1100
Supporting frame	500
Foundation	800
Total	2400

Table 3.1: Weight of each template segment

Monopile main properties

The monopile that is installed by means of the He Dreih template has the following specifications as stated in table 3.2. The weight of the monopile is carried by the seabed, however the monopile can have a maximum inclination of 0.5° . This would result in an additional load on the template.

Item	Value	Unity
Height	75	m
Diameter (top)	7	m
Diameter (bottom)	9.5	m
Wall thickness	75	mm
Weight	1600	mT

Table 3.2: Monopile main properties

3.2. Environmental conditions at the He Dreih Wind Farm location

In order to determine the governing environmental loads that act on the template a significant wave height (H_s) and peak period (T_p) should be stated. In order to do this accurately, the metocean data of the He Dreih Wind Farm is obtained and is converted to a wave scatter diagram as stated in figure 3.3. Afterwards, a significant wave height and peak period is stated in order to determine the governing environmental loads acting on the template during the template set down and contingency case.

Wave scatter diagram

Metocean data is used to create a wave scatter diagram of the He Dreih Wind Farm. This data covers the wave conditions ranging from 1979 to 2020, and considers only the operational months (March until October). The value stated in a cell represents the occurrence in percentage of those conditions based on the Metocean data. As an example, from the determined wave scatter diagram stated in figure 3.3 it can be observed that a peak period of 4 - 8 seconds with a significant wave height between 0.5 - 2.5 meter occurs approximately 60% of the time.

The operability of each developed foundation concept can be determined by combining the operability curve obtained from the hydrodynamic analysis and the corresponding wave scatter diagram from figure 3.3.

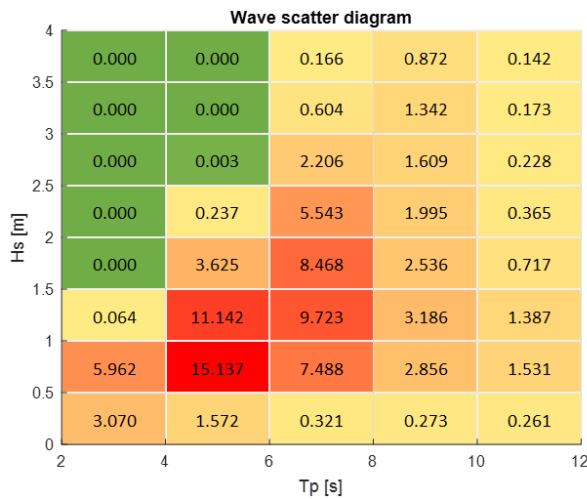


Figure 3.3: Wave scatter diagram of the He Dreih Wind Farm location (based on operational months of 1979-2020)

3.2.1. Weather restricted conditions

The execution of each critical phase is considered as a weather restricted operation. Weather restricted operations are defined by DNV as marine operations with a reference period (T_R) less than 96 hours and a planned operation period (T_{POP}) less than 72 hours. This shall therefore only be planned to be executed within a reliable weather window [15].

Set down case

The following environmental conditions are stated to determine the environmental loads during the weather restricted conditions of the template set down case:

- Maximum significant wave height of $H_s = 2.5$ m, limited by:
 - Wave breaking limit
 - $H_{max} = 2 * H_s$
- Peak period of $T_p = 4$ seconds
- Surface current velocity of $v_{current} = 0.70$ m/s based on a 1-year return period
- Maximum wind velocity of $v_{wind} = 25$ m/s

Contingency case

For the weather restricted conditions during the contingency case, the template configuration should be able to withstand the following environmental conditions:

- Maximum significant wave height of $H_s = 3.0$ m, limited by:
 - Wave breaking limit
 - $H_{max} = 2 * H_s$
- Peak period of $T_p = 4$ seconds
- Surface current velocity of $v_{current} = 0.90$ m/s, based on a 50 year return period
- Maximum wind velocity of $v_{wind} = 30$ m/s, based on a 10 year return period

For the calculation of the environmental loads the following shall be taken into account:

- Waves, current and wind shall be taken from the same direction;
- Waves, current and wind shall be unidirectional (no wave spreading);
- Current profile is constant over depth
- Water depth of 45 meter

The environmental conditions stated above are summarized in Table 3.3 below.

Parameter	Value
T_p	4 s
H_s	2.5 - 3.0 m (depending on the load case)
H_{max}	$2.0 * H_s$ (in meter)
Directions	$0^\circ - 360^\circ$ (with increments of 15 degrees)
Current velocity v_c	0.7 or 0.9 m/s (depending on the load case)
Direction	Colinear with waves
Method	Constant with water depth
Wind velocity v_w	25 or 30 m/s
Water depth d	45 m

Table 3.3: Considered environmental conditions during the critical cases

3.2.2. Soil conditions

The soil conditions that are considered in this thesis are soils that generally occur in the North Sea and that are suitable for monopile installation. For this research thesis an uniform clay seabed and an uniform sand seabed are chosen for the design of the template foundation. For clay a relatively hard seabed is considered, having an undrained shear strength of $s_u = 150$ kPa, which corresponds with a saturated soil unit weight of $\gamma_{clay} = 20$ kN/m³. For sand, an uniform seabed with an internal friction angle of $\phi = 40^\circ$ is chosen, corresponding with a dry soil unit weight of $\gamma_{sand} = 17.60$ kN/m³. An undrained behavior is considered for clay and a drained behavior for sand. Table 3.4 below shows an overview of the soil properties that are considered during this thesis.

Clay layer	Properties	Behavior
Shear strength s_u [kPa]	150	Undrained
γ_{clay} [kN/m ³]	20	
Sand layer	Properties	Behavior
Friction angle ϕ [°]	40	Drained
γ_{sand} [kN/m ³]	17.60	

Table 3.4: Soil properties considered during this thesis

3.3. Modelling the environmental loads acting on the template

This section discusses the simplification made to the template construction to determine the environmental loads acting on it. It will be investigated if a simplification of the template can be made that considers only the NMS as a cylindrical structure. That would imply that the supporting frame and foundation can be neglected. This is only possible if the environmental loads acting on the supporting frame can be considered small compared to the loads acting on the NMS.

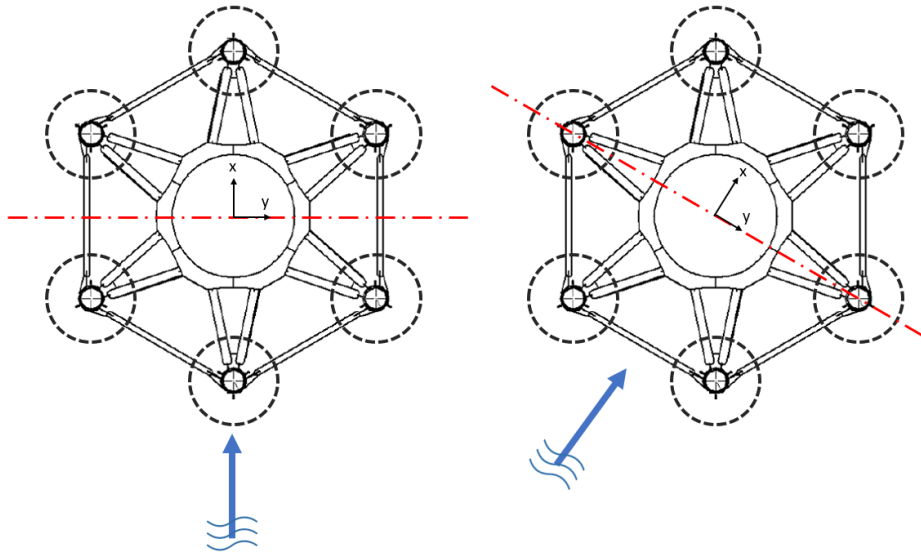


Figure 3.4: Wave load directions, horizontal (left) and diagonal (right)

Template simplification

A simplification of the template construction is made for the calculation of the horizontal environmental loads acting on the template during the set down and contingency case. The water depth is estimated as an intermediate water depth in order to determine the wave particle motion. Since the magnitude of the hydrodynamic loads decrease over depth, the largest loads are obtained at the upper part of the template. The wave loading decreases quadratic-ally, with approximately 2% of the load at sea level is obtained near the seabed. This is based on wave theory considering an intermediate water depth. As stated in section 1.3.1, the construction can be divided in three segments, namely the NMS, the supporting frame and the foundation. The NMS is a vertical cylinder with a diameter of 13.6 meter and extends over the full water depth. The supporting frame has a relatively small area, with a member diameter ranging from 0.5 - 0.9 meter, and reaches up to a height of 32 meter from the seabed. The foundation is close to the seabed, or penetrated into the seabed. Therefore it is assumed that the foundation will encounter a negligible amount of wave forces. Since the supporting frame does not extend over the full water depth and is relatively small compared to the width of the NMS, the supporting frame is neglected when determining the loads. It is determined that the environmental loads acting on the supporting frame and foundation footing are approximately 10% of the loads acting on the NMS. Based on the statements above, the template is simplified to only the NMS modelled as a vertical cylinder with a diameter of 13.6 meter. This simplification is shown in figure 3.5. The environmental loads acting on the template are calculated by means of Morison's equation as stated in section 2.4.

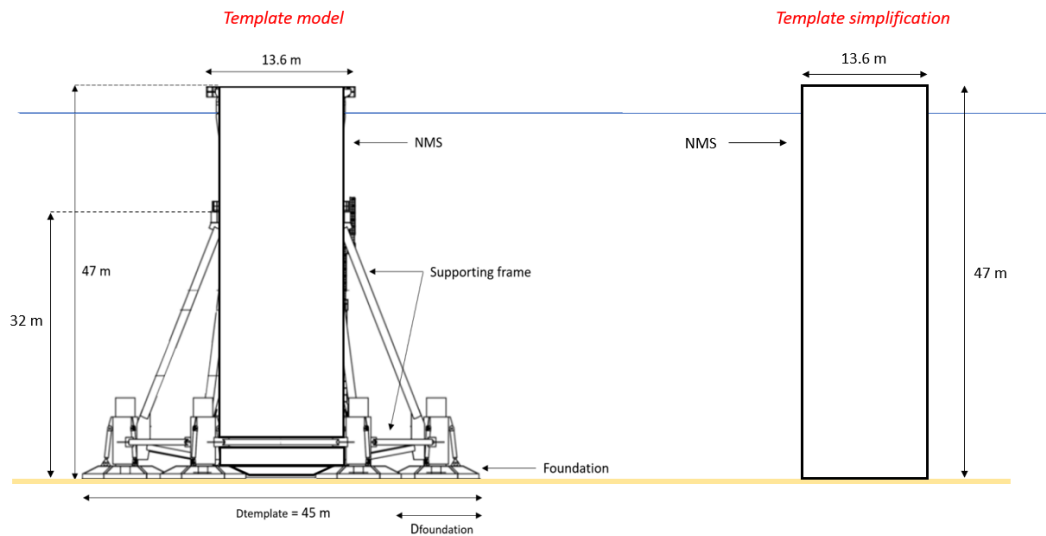


Figure 3.5: Template simplification

Section 2.4 states the theory of Morison's equation that is used to calculate the environmental loads acting on the simplified template, which assumes that the NMS can be considered as a slender structure. The NMS can only be considered as a slender structure for wavelengths $\lambda \geq 5 * D$, which corresponds to a wave period of $T \geq 6.6$ s. For wave periods $T \leq 6.6$ s, diffraction and radiation will occur. The application of Morison's equation will then result in an overestimation of the loads acting on the structure. However, the loads determined by Morison's equation are in the right order of magnitude. Therefore Morison's equation will be used since this thesis covers a preliminary design stage of the template. In a more detailed design stage also the influence of the loads acting on the supporting frame and the foundation should be taken into account.

Results of environmental loads

By means of the Morison equation and the environmental conditions stated above, the results of the hydrodynamic loads acting on the structure are stated in table 3.5 below. These are the unfactored loads that act on the template during the set down case and contingency case considered in section 3.2.1. This table provides an overview of the loads for the set down and contingency case.

Set down case		Contingency case	
H_s	2.5 m	H_s	3.0 m
H_{max}	5 m	H_{max}	6 m
T_p	4 sec	T_p	4 sec
$v_{current}$	0.7 m/s	$v_{current}$	0.9 m/s
Horizontal load	8.8 MN	Horizontal load	11.7 MN
Vertical static load	24.5 MN	Vertical static load	20.9 MN
Total overturning moment	335.1 MNm	Total overturning moment	483.2 MNm

Table 3.5: Environmental conditions and corresponding loads during set down and contingency case

The vertical load during each case is related to the corresponding weight of the template for that case. The governing vertical static load during the set down case consists of the submerged weight of the template plus the weight of the pile and hammer on the template, at a maximum inclination angle of 0.5° . See figure 3.1. If the pile and hammer would have no inclination angle, the weight would be carried by the seabed. Therefore at an inclination angle of 0.5° , the weight carried by the template is considerably small. The vertical static load during the contingency case is the weight of the template during the survival conditions, stated in table 3.1.

Considering the contribution of wind loads during monopile installation a concise estimation is made. In order to do so, the overturning moment due to the wind load is compared to the overturning moment due to wave and current loads. With the considered maximum wind velocity of $v_w = 30\text{m/s}$, this is estimated to have a contribution of less than 2% and can therefore be neglected. This simplifies the environmental loads to wave and current loads only. The wind loads are calculated as follows:

$$F_{wind} = A * 0.613v_{wind}^2 * C_d \quad (3.1)$$

where:

- A is the vertical surface area subjected to wind loading [m^2]
- v_{wind} is the wind velocity [m/s]
- C_d is the drag coefficient, stated as 1.2 for cylinders [-]

3.4. Choosing which foundation concepts to consider

The foundation techniques described in section 2.1 are a concrete GBS, a mudmat foundation and a suction bucket foundation technique. For deep pile foundations a conventional driven pile, a push-in pile and a helical pile foundation are discussed. The choice of the foundation techniques that will be developed further throughout this research are based on the limitations, assumptions and boundary conditions stated above and on basic calculations.

The concrete GBS foundation technique will not be considered further throughout this research. This is based on its material strength and a first estimation of the dimensions of a concrete GBS compared to a steel mudmat. The concrete used for Gravity Based Structures is assumed to have a unit weight of 2400 kg/m^3 [32]. For steel a unit weight of 8000 kg/m^3 is considered [32]. A large weight of the template is preferred since this is in favor for the stability of the template on the seabed. In order to obtain the same template weight without adding any extra ballast, the required volume will therefore be approximately three times as large. A larger foundation volume results in a larger buoyancy of the foundation, which is undesirable when lifting the template through the wave zone. On top of that, a steel mudmat would have a much larger strength than a concrete GBS foundation due to its material characteristics. Therefore, it can be stated that a GBS is less desirable compared to a mudmat foundation. For that reason a concrete GBS will not be developed further throughout this research.

The mentioned drilled and grouted pile foundations will not be developed throughout this research. The installation of this foundation technique is stated to be costly and is preferable for rock soils [37]. Since only sand and clay soils are considered, only the push-in pile and helical pile foundation concepts will be investigated.

Conventional pile foundations will not be considered since this would imply the usage of a driving or drilling system, which produces noise emissions. Since the NMS incorporated within the template to comply with the German governmental regulations, it would not be in line with the sustainable ambitions to reduce the noise production as much as possible.

The push-in pile and helical pile foundations can only be installed separately after the template is set down on the seabed. For these concepts the initial stability is not obtained by the pile foundations. Therefore an additional foundation technique is required to ensure the initial stability during the set down case. The additional foundation technique that will be considered for the push-in pile and helical pile foundation concepts is a suction bucket.

Development of the foundation concepts

This chapter states the development of the foundation concepts considered throughout this thesis. First the maximum compression ($F_{compression,max}$) and tension force ($F_{tension,max}$) acting on the template are determined. This is based on the environmental loads determined in section 3.3. The template should be designed to resist these loads in order to ensure stability. The design considers the dimensions in terms of diameter, length of the skirt/pile if required and the wall thickness of the suction bucket or pile. The dimensions are calculated based on the API theory stated in section 2.3. At the end of this chapter the results of the dimensions are stated for each foundation concept. The results also consider the design of the foundation concepts that are required for the pile foundation techniques to ensure initial stability during the set down case. This is required since the pile foundations can only be installed after the template is set down on the seabed. A suction bucket concept is chosen to ensure this initial stability.

4.1. Calculating required dimensions of the foundation concepts

This section provides the design of the foundation concepts that are considered throughout this thesis, based on the API foundation theory stated in section 2.3. The equations are computed in a matlab calculation model to determine the required dimensions of each foundation technique. This model iterates over the diameter and skirt or pile length of a foundation concept, based the capacity that is required to ensure stability. Figure 4.1 below shows an indication of the design of each considered foundation concept. The foundation concepts stated in the figure are not to scale, but do give a proper indication of the concept.

- Mudmat
- Suction bucket
- Push-in pile
- Helical pile

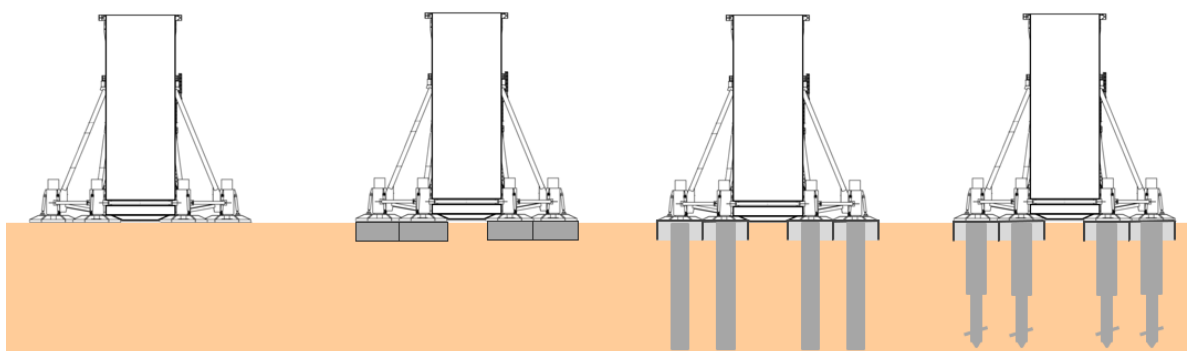


Figure 4.1: Artist impression on the foundation concepts; from left to right: Mudmat; Suction bucket; Push-in pile; Helical pile (foundation concepts are not to scale)

As stated in chapter 3 a fixed supporting frame is assumed throughout this research. The supporting frame consists of six legs connected to six identical foundations. The template configuration is depicted

in Figure 3.2 and each segment is mentioned.

The dimensions of the foundation concepts are determined based on the environmental loads stated in Table 3.5. From this the governing loads acting on a foundation leg is determined due to the environmental loads acting in horizontal direction, and the selfweight of the template acting in vertical direction. The environmental loads result in an overturning moment acting on the template and can cause sliding. Figure 4.2 below shows on the left the lateral reaction forces to the loads acting on the template. On the right the vertical reaction forces to the loads acting on the template are shown.

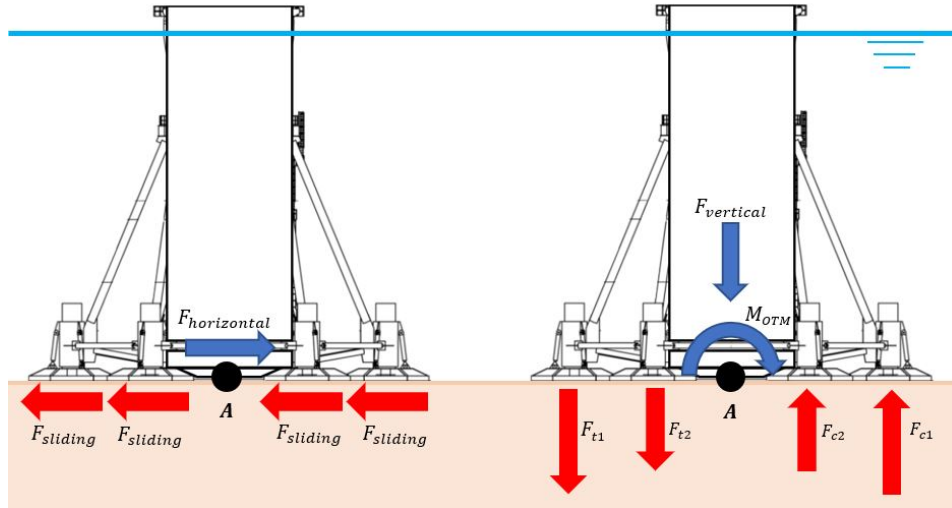


Figure 4.2: Lateral (left) and axial (right) foundation reactions due to the loads acting on the template

Moment equilibrium

The overturning moment is calculated around point A, as stated in figure 4.2. This results in tension and compression reaction forces obtained from the interaction between the template and the seabed. The equilibrium of forces due to the loads acting on the template is stated in the equations below.

Overturning moment around point A:

$$OTM = F_{c1,M} * \left(\frac{1}{2}D_{template} - \frac{1}{2}D_{foundation}\right) + 2F_{c2,M} * \left(\frac{1}{4}D_{template} - \frac{1}{2}D_{foundation}\right) - F_{t1,M} * \left(\frac{1}{2}D_{template} - \frac{1}{2}D_{foundation}\right) - 2F_{t2,M} * \left(\frac{1}{4}D_{template} - \frac{1}{2}D_{foundation}\right) \quad (4.1)$$

This results in the following equations to determine the maximum loads in compression and tension:

$$F_{tension} = \max((F_{t1,M} - F_{res,G}), (F_{t2,M} - F_{res,G})) \quad (4.2)$$

$$F_{compression} = \max((F_{c1,M} + F_{res,G}), (F_{c2,M} + F_{res,G})) \quad (4.3)$$

Where $F_{res,G}$ is the weight of the template that is carried by one foundation leg. This is considered to be $\frac{1}{6}$ th of the template self weight. Taking the loads stated in table 3.5 into account, the maximum compression and tension force resulted in $F_{compression} = 15334 \text{ kN}$ and $F_{tension} = 4595 \text{ kN}$.

Mudmat

The mudmat foundation concept obtains its stability from distributing the load over the horizontal surface area to the seabed. Since a mudmat foundation does not penetrate into the soil, the foundation capacity is only dependent on the diameter of the mudmat. On top of that, tension forces cannot occur. It is therefore assumed that the overturning moment on a mudmat foundation will only result in a compression force.

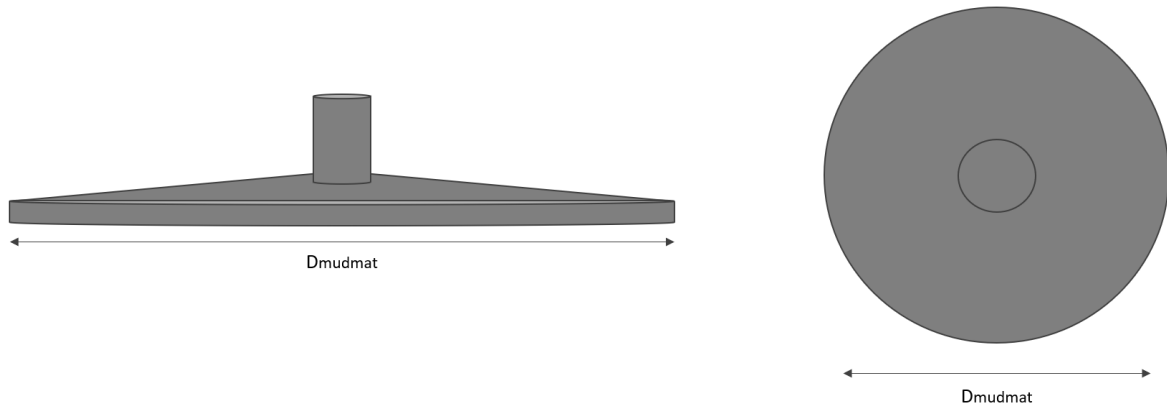


Figure 4.3: Mudmat foundation schematic drawing; side view (left) and top view (right)

Based on the loads acting on the structure the required diameter is determined for each type of seabed by means of the following equations:

Sand seabed

Vertical capacity:

$$Q'_{d,sand} = (p'_o(N_q - 1)K_q + 0.5\gamma' B' N_\gamma K_\gamma) * \frac{1}{4} \pi D_{mudmat}^2 \quad (4.4)$$

where B' is the effective width of the foundation which is considered to be the diameter of the mudmat, thus equal to D_{mudmat} .

Lateral capacity:

$$H'_{d,sand} = F_{G,TP} \tan(\phi') \quad (4.5)$$

Clay seabed

Vertical capacity:

$$Q'_{d,clay} = 6.05 s_u A \quad (4.6)$$

Lateral capacity:

$$H'_{d,clay} = s_{uo} A \quad (4.7)$$

Suction bucket

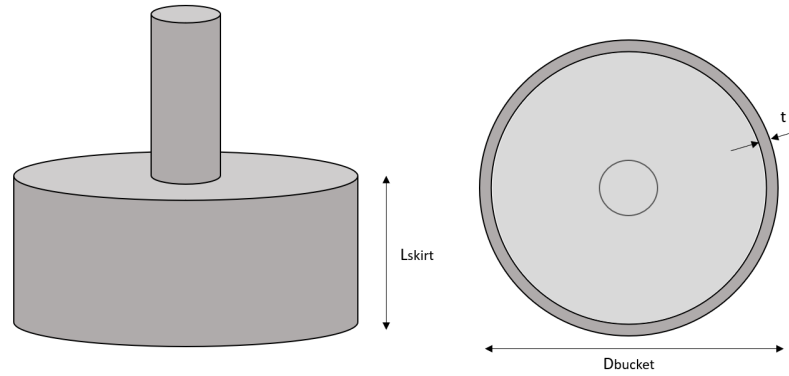


Figure 4.4: Suction bucket schematic drawing; side view (left), bottom view (right)

This section states the calculation of the minimum required diameter and skirt length of the suction bucket to ensure stability on the seabed. This is based on the maximum compression and tension forces stated previously. The diameter is iterated from 1 - 10 m and the skirt length is iterated over a length of 1 - 6 m in the calculation model. The embedment ratio limit stated in section 2.1.1 should also be taken into account. Calculation of the dimensions of the suction bucket are based on the shallow and deep foundation theory stated by API standards. This is obtained from the theory stated in section 2.3. The governing dimensions to ensure stability were obtained when considering the deep foundation theory. Therefore the dimensions of the bucket are determined based on the axial and lateral capacity due to tension and compression loads.

The equations stated above are solved in a matlab model to calculate the minimum required diameter D to ensure stability, iterating over an increasing skirt length L . The results are shown in section 4.2.

Sand seabed

Vertical capacity

The required diameter to withstand the vertical load can be determined by means of the tension and compression capacity of the suction buckets. This is determined by the skin friction and tip resistance of the bucket as follows:

$$Q_t = Q_{f,t} = f(z)A_s$$

$$Q_t = \int_0^L \pi D z f_{outside,sand}(z) dz + \int_0^L \pi (D - 2t) z f_{inside,sand}(z) dz \quad (4.8)$$

$$Q_c = Q_{f,c} + Q_p = f(z)A_s + qA_p$$

$$Q_c = \int_0^L \pi D z f_{outside,sand}(z) dz + \int_0^L \pi (D - 2t) z f_{inside,sand}(z) dz + \frac{1}{4} \pi (D^2 - (D - 2t)^2) N_q \sigma_v \quad (4.9)$$

Where L is the skirt length of the suction bucket, A_s is the vertical side surface of the skirt, t is the thickness of the skirt and σ_v is the effective unit weight at the depth of the skirt tip. It is assumed that the outside skin friction is equal to the inside skin friction [4].

Lateral capacity

The lateral capacity based on the deep foundation theory stated in equations 2.33 and 2.34 by API for a sand seabed is dependent on the skirt length, diameter and the angle of internal friction. It is calculated as follows:

$$\begin{aligned}
H'_{d,s} &= \int_0^L ((C_1 z + C_2 D) \gamma' z) dz \\
H'_{d,d} &= \int_0^L (C_3 D \gamma' z) dz \\
H'_d &= \min(H'_{d,s}, H'_{d,d})
\end{aligned} \tag{4.10}$$

The index d, s and d, d stand for the design value when shallow foundation has to be considered and for the design value when deep foundation has to be considered. The coefficients C_1, C_2 and C_3 are dependent on the angle of internal friction, and can be determined as follows:

$$\begin{aligned}
C_1 &= \frac{(\tan \beta)^2 \tan \alpha}{\tan(\beta - \phi')} + K_o * \left[\frac{\tan \phi' \sin \beta}{\cos \alpha \tan(\beta - \phi')} + \tan \beta * (\tan \phi' \sin \beta - \tan \alpha) \right] \\
C_2 &= \frac{\tan \beta}{\tan(\beta - \phi')} - K_a \\
C_3 &= K_a [(\tan \beta)^8 - 1] + K_o \tan \phi' * (\tan \beta)^4 \\
\alpha &= \frac{\phi'}{2}; \\
\beta &= 45 + \frac{\phi'}{2}; \\
K_o &= 0.4; K_a = \frac{1 - \sin \phi'}{1 + \sin \phi'}
\end{aligned}$$

Clay seabed

Vertical capacity

The determination of the vertical capacity in a clay layer is very similar to the theory when considering a sand layer. The tension capacity (Q_t) consists of the outside and inside skin friction. The compression capacity (Q_c) is the sum of the skin friction and the pile tip resistance. However, the pile tip resistance in a clay layer is determined by the undrained shear strength which is assumed constant along the depth. Therefore, increasing the skirt length will not result in an increase in skirt tip resistance. The following formula are considered:

$$\begin{aligned}
Q_t &= Q_{f,t} = f(z) A_s \\
Q_t = F_{tension} &= \int_0^L \pi D z f_{outside,sand} dz + \int_0^L \pi (D - 2t) z f_{inside,sand} dz \\
Q_c &= Q_{f,c} + Q_p = f(z) A_s + q A_p \\
Q_c = F_{compression} &= \int_0^L \pi D z f_{outside,sand} dz + \int_0^L \pi (D - 2t) z f_{inside,sand} dz + \frac{1}{4} \pi (D^2 - (D - 2t)^2) * 9c_u
\end{aligned} \tag{4.11}$$

Lateral capacity

For calculating the lateral capacity for deep foundations in an undrained situation, the following equations stated by the API are used:

$$H'_d = \int_0^L (3s_u D + \gamma' z D + J s_u z) dz \tag{4.13}$$

but is limited by:

$$H'_d = \int_0^L (9s_u D) dz \tag{4.14}$$

where:

- s_u is the ultimate resistance, units of pressure
- D is the pile outside diameter
- γ' is the submerged soil unit weight
- J is the dimensionless empirical constant, taken here as 0.25

Push-in pile

For calculating the dimensions of a deep foundation pile the axial pile capacity should be considered. The axial capacity of the pile at compression loads is determined by the sum of the inner and outer shaft resistance plus the bearing capacity at the pile tip. The axial capacity of the pile at tension loads is determined by the sum of the inner and outer shaft resistance, based on API standards [4]. A schematic overview of the pile is shown in figure 4.5 below.

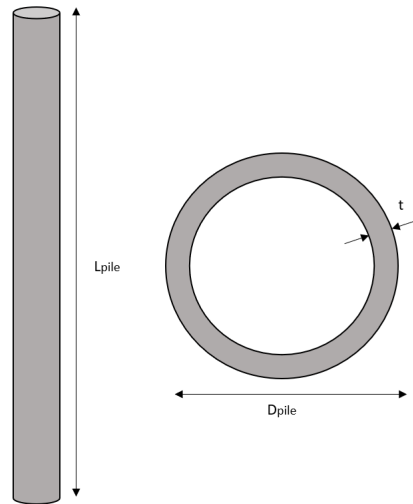


Figure 4.5: Push-in pile schematic drawing; Side view (left) and top view (right)

In order to avoid local buckling at stresses up to the yield strength of the pile material, the D/t ratio of the length of the pile should be small. The minimum wall thickness t_{min} to avoid local buckling should not be less than the values calculated by the following equation [24]:

$$t_{min} = 6.35 + \frac{D}{100} \quad (4.15)$$

It should be noted that this would be a conservative approach since this limitation is stated for piles that are to be installed by driving with sustained hard driving (820 blows/m with the largest size hammer to be used) [24]. Push-in piles will be pushed into the soil due to the weight of the opponent piles which would result in lower stresses in the pile. Therefore local buckling is less likely to occur.

The theory considered for determining the capacity and the required diameter of the push-in pile is the same as the deep foundation theory used for calculating the suction bucket dimensions. Both concepts are a steel cylinder with a certain pile length. The equations stated below are solved in a matlab model to determine the minimum required diameter D to ensure stability, when iterating over an increasing pile length. The results are shown in section 4.2.

Sand seabed

Vertical capacity

The ultimate compression capacity of a pile foundation can be determined by the skin friction of the pile and the end bearing capacity. The ultimate tension capacity of a pile foundation is determined by only the skin friction of the pile. It is known from practice that open-ended foundation piles show unplugged behavior during installation. The total skin friction is calculated by the summation of the internal and external skin friction, plus the end bearing capacity of the pile tip. This results in the following equations for calculating the capacity in compression and tension:

$$Q_t = Q_{f,t} = f(z)A_s$$

$$Q_t = \int_0^L \pi D z f_{outside,sand}(z) dz + \int_0^L \pi (D - 2t) z f_{inside,sand}(z) dz \quad (4.16)$$

$$Q_c = Q_{f,c} + Q_p = f(z)A_s + qA_p$$

$$Q_c = \int_0^L \pi D z f_{outside,sand}(z) dz + \int_0^L \pi D z f_{inside,sand}(z) dz + \frac{1}{4} \pi (D^2 - (D - 2t)^2) N_q \sigma_v \quad (4.17)$$

Inserting equations 4.16 and 4.17 in the matlab calculation model yields the minimum required diameter and pile length to ensure stability.

Lateral capacity

The lateral capacity is to be determined for shallow and deeper depths which is stated below by $H'_{d,s}$ for shallow and $H'_{d,d}$ for deep depths. Both equations have to be considered for which the smallest value should be used as the governing lateral capacity. The calculations of the coefficients C_1 , C_2 and C_3 are elaborated in section 2.3.2.

$$H'_{d,s} = \int_0^L ((C_1 z + C_2 D) \gamma' z) dz$$

$$H'_{d,d} = \int_0^L (C_3 D \gamma' z) dz \quad (4.18)$$

$$H'_d = \min(H'_{d,s}, H'_{d,d})$$

Clay seabed

Vertical capacity

The ultimate axial capacity of a pile foundation under vertical loading can be determined by the skin friction of the pile and the end bearing capacity. It is known from practice that open-ended foundation piles show unplugged behavior during installation. Therefore the total skin friction is calculated by the summation of the internal and external skin friction. The end bearing capacity acts on the pile tip annulus only. This results in the following equation:

$$Q_t = Q_{f,t} = f(z)A_s$$

$$Q_t = F_{tension} = \int_0^L \pi D z f_{outside,sand} dz + \int_0^L \pi (D - 2t) z f_{inside,sand} dz \quad (4.19)$$

$$Q_c = Q_{f,c} + Q_p = f(z)A_s + qA_p$$

$$Q_c = F_{compression} = \int_0^L \pi D z f_{outside,sand} dz + \int_0^L \pi D z f_{inside,sand} dz + \frac{1}{4} \pi (D^2 - (D - 2t)^2) * 9c_u \quad (4.20)$$

The calculation for the axial capacity for cohesive soils, such as stiff clay, is elaborated in section 2.3.2. It should be noted that the shaft friction resistance and end bearing capacity computed by the formulas above represent long-term capacities [4]. The axial capacity immediately after installation is usually lower, which should be taken into account for a template construction which is placed on the seabed for a relatively short period of time.

Lateral capacity

For lateral action on the pile in an undrained situation the standards stated by the API are used, since it considers the calculation of the lateral capacity for deep pile foundations. The same formula can be used for calculating the lateral capacity for stiff clay as for soft clay. The formula used is as follows [4]:

$$H'_d = \int_0^L (3s_u D + \gamma' L D + J s_u z) dz \quad (4.21)$$

but is limited by:

$$H'_d = \int_0^L (9s_u D) dz \quad (4.22)$$

where:

- s_u is the ultimate resistance, units of pressure
- D is the pile outside diameter
- γ' is the submerged soil unit weight
- J is the dimensionless empirical constant, taken here as 0.25

Helical pile

The helical pile consists of an upper and a lower shaft, where it is assumed that the upper shaft is two times the diameter of the lower shaft. The wall thickness is dependent on the pile diameter by the following relation $t = 6.35 + \frac{D}{100}$, in order to prevent buckling. There will be one helix present at the bottom of the bottom shaft and one at the bottom of the upper shaft. Figure 4.6 below shows a schematic overview of a helical pile.

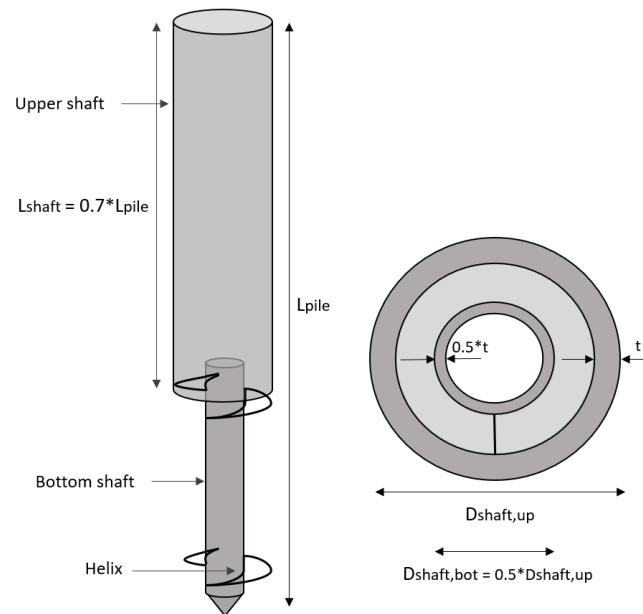


Figure 4.6: Helical pile schematic overview; side view (left), top view (right)

Calculation of the required diameter is done by means of the cylindrical shear method, stated by Mohajerani et al. (2016) [34]. For compression, the cylindrical shear method determines the axial capacity by the sum of the end bearing resistance below the bottom helix plus the skin friction of the upper shaft and the bottom shaft. For tension the top helix accounts for bearing resistance plus the sum of the skin friction of the upper shaft and the bottom shaft. It is therefore assumed that soil is entrapped in the upper shaft. The helix at the bottom shaft has the same properties as the helix at the top shaft. Figure 4.7 shows the shaft friction and bearing capacity for a compression and tension load.

The methods to determine the capacity of a helix foundation are stated by Mitsch and Clemence et al. (1985) [33] for helicals in cohesionless soils and by Mooney and Narasimha et al. (1991) [38] for piles in cohesive soils. The equations that are used in the matlab model are stated below.

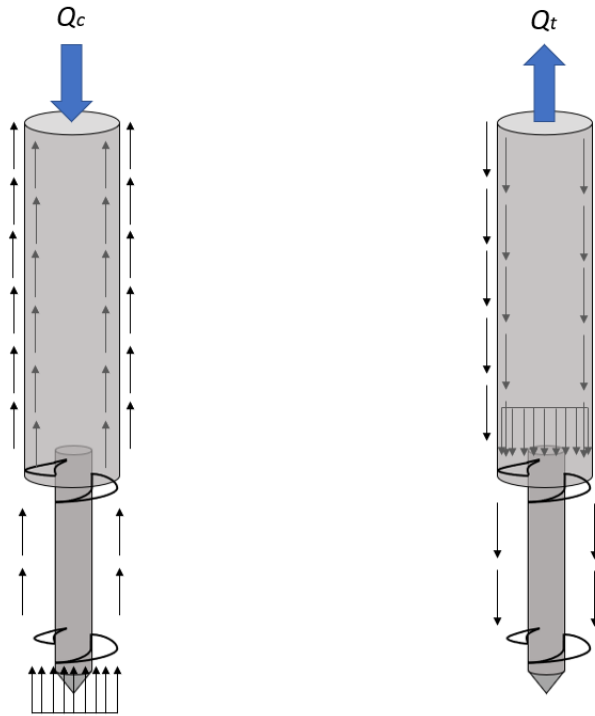


Figure 4.7: Left: Pile in compression; Right: Pile in tension

Sand seabed

Vertical loading

The equation of the cylindrical shear method to determine the ultimate compression capacity of a helical pile in a cohesionless soil is proposed by Mitsch and Clemence [33], and can be determined by the following equations for compression (Q_c) and tension (Q_t):

$$Q_c = Q_{helix} + Q_{bearing} + Q_{shaft}$$

$$Q_c = \frac{1}{2}\pi D_a \gamma' (H_b^2 - H_t^2) K_s \tan \varphi + \gamma' H A_H N_q + \frac{1}{2} P_S H_{eff}^2 \gamma' K_S \tan \phi \quad (4.23)$$

Under tension loading the equation becomes the following:

$$Q_t = Q_{helix} + Q_{bearing} + Q_{shaft}$$

$$Q_t = \frac{1}{2}\pi D_a \gamma' (H_b^2 - H_t^2) K_u \tan \varphi + \gamma' H A_H F_q^* + \frac{1}{2} P_S H_{eff}^2 \gamma' K_u \tan \varphi \quad (4.24)$$

$K_S = \frac{1 - \sin \phi}{1 + \sin \phi}$ is the active lateral earth pressure (due to compression), whereas $K_u = \frac{1 + \sin \phi}{1 - \sin \phi}$ is the passive lateral earth pressure (due to tension).

Lateral capacity

For the lateral capacity the deep foundation theory stated by the API is considered. This theory is equal to the theory used for suction buckets and push-in pile, but rewritten for the design of the helical pile. The lateral capacity is to be determined for shallow and deeper depths which is stated below by $H'_{d,s}$ for shallow and $H'_{d,d}$ for deep depths. Both equations have to be considered for which the smallest value should be used as the governing lateral capacity. The calculations of the coefficients C_1, C_2 and C_3 are elaborated in section 2.3.2.

$$\begin{aligned}
H'_{d,s} &= \int_0^{0.7L_{pile}} ((C_1 * 0.7z + C_2 D_{shaft,up}) \gamma' * 0.7z) dz + \int_{0.7L_{pile}}^{L_{pile}} ((C_1 * 0.3z + C_2 D_{shaft,bot}) \gamma' * 0.3z) dz \\
H'_{d,d} &= \int_0^{0.7L_{pile}} (C_3 * D_{shaft,up} * \gamma' * 0.7z) dz + \int_{0.7L_{pile}}^{L_{pile}} (C_3 * D_{shaft,bot} * \gamma' * 0.3z) dz \\
H'_d &= \min(H'_{d,s}, H'_{d,d})
\end{aligned} \tag{4.25}$$

Clay seabed

Vertical capacity

The ultimate compressive strength of the pile consists of the sum of the bearing strength at the tip of the pile, plus the bearing capacity obtained from the helices and the skin friction. The ultimate compression capacity in a clay seabed can be determined as follows [38]:

$$Q_c = Q_{helix} + Q_{bearing} + Q_{shaft} \tag{4.26}$$

$$Q_c = S_f(\pi D_{shaft,bot} L_c) c_u + A_H c_u N_c + \pi D_{shaft,bot} H_{eff} \alpha c_u + \pi D_{shaft,up} H_{eff} \alpha c_u + \pi D_{shaft,up} H_{eff} \alpha c_u \tag{4.27}$$

where:

S_f	spacing ratio factor
D	diameter of the pile helix
N_c	compressive bearing capacity factor for cohesive soils
d	diameter of the pile shaft
H_{eff}	effective length of the pile above the top helix
L_c	distance between top and bottom helical plates
A_H	area of the helix
α	adhesion factor

The ultimate tension capacity of a helical pile is derived similarly to the compression capacity. However, there is a difference since the soil is undisturbed by installation of the pile during compressive loading. For tension loading the soil properties of the disturbed soil will be used. The bearing capacity is increased due to the uplift bearing resistance by the top helix. This results in a contribution of the effective stress γ' times the depth of the top helix H .

$$Q_t = Q_{helix} + Q_{bearing} + Q_{shaft}$$

$$Q_c = S_f(\pi D_{shaft,bot} L_c) c_u + A_H (c_u N_c + \gamma' H) + \pi D_{shaft,bot} H_{eff} \alpha c_u + \pi D_{shaft,up} H_{eff} \alpha c_u + \pi (D_{shaft,up}) H_{eff} \alpha c_u \tag{4.28}$$

From the difference in the equation for the tensile and compressive capacity, it can be obtained that the increase in tensile capacity compared to compressive capacity is larger when the length of the shaft from seabed to top helix is increased.

Lateral capacity

For the lateral capacity the deep foundation theory stated by the API is considered. This theory is equal to the theory used for suction buckets and push-in pile, but rewritten for the design of the helical pile.

$$H'_d = \int_0^L (3s_u D_{out} + \gamma' z D_{out} + J s_u z) dz \tag{4.29}$$

but is limited by:

$$H'_d = \int_0^L (9s_u D_{out}) dz \tag{4.30}$$

where:

- s_u is the ultimate resistance, units of pressure
- D is the pile outside diameter
- γ' is the submerged soil unit weight
- J is the dimensionless empirical constant, taken here as 0.25

The calculations of the coefficients C_1 , C_2 and C_3 are elaborated in section 2.3.2. The index d, s and d, d stand for the design value when shallow foundation has to be considered and for the design value when deep foundation has to be considered.

4.2. Results of the calculation model

This section shows the results of the models used to calculate the minimum required diameter and skirt or pile length, if applicable. These dimensions are based on the governing total loads acting on the structure throughout the critical load cases, considering the homogeneous sand and clay seabed. The loads are calculated in section 3.3. In the model, the calculated compression, tension and lateral loads are kept constant. Meaning, each point on the 'Tension capacity'-line shown in the graphs below represent the same required tension capacity based on the tension load acting on the foundation. First it is determined which load shows to be governing in terms of dimensions. Then, taking the weight of each concept into account, the dimensions for each concept are determined. For the suction bucket, push-in pile and helical pile foundations each graph shows the diameter against the corresponding skirt or pile length. Within the model also the wall thickness is incorporated. For the suction bucket, the wall thickness is dependent on the diameter via the relation $t = \frac{D}{100}$. For the helical pile and push-in pile, the wall thickness is considered as: $t = 6.35 + \frac{D}{100}$ in millimeter [24]. The compression and tension capacity showed to be the governing criteria for the dimensions of the suction bucket, push-in pile and helical pile foundation concepts. Therefore the results considering the sliding capacity are not shown in order to keep a clear overview of the graphs.

Mudmat

The minimum required diameter considering a mudmat foundation on a sand or clay seabed resulted to be 14 m at each foundation leg. Since there is no penetration of a mudmat into the soil it is obtained that the governing diameter is due to instability caused by sliding.

Suction Bucket

The results for the suction bucket concept when iterating over the diameter and skirt length are shown in figure 4.8 below. On the x-axis the skirt length is ranging from 1 - 12 m and the y-axis considers the suction bucket diameter. As mentioned in section 2.1.1, the dimensions of the suction bucket should also take the embedment ratio into account in order to avoid fluidization. Therefore the upper and lower limit of the foundation embedment ratio are also included in the graphs below.

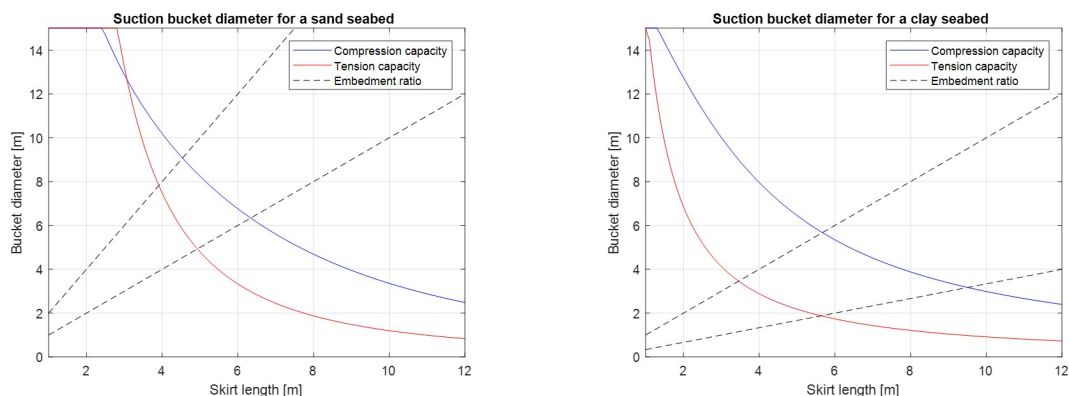


Figure 4.8: Suction bucket dimensions for sand (left) and clay (right)

For both type of seabeds the required capacity in compression is governing for the dimensions. When

taking the embedment ratio limit into account the diameter of the suction bucket foundations lie within the range stated in the table below.

	D_1 [m]	D_2 [m]	L_1 [m]	L_2 [m]
Sand seabed	9.1	6.3	4.5	6.3
Clay seabed	5.8	3.1	5.8	9.5

Table 4.1: Outer limits of the suction bucket dimensions considering the foundation embedment ratio

where:

D is the diameter of the suction bucket [m]

L is the skirt length [m]

Besides the embedment ratio limit also the maximum allowable foundation weight of 800 mT should be taken into account. Figure 4.9 below shows the diameter of the suction bucket as a function of the weight, shown for the governing compression capacity for a sand and clay seabed.

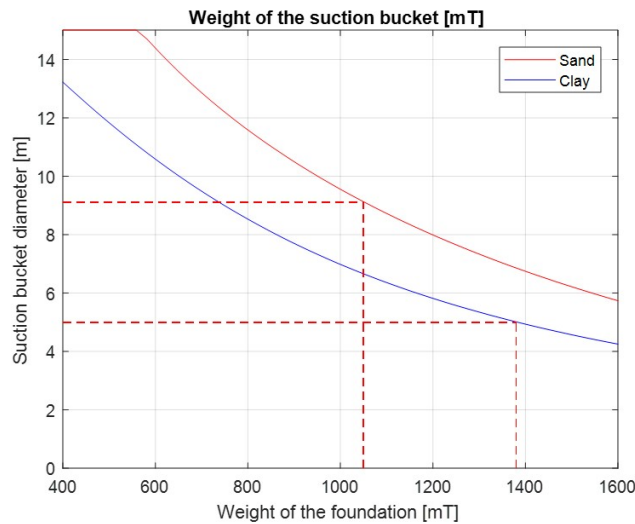


Figure 4.9: Weight of the suction bucket foundation [mT]

It can be obtained from the figure that the weight increases with a decreasing diameter. The weight limit of 800 mT is reached for a diameter of $D_{sand} = 11.7m$ and $D_{clay} = 8.5m$. However, since the embedment ratio limit stated in section 2.1.1 should be taken into account, the results of the dimensions of the suction bucket are as follows:

	D [m]	L_{skirt} [m]
Sand seabed	9.1	4.5
Clay seabed	5.0	6.4

Table 4.2: Determined dimensions of the suction bucket

These results take the embedment ratio limit into account, however the maximum weight of 800 mT is exceeded. This would result in adjustments to be made to the supporting frame in a more detailed design stage.

4.2.1. Initial stability of the pile foundation concepts

The piles of the concepts can only be installed after the template is set down on the seabed. Without these piles there is only little stability reached and failure will occur. Therefore, additional foundation concepts are required that ensure stability during the template set down phase until the piles are fully

installed. For the design of the additional foundation a suction bucket is considered. It is assumed that the environmental loads during set down and complete installation of the foundation piles is constant. This foundation should be able to ensure the overturning moment and vertical loading during the set down case, which is stated in table 3.5. This resulted in the following dimensions:

Item	Sand	Clay
Diameter [m]	8.6	5
Skirt length [m]	4.3	5.5
Weight [mT]	770	890
Wall thickness [m]	0.086	0.05

Table 4.3: Dimensions for initial stability

The dimensions are checked whether the required penetration depth due to self weight penetration is reached, due to the soil resistance and the weight of the template, excluding the pile foundations. The penetration depth is calculated as follows:

$$W_{template} > 6 * Q_c \quad (4.31)$$

where:

Q_c is the soil resistance of one leg, calculated as the sum of skin friction and pile tip resistance [kN]
 $W_{template}$ is the weight of the template [kN]

This results in the following graph that shows the soil resistance as a function of the penetration depth, for the considered clay and sand seabed.

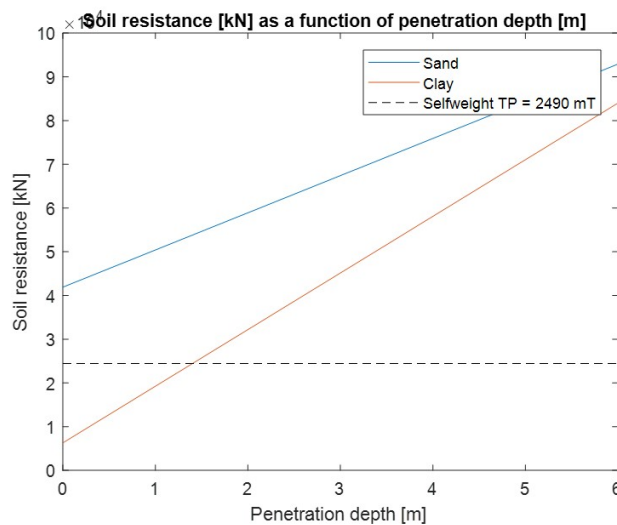


Figure 4.10: Soil resistance as a function of the penetration depth

The self weight of the template is based on the weight of the NMS, the supporting frame and the weight of the initial foundation in clay added to the concept, since this weight is governing. It can be obtained from the figure that the required penetration depth is not reached due to the self weight in a clay and sand seabed. Therefore additional suction pressure is needed to reach the required penetration depth. This leads to the additional foundation concept to be a suction bucket. The weight of the suction bucket should be taken into account when determining the weight of the pile foundations. The pile foundations need to ensure stability based on the difference in loading between the set down case and contingency case, stated in table 3.5.

Push-in Pile

The total length of the pile foundation is the sum of the skirt length of the suction bucket that is required for initial stability, plus the required pile length to ensure stability during the contingency case. This is reasonable for a clay seabed, however, for the sand seabed this results in an overestimation. As stated in section 2.2, the strength of sand increases linearly with depth. The dimensions for the pile foundations are calculated considering the piles at seabed level. Therefore, the total capacity at depth $L_{skirt} + L_{pile}$ is larger than at L_{pile} .

The graphs below show the dimensions of the push-in pile foundation with the pile length on the x-axis and the corresponding diameter on the y-axis. As mentioned in section 2.1.2 the diameter that is calculated is the overarching diameter of the four smaller pile foundations. It is shown in the figures that the compression capacity and tension capacity are both governing, depending on the chosen dimensions of the pile.

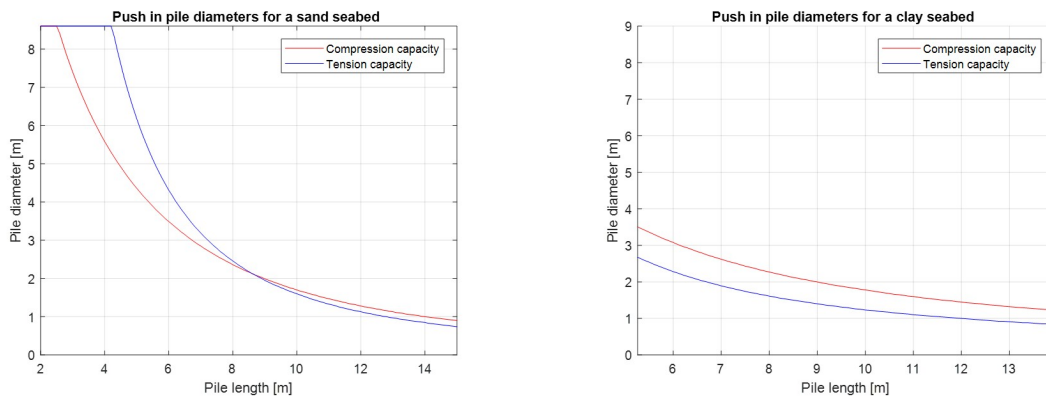


Figure 4.11: Diameter and pile length dimensions for a sand (left figure) and clay (right figure) seabed

The dimensions of the push-in pile for a sand and clay seabed are determined to be the following:

	D [m]	L_{pile} [m]
Sand seabed	3.0	7.2
Clay seabed	3.0	6.1

Table 4.4: Determined dimensions of the push-in pile

Additionally, the corresponding weight to these dimensions are calculated. This results in the following:

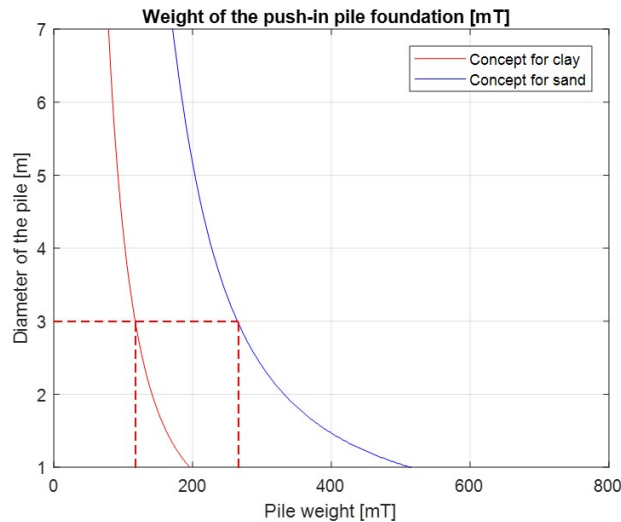


Figure 4.12: Weight of the push-in pile foundations [mT]

This results in a corresponding weight of 270 mT for the sand concept and 130 mT for the clay concept. As mentioned previously, the total length of the pile foundation is the skirt length of the suction bucket plus the length of the pile stated in table 4.4. The results for the push-in pile foundation including the suction buckets to ensure initial stability are summarized in table 4.5 below.

	Diameter [m]	Length [m]	Weight [mT]
Sand seabed			
Suction bucket	8.6	4.3	770
Push-in pile	3	11.5	550
Clay seabed			
Suction bucket	5	5.5	890
Push-in pile	3	11.6	555

Table 4.5: Dimensions of the push-in pile concepts

Helical Pile

Consequently for the helical pile foundation, the total length of the pile is the sum of the skirt length of the suction bucket plus the required pile length to ensure stability during the contingency case. The graphs below show the dimensions of the helical pile foundation with the pile length on the x-axis and the corresponding diameter on the y-axis. The diameter that is stated in the graphs below is the outer diameter of the top section of the pile. It is shown in the figures that for the sand seabed the compression capacity or tension capacity is governing, depending on the chosen dimensions of the pile.

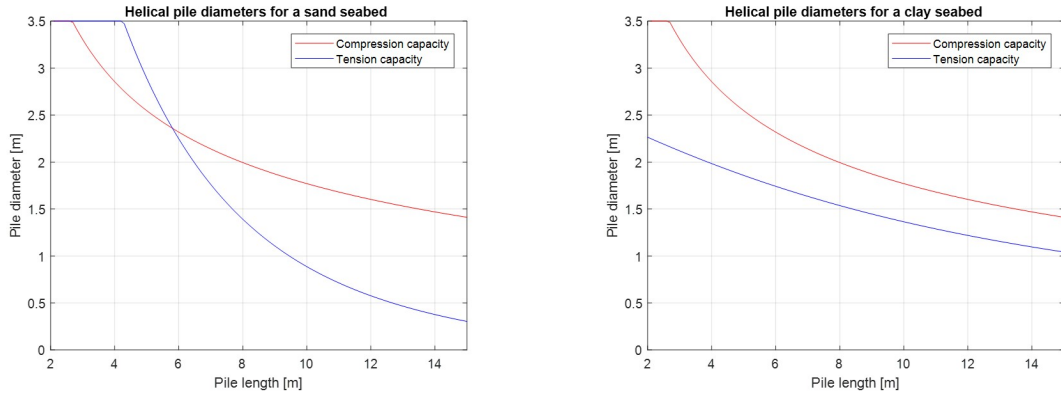


Figure 4.13: Diameter and pile length dimensions for a sand (left) and clay (right) seabed

The dimensions of the helical pile for a sand and clay seabed are determined to be the following:

	D [m]	L_{pile} [m]
Sand seabed	2.5	5.6
Clay seabed	2.5	5.2

Table 4.6: Determined dimensions of the helical pile

Additionally, the corresponding weight to these dimensions are calculated. This results in the following:

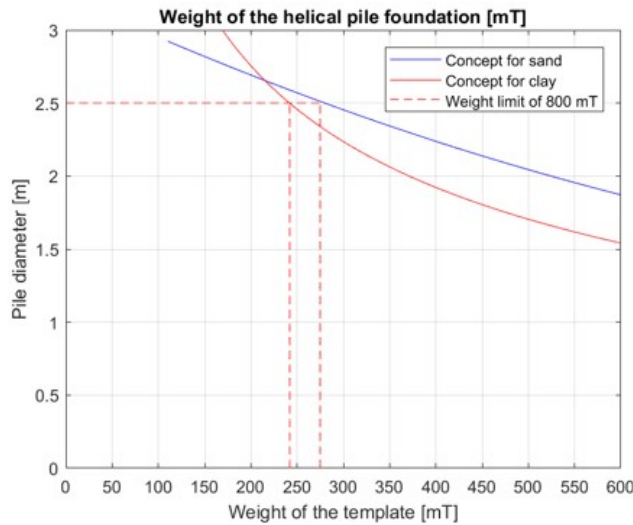


Figure 4.14: Weight of the helical pile foundations [mT]

This results in a corresponding weight of 275 mT for the sand concept and 240 mT for the clay concept. As mentioned previously, the total length of the pile foundation is the skirt length of the suction bucket plus the length of the pile stated in table 4.6. The results for the helical pile foundation including the suction buckets to ensure initial stability are summarized in table 4.5 below.

	Diameter [m]	Length [m]	Weight [mT]
Sand seabed			
Suction bucket	8.6	4.3	770
Helical pile	2.5	9.9	485
Clay seabed			
Suction bucket	5	5.5	890
Helical pile	2.5	10.7	525

Table 4.7: Dimensions of the helical pile concepts

4.2.2. Discussion

The calculated dimensions of the foundation concepts stated above is based on the environmental loads shown in table 3.5. This considers the environmental loads acting on the template during the set down case and the contingency case. The pile foundations can only be installed when the template is set down on the seabed. Hence, an additional foundation technique is required in order to ensure stability during the set down case. The results of each foundation concept is stated in table 5.3 and 5.4 below.

Foundation technique	Diameter [m]	Skirt length [m]	Wall thickness [m]	Foundation weight [mT]
Mudmat	14	-	-	800
Suction bucket	9.1	4.5	0.091	1050
Push-in pile	3	11.5	0.094	550
<i>Suction bucket</i>	8.6	4.3	0.086	770
Helical pile	2.5	9.9	0.086	485
<i>Suction bucket</i>	8.6	4.3	0.086	770

Table 4.8: Foundation dimensions of each concept for a sand seabed

Foundation technique	Diameter [m]	Skirt length [m]	Wall thickness [m]	Foundation weight [mT]
Mudmat	14	-	-	800
Suction bucket	5	6.4	0.05	1380
Push-in pile	3	11.6	0.094	555
<i>Suction bucket</i>	5	5.5	0.05	890
Helical pile	2.5	10.7	0.086	525
<i>Suction bucket</i>	5	5.5	0.05	890

Table 4.9: Foundation dimensions of each concept for a clay seabed

It should be noted that most foundation techniques exceed the weight limit of 800 mT. The influence of this increase in weight has to be determined in a more detailed design stage. This could have an effect on the design of the supporting frame, but also on the crane behavior when lifting the template through the wave zone. It should be checked whether the crane capacity is still sufficient to lift the template. Also, an increase in weight influences the dynamic behavior of the ship when lifting the template through the wave zone. Therefore the corresponding resonance period when the template is lifted by the crane should be determined for each foundation concept. Additionally, the influence of the installation method on the soil capacity is not considered here. The installation method should consider the effect of buckling of the foundation technique. This could become an important aspect when investigating the installation method of the concepts, considering the fact that 64 monopiles have to be installed by means of this template. Also the effect of adjacent pile foundations can result in an increase or decrease of the soil capacity. The reaction of the soil to the installation method and the effect of adjacent piles can be determined empirically by means of model scale tests, or theoretically by means of [31].

5

Lifting the template through the wave zone

For the installation of the template construction, the lifting operation through the wave zone until landing on the seabed is an important procedure. During this operation the template and crane hoist obtain large hydrodynamic forces. The behaviour of the template during this operation can significantly influence the performance of the full template installation sequence. This operation can generally be divided in three main phases:

- Lifting through the wave zone
- Submerged lowering operations
- Landing on seabed and retrieval

This chapter investigates the phase where each foundation concept is lifted through the wave zone. It elaborates on the hydrodynamic theory given in section 2.5 and states the boundary conditions and limitations that are considered for the hydrodynamic analysis. This theory considers the DNV simplified method and is applied to the foundation concepts developed in chapter 4. The DNV simplified method provides conservative estimates of the loads acting in vertical direction on the template during this lifting phase, due to the assumptions that are considered throughout this method [18]. These are the following:

- The horizontal extent of the lifted object is relatively small compared to the wave length.
- The vertical motion of the object follows the crane tip motion.
- The load case is dominated by the vertical relative motion between object and water - other modes of motions can be disregarded.

Section 5.7 states a discussion on what is taken into account by the assumptions made in this method and discusses aspects that are not considered. In order to determine the hydrodynamic loads acting on the template the crane-tip motions and the hydrodynamic forces are determined. First, a wave database is generated and used as an input from which the wave energy spectrum and crane tip motions can be determined. This is followed by the calculation of the hydrodynamic forces acting on the structure when lifting through the wave zone. These will be calculated for two load cases, one where the template is in air and second where the template is submerged. Based on the Dynamic Amplification Factor (DAF) limit the maximum allowable significant wave height (H_s) can be determined, which yields the operability. The operability shows the maximum allowable H_s for each corresponding peak period (T_p). In combination with the determined wave scatter diagram at the He Dreiht Wind Farm location, stated in figure 3.3, the operability of each developed concept based on the DAF-limit can be determined. The operability is the amount of time, expressed in percentage (%), for which the template can be lowered through the wave zone within the DAF-limit. Exceeding this DAF-limit can result in failure of the lifting operation. When using the DNV simplified method, only the DAF-limit is considered. Therefore only the motion in heave direction is of interest. In the last section of this chapter the applied method will be discussed.

5.1. Consideration and assumptions

5.1.1. Lifting operation

The installation of the template for the He Dreih Wind Farm project is executed by the SSCV Thialf. Therefore this vessel is considered for the hydrodynamic analysis during this thesis. The lifting operation is done by a single crane. It is assumed that the motion of the vessel is not affected by the lifting operation of the template [18]. This assumption can be made since the weight of the template is less than 1-2% of the displacement of the crane vessel. On top of that it is determined that the weight of the template hanging in the crane has little influence on the center of gravity of the Thialf. As a consequence, the template will have little influence on the behavior of the vessel. In addition it is assumed that the connection between the the crane tip and the template is a rigid connection. Hence, the motion of the template is equal to the crane tip motion. Argumentation on the validity of this assumption is stated in the discussion of this chapter, in section 5.7

Based on the hydrodynamic analysis of the initial design, it is stated that the vertical forces acting on the template are dominant when considering the operability. Based on this, only the forces in vertical direction are considered and the influence of horizontal forces are neglected. Therefore the simplified method stated by DNV [18] can be used.

5.1.2. Crane position

During the lifting operation the Thialf will be in Dynamic Positioning (DP) mode, in order to stay in the required position in terms of wave shielding. Generic specifications of the Thialf are stated in appendix A. Appendix G states an overview of the positions of interest with respect to the global origin. During the lifting operation, the position of the crane is considered to be at 135° from starboard side and has a constant crane lowering velocity of 0.1 m/s during the full lowering sequence. The crane position with respect to starboard (SB) and portside (PS) is shown in figure 5.1 below.

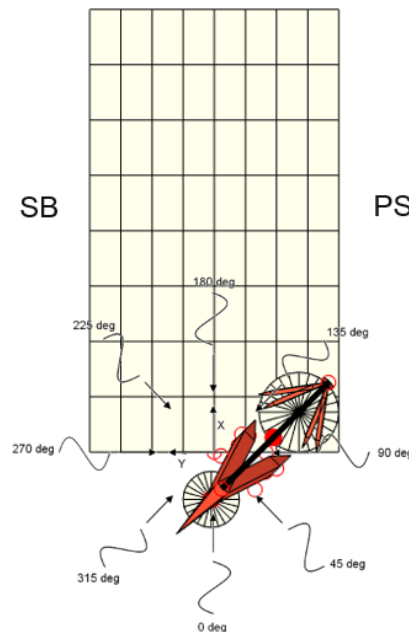


Figure 5.1: Crane position of portside (PS) crane

The position of the crane tip and the center of gravity (CoG) of the Thialf with respect to the global origin is as follows:

	x	y	z
Thialf CoG	72.530	0.000	-4.440
Crane tip main block	-28.188	12.425	118.480

Table 5.1: Position of Thialf CoG and crane tip w.r.t. global origin

5.1.3. Template position

During the lifting operation the template is hanging in the crane that is positioned as stated in table 5.1. The length of the crane hoisting system between the crane tip and the connection point of the template is approximately 48 m. The position of the CoG of the template with respect to the global origin is stated in table 5.2. This is shown in more detail in appendix G. Since the template is symmetric, the x and y position of the CoG of the template is equal to the position of the crane tip main block.

	x	y	z
Template CoG	-28.188	12.425	6.100

Table 5.2: Template CoG position w.r.t. global origin

5.1.4. Shielded and undisturbed waves

The waves are considered at an incoming wave direction of 135° . Due to the Dynamic Positioning (DP) system present at the Thialf the position relative to the incoming waves can be kept approximately constant. The Thialf can adjust its position if incoming waves are changing direction. Considering the crane tip position at an angle of 135° , the template will be partly shielded by the vessel with incoming waves at 135° . As a consequence, the height of the incoming waves will decrease when encountering the template, since the vessel absorbs energy from the incoming wave spectrum. Figure 5.2 below shows the significant wave height of an incoming unit wave of 1 meter when being undisturbed and when being shielded at 135° . Therefore this position is most preferable in terms of hydrodynamic loading on the template.

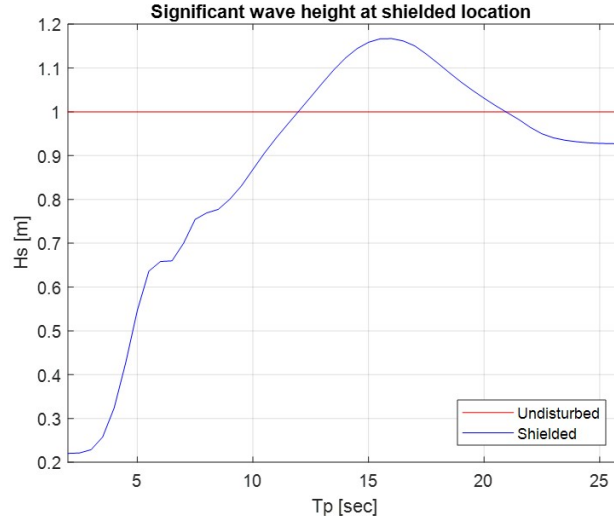


Figure 5.2: Significant wave height for an undisturbed and shielded incoming unit wave of $H_s = 1m$, with an incoming angle of 135°

It can be obtained from the figure that the energy of the incoming wave is absorbed by the Thialf for low wave periods, up to around 12 seconds. The motion of the vessel is not much affected by the incoming wave spectrum. However, at larger wave periods ranging from 12 to around 21 seconds, the wave height is increased by the presence of the Thialf. This effect is caused by radiation. The incoming waves induce a motion of the vessel, resulting in radiated waves that lead to an input of energy to the wave spectrum. For larger peak periods ($T_p > 21s$), the motion of the vessel results in energy absorption of the waves yielding a lower significant wave height at the template. However, only peak periods

ranging between 2 - 12 seconds are considered for the hydrodynamic analysis since these occur most frequently at the location of the He Dreiht Wind Farm.

5.2. Template model

The foundation of the template for each concept is simplified in order to determine the hydrodynamic forces acting on the structure. The horizontal surface area of the six legs is modelled as one large circular disc, containing skirts if applicable. Figure 5.3 below shows an overview of the template for the mudmat foundation concept, obtained from Liftodyn.

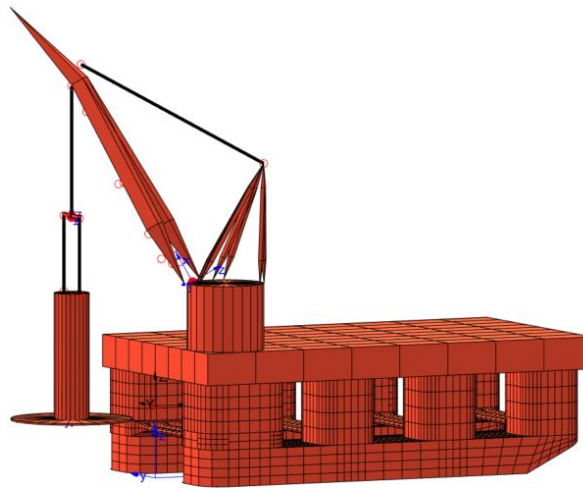


Figure 5.3: Overview of the mudmat foundation concept model during lifting

From the figure it can be observed how the mudmat foundation is modelled. For each considered concept the area of the horizontal disc is equal to the foundation area determined in chapter 4. However, when considering the foundations that include skirts, simplifying the model to one large circular disc will result in a lower force contribution than the six circular discs separately. This is since the circumference of one disc with a certain surface area is smaller than the total circumference of six smaller discs equal to this surface area. Therefore, in reality the slamming forces would have a larger contribution to the total hydrodynamic forces acting on the foundation. This is due to the influence of the skirts, resulting in an increase in slamming velocity inside the bucket.

5.3. Hydrodynamic forces acting on the template

As stated in section 2.5, the hydrodynamic forces that are considered by the DNV are the mass force, buoyancy force, drag force and slamming impact force. Figure 5.4 below shows an overview of the forces acting on the template foundation for both considered load cases described in the next section.

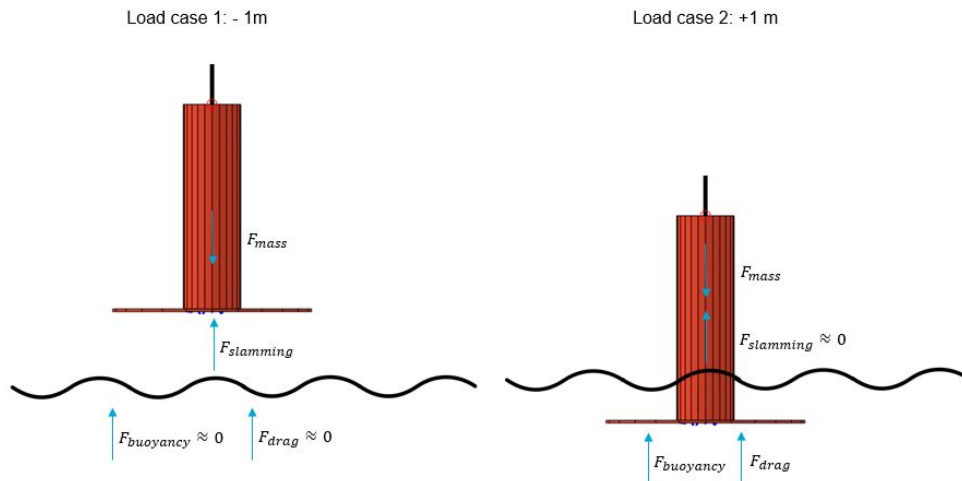


Figure 5.4: Hydrodynamic forces in vertical direction acting on the template, for both considered load cases

Load cases

In order to determine the governing hydrodynamic forces that act on the structure when lifting through the wave zone, the template is considered at two stages. To determine the hydrodynamic forces in vertical direction, the forces acting on the supporting frame and NMS are not taken into account. This is done since the horizontal surface area of the supporting frame and NMS are considerably small compared to the horizontal surface area of the foundation. Hence, the vertical loading acting on the supporting frame and NMS is negligible. The first load case considers the foundation to be in air. The second load case considers the foundation to be submerged. These stages are shown in figures 5.5 and 5.6. By calculating the hydrodynamic forces at these two stages during lowering, the operability curve of both load cases is determined. Based on this the governing operability curve is computed. The sections below state the load cases that are considered with their corresponding submergence level to the mean sea level.

The vertical position of the governing horizontal surface area of each foundation concept is chosen as reference point. This area has the largest contribution to the horizontal water plane surface area. On top of that, this surface area is different for each foundation concept and will therefore be of influence in terms of operability when lowering the foundation of the template through the wave zone.

Load case 1: +1 m

During the first load case the horizontal surface area of the foundation concept is in air and is located 1 meter above the waterline with respect to the circular disc. At this stage the slamming force that act on the surface area is present and has a large contribution to the hydrodynamic forces on the structure. For the mudmat foundation, the added mass, drag and buoyancy forces are considered to be zero since the structure is hanging completely in air since no skirts are present. For the bucket foundation concepts the structure is partly submerged. However the mass, drag and buoyancy forces are assumed to be negligible since the horizontal projected area of the skirt tips is small.

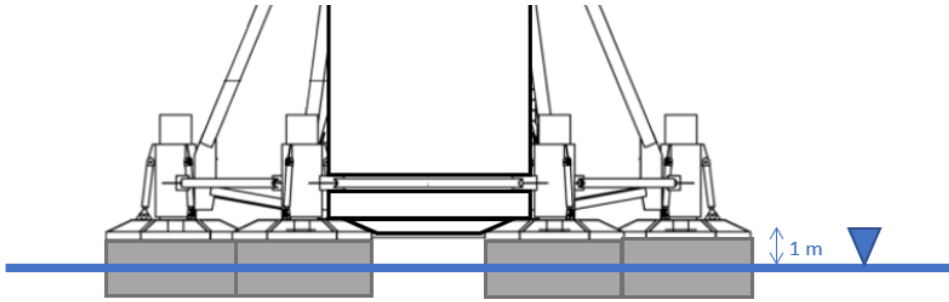


Figure 5.5: Load case 1: +1 m below waterline

Load case 2: -1 m

For the second load case the foundation concept is assumed to be fully submerged and is located 1 meter below the waterline with respect to the circular disc area. At this stage the slamming loads acting on the circular disc area are reduced to zero since the foundation concept is fully submerged. However, the added mass, drag and buoyancy force are now present and describe the hydrodynamic forces acting on the foundation.

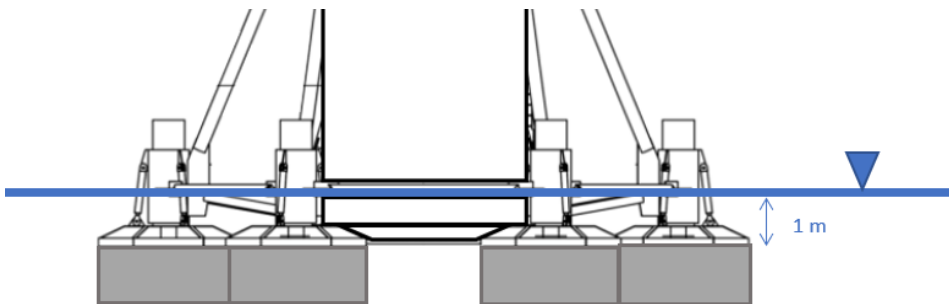


Figure 5.6: Load case 1: -1 m below waterline

5.4. Limitations and criteria

Converted dynamic amplification factor limit

The dynamic amplification factor is the ratio of the maximum amplitude of the dynamic load divided by the maximum amplitude of the static weight, stated in equation 5.1 below. It is therefore a ratio to define the dynamic effect due to sudden loading on the structure. A limit is set to the DAF in order to avoid failure of the crane, or to be conservative and to ensure a safe lifting operation. Since the static forces are constant during the lifting operation, the DAF limit limits the maximum allowable dynamic loading acting on the template. The dynamic forces considers only the hydrodynamic forces acting on the template in vertical direction.

$$DAF = \frac{|F_{dyn}(t)|}{Mg} = 1.3 \quad (5.1)$$

$$F_{dyn}(t) = Mg + F_{hydrodynamic,vertical}(t)$$

As mentioned in section 2.5, the DAF is converted to forces, resulting in a ratio of forces. The limit for which the operability in heave motion will be designed on is $DAF = 1.3$ and is stated by Heerema [8]. Based on the DAF limit and the calculated hydrodynamic forces acting on the structure the maximum allowable significant wave height H_s can be determined.

Crane capacity

The minimum required radius of the crane is determined at 44 meter with respect to the center of the crane. This radius is calculated with a minimum required clearance of 5 meter between the outer point

of the template and the outer point of the Thialf, stated by Heerema. This value corresponds to the x-position of the crane tip stated in table 5.1. It is assumed that the crane capacity corresponding to a radius of 44 meter is approximately 6700 mT.

Resonance of the hoisting system

Since the assumption is made that the template follows the crane tip motion, the connection between the template and the crane tip is assumed to be rigid. For this case, only the resonance period of the Thialf is of interest and the resonance period of the hoisting system can be neglected. However, in reality the crane connection is not a rigid connection. Therefore, the resonance period of the hoisting system is of interest and should be considered. In order to determine whether resonance of the hoisting system occurs the resonance period of the hoisting system should be determined. Resonance may be present if the crane tip oscillation period or wave period is close to the determined resonance period T_0 of the hoisting system [18]. This resonance period is determined as follows:

$$T_0 = 2\pi \sqrt{\frac{M + A_{33} + \theta * mL}{K}} \quad (5.2)$$

where

- m is the mass of hoisting line per unit length [kg/m]
- L is the length of the hoisting line [m]
- M is the mass of the template in air [kg]
- A_{33} is the heave added mass of the template [kg]
- K is the stiffness of the hoisting system [N/m]
- θ the adjustment factor taking the effect of mass of hoisting line and possible soft springs into account

The calculation of the stiffness of the hoisting system K is stated in section 2.5. The adjustment factor θ is considered zero, since the soft system is located just above the lifted object [18]. Since the mass of each developed concept is different, the resonance period of each alternative will vary. The resonance period is not taken into account by the DNV simplified method, but its effect on the operability will be discussed in section 5.7.

5.5. Software applied

The software program Liftodyn is used in order to determine the Response Amplitude Operator (RAO) of the crane tip motions of the Thialf. As mentioned in section 2.5, the RAO is a characteristic that describes the behavior of a ship under defined circumstances for each ship motion. Within Liftodyn the stiffness of the crane boom is taken into account, and determines the equations of motion of the CoG of all bodies in the model. The RAO's of the crane tip can be determined from the incoming wave spectrum. Liftodyn is an in-house developed computer code to model and solve general linear hydrodynamic problems in the frequency domain. From Liftodyn the obtained RAO's can be post-processed to a motion, velocity or acceleration RAO at any point relative to another point. By means of the RAO's the crane tip motions relative to the wave elevation of a known seastate can be determined. By means of Liftodyn the RAO's of the crane tip are determined, and afterwards post-processed in matlab.

Post-processing of the crane tip RAO's is done to calculate the assumed behavior of the crane tip when being subjected to a certain wave spectrum. Thereafter the hydrodynamic forces based acting on the template are calculated, based on the theory stated in section 2.5. Each developed concept for a sand seabed is post-processed to determine the operability, only considering the motions in heave direction. Table 5.3 below shows the results determined in chapter 4 and the corresponding added mass of each foundation concept. For the push-in pile and helical pile foundation concepts, only the subitem '*Suction bucket*' is of relevance for the operability since this is the foundation that is required to provide initial stability. The reason behind this is that the installation of the push-in pile and helical pile concept is done in multiple lifts. The first lift considers the template construction including the suction buckets that

are required to provide initial stability. The piles are separately installed after the template is set down on the seabed and initial stability is obtained.

Foundation concept	Diameter [m]	Area [m ²]	Template weight [mT]	Added mass [mT]
Mudmat	14	924	2400	8836
Suction bucket	9.1	390	2650	3344
Push-in pile	3	-	270	-
<i>Suction bucket</i>	8.6	306	2370	2597
Helical pile	2.5	-	240	-
<i>Suction bucket</i>	8.6	319	2370	2678

Table 5.3: Foundation dimensions of each concept for a sand seabed

Foundation concept	Diameter [m]	Area [m ²]	Template weight [mT]	Added mass [mT]
Mudmat	14	924	2400	8836
Suction bucket	5	117	2980	1029
Push-in pile	3	-	270	-
<i>Suction bucket</i>	5	75	2490	626
Helical pile	2.5	-	240	-
<i>Suction bucket</i>	5	88	2490	722

Table 5.4: Foundation dimensions of each concept for a clay seabed

5.6. Results

Based on the hydrodynamic analysis by means of the DNV simplified method and the Liftodyn model, the total characteristic hydrodynamic forces acting on each foundation concept is determined. This section provides the results of the static and hydrodynamic forces acting on the foundation concept for both considered load cases stated in 5.3. The static forces are constant throughout both load cases. As mentioned previously an incoming wave direction of 135° is considered. This angle is based on the reference axis shown in figure 5.1. A peak period range from 2 - 12 seconds is considered, since these are dominant at the considered He Dreiht Wind Farm location.

Static forces

The static forces of each developed concept should be taken into account when calculating the DAF. This force is constant over time for both load cases and is equal to the static weight of the template in air (in kN) that is lifted through the wave zone. Therefore, this excludes the weight of the piles for the pile foundation concepts. These are installed separately after the template is set down on the seabed. The static weight of each concept for the considered sand seabed is summarized in table 5.5 below.

Foundation concept	Static force [MN] - sand	Static force [MN] - clay
Mudmat	23.5	23.5
Suction bucket	26.0	29.2
Push-in pile	23.3	24.4
Helical pile	23.3	24.4

Table 5.5: Static forces of each developed foundation concept

Wave spectrum

First the crane tip motions as a result of the incoming wave spectrum are stated. This is followed by the relative motion, velocity and acceleration between the crane tip and the wave elevation of the incoming wave spectrum. These are independent of the type of template concept that is lifted, and follow as a result of the assumptions made by the DNV simplified method.

Crane tip motions

As a result of the dimensions and weight of the Thialf, the waves corresponding with a low peak period have only little influence on the elevation of the Thialf, and therefore also on the heave motion of the

crane tip. However, when considering larger peak periods, the wave elevation of the incoming waves does result in a heave motion of the crane tip. This can be obtained from figure 5.7 shown below. The motion of the Thialf is affected by the waves at an increasing peak period, due to an increase in wave length. However, this effect decreases when considering very large peak periods, in the range of minutes to hours. Then the motion of the Thialf is not affected by the incoming waves and the heave motion of the crane tip will also decrease.



Figure 5.7: Heave motion of the crane tip due to the incoming wave

Relative crane tip motion, velocity and acceleration

Next, the relative motion between the crane tip motion and the wave elevation is determined. This is done since the assumption is made that the heave motion of the template follows the heave motion of the crane tip [18]. In order to determine the hydrodynamic forces acting on the template the relative motion, velocity and acceleration is of interest.

The results shown below are based on a Most Probable Maximum (MPM) of 200 cycles. With a median peak period of 7 seconds, this corresponds to an incoming wave set during approximately 20 minutes. This is in the same order of magnitude of the lifting operation, since a duration of less than 30 minutes considered as stated in section 2.5).

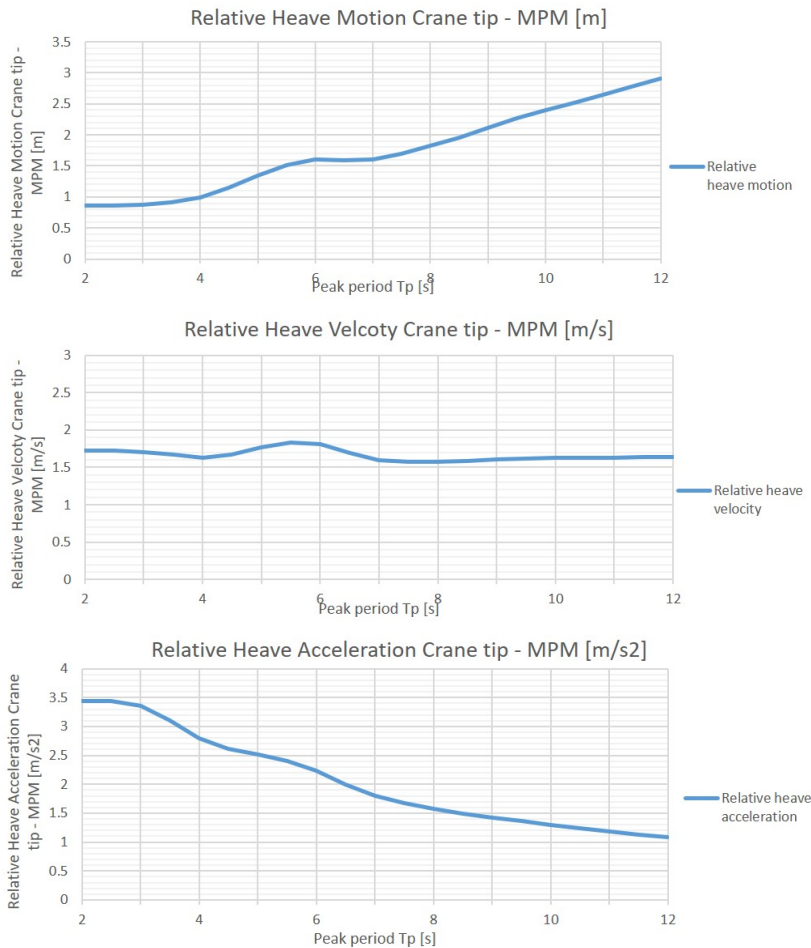


Figure 5.8: Relative heave motion, velocity and acceleration of the crane tip

It can be obtained from the figure that the relative heave acceleration between the crane tip and the wave elevation decreases with an increasing peak period. Also the acceleration of the crane tip will be in more correspondence with the wave acceleration since the Thialf will follow the motion of the waves. This results in a decrease of the relative heave acceleration between the wave elevation and the crane tip.

Based on the assumption that the heave motion of the template follows the heave motion of the crane tip, the relative heave motion, velocity and acceleration of the template are equal to what is shown in figure 5.8.

Hydrodynamic forces

With respect to the theory stated in section 2.5 and in combination with the results stated above, the characteristic total hydrodynamic forces are determined for each foundation concept. The total hydrodynamic forces are based on the mass force, buoyancy force, drag force and slamming impact force. The resulting hydrodynamic forces are dependent on the area of each foundation concept and is a function of the relative heave motion, velocity and acceleration between the template and the water particles. Below, the resulting total hydrodynamic forces are stated considering both load cases. The results are used to determine the DAF as stated in equation 5.1.

Load case 1: +1 m

The total hydrodynamic forces are determined for the considered peak periods, ranging from 2 - 12 seconds. In figure 5.10 the resulting hydrodynamic force when the template is above the waterline is determined for each developed foundation concept. Up to a peak period of approximately 5 seconds, the suction bucket foundation concept obtains the largest hydrodynamic force. This is mainly since this concept has the largest mass force, which is dependent on the added mass and the relative heave acceleration. For peak periods larger than 5 seconds, the mudmat obtains the largest loads. Considering the push-in pile and helical pile foundation concepts, the suction buckets that are added to provide initial stability are considered as stated in section 5.5. Since the dimensions are approximately equal for both concepts, the hydrodynamic forces acting on the template are also approximately equal.

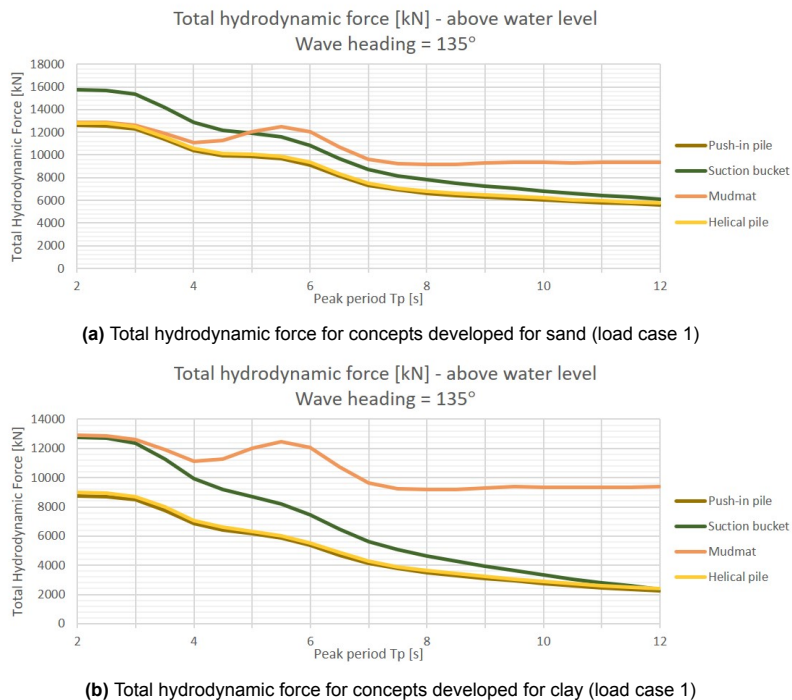


Figure 5.9: Total hydrodynamic force for each foundation concept for load case 1

Load case 2: -1 m

The second load case considers a draft of 1 meter below water level. During this case there are no slamming forces present. For each considered concept, the total hydrodynamic force decreases with an increasing peak period. From the forces acting on the template, the total mass force has the dominant contribution. The decrease in total hydrodynamic force is caused by a decreasing relative heave acceleration with an increasing peak period. The mudmat concept has the largest foundation area, and therefore also the largest added mass (see equation 2.64).

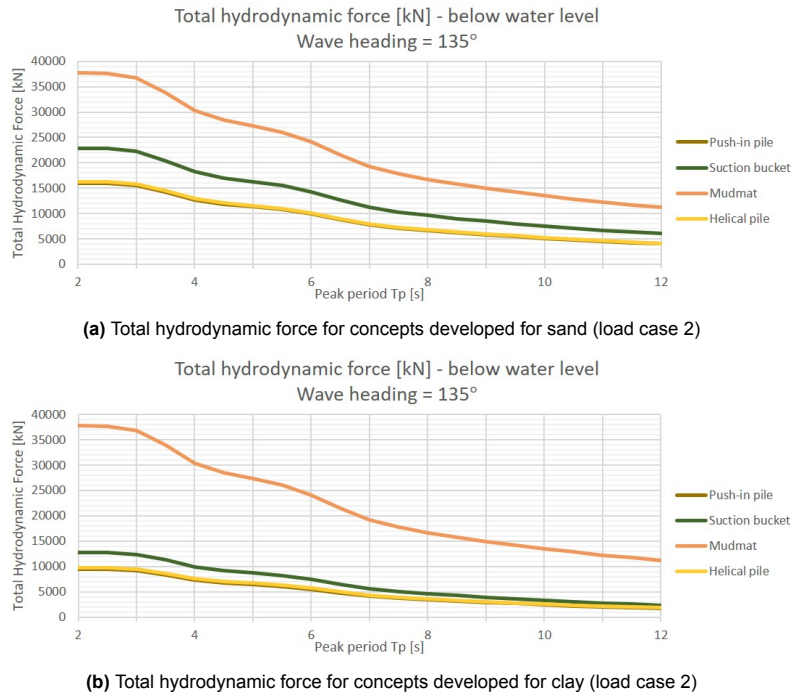


Figure 5.10: Total hydrodynamic force for each foundation concept for load case 2

Operability

Based on the results of the total hydrodynamic forces and the static forces the DAF can be determined for each developed concept and for each load case. As mentioned in section 5.4, a DAF limit of 1.3 is considered. Considering this limit the maximum allowable significant wave height can be determined, which yields the operability of each foundation concept. The figures stated below show the maximum allowable significant wave height for each load case for the foundation concepts developed for a sand seabed.

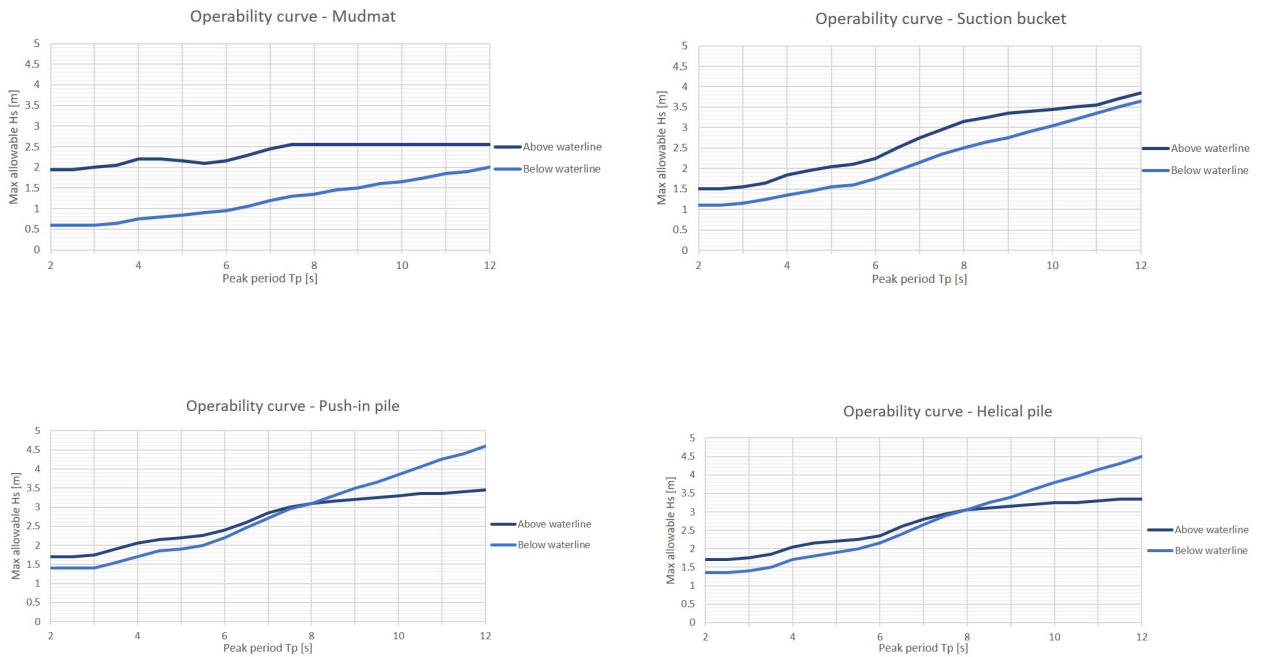


Figure 5.12: Operability curves based on a DAF limit of 1.3

The lowest maximum allowable significant wave height is the governing value when considering both load cases. For the mudmat and suction bucket concept, the load case below the waterline is shown to be governing. For the helical pile and push-in pile the load case below the waterline is governing for a peak period up to approximately 8 seconds. For peak periods from 8 up to 12 seconds the load case above the water line is governing. The maximum allowable significant wave height increases with an increasing peak period. This is caused by a decrease in hydrodynamic forces and a constant static force.

The governing operability curve of each considered foundation concept is shown in figure 5.13 below. This figure clearly shows that the mudmat foundation obtains the lowest operability when lifting through the wave zone. Meaning that for the mudmat foundation the period for waiting on weather for which the operation can be executed will be the longest.

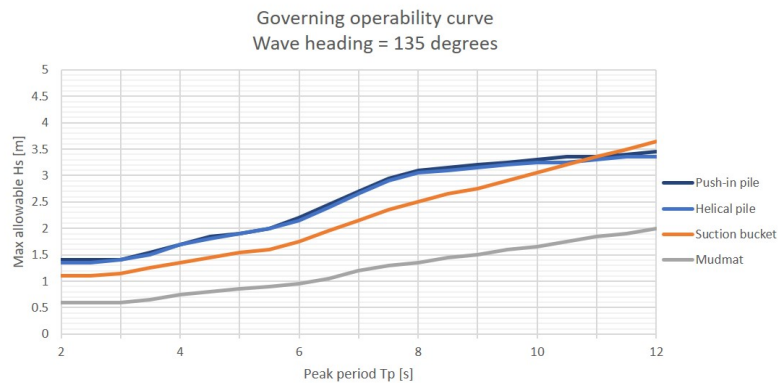


Figure 5.13: Governing operability curve for each foundation concept developed for a sand seabed

The figures stated below show the maximum allowable significant wave height for each load case for the foundation concepts developed for a clay seabed.

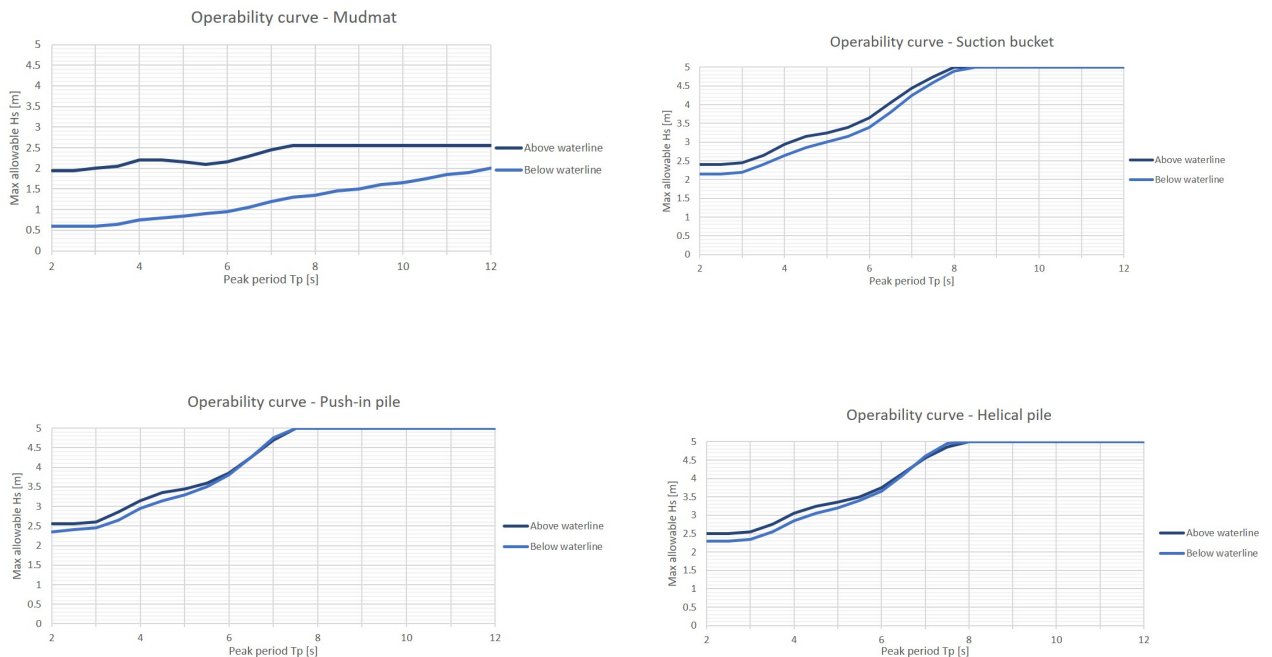


Figure 5.15: Operability curves based on a DAF limit of 1.3

The approach to determine the operability of the foundation concepts developed for a clay seabed are the same as for the concepts developed for a sand seabed. Since the dimensions of the mudmat foun-

dation concept are for both seabeds the same, the operability curve also yield the same result. For the suction bucket foundation concept, push-in pile and helical pile foundation concepts developed for a clay seabed, the operability of the load case below the waterline proved to be governing.

The results in terms of operability are shown in figure 5.16. The horizontal surface areas of the suction bucket, push-in pile and helical pile foundation concepts are much smaller. Therefore the operability is much better when only looking at the vertical forces acting in heave direction. The dimensions of the mudmat foundation concept for a clay or sand seabed are equal, as stated in section 4.2.2. Therefore the operability of the mudmat foundation concept is the same for both seabed types.

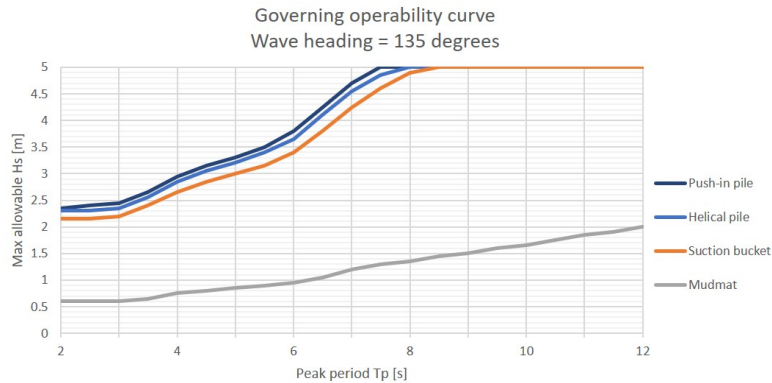


Figure 5.16: Governing operability curve for each foundation concept developed for a clay seabed

In order to determine the resulting operability of each foundation concept, the operability curves should be combined with the wave scatter diagram stated in section 3.2. This is stated in appendix F. The operability of each foundation concept is determined and resulted in the following:

Foundation concept	Operability [%] - sand concepts	Operability [%] - clay concepts
Mudmat	23.0	23.0
Suction bucket	67.2	94.0
Push-in pile	78.0	94.8
Helical pile	78.0	94.8

Table 5.6: Operability of each developed foundation concept for both type of seabeds

5.7. Discussion

This section discusses the drawbacks of the applied DNV simplified method [18]. In order to do so, the assumptions that are made will be shortly recalled. These are the following:

- The vertical motion of the object follows the crane tip motion;
- The horizontal extent of the lifted object is relatively small compared to the wave length;
- The load case is dominated by the vertical relative motion between the object and water - other modes of motions can be disregarded.

The vertical motion of the object follows the crane tip motion

This assumption considers a rigid connection between the crane tip and the template, meaning that the hoisting system is assumed to be rigid. However, in reality this is not the case. Hence, the motion of the template will not follow the exact motion of the crane tip. In order to determine if the stated assumption can be made, a realistic stiffness of the hoisting system is to be considered and should be compared to a stiff hoisting system. Based on reference material within Heerema, a spring stiffness of $K = 400 * 10^3 kN/m$ is considered as a realistic value for the hoisting system. The figure below shows the RAO of the relative distance between the template and the crane tip. The top figure shows an infinite stiffness (rigid) and the bottom figure presents a hoisting stiffness of $400 * 10^3 kN/m$.

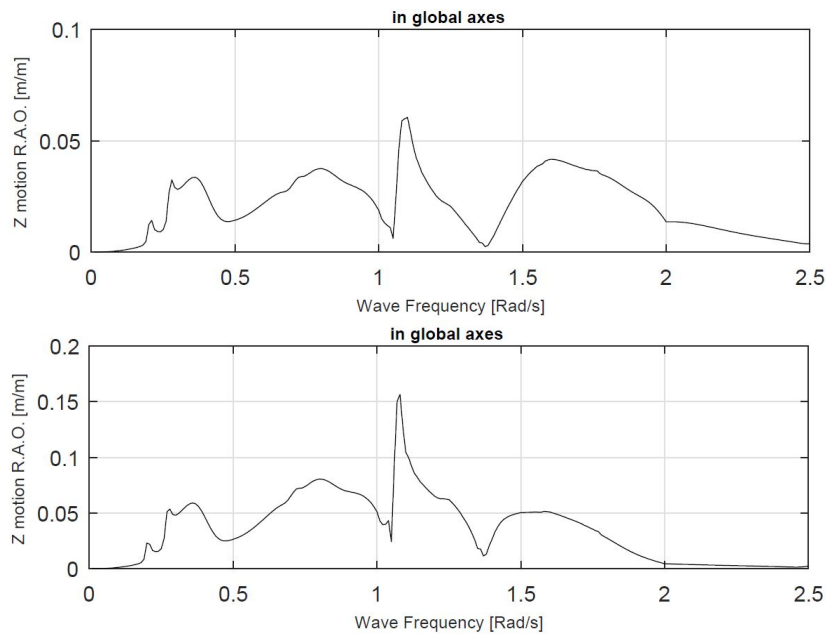


Figure 5.17: RAO of the relative distance between template and crane tip

The RAO of the relative distance between the crane tip and the template is very small for both cases. From the difference in RAO between the top figure and bottom figure, it can be obtained that the stiffness has little influence on the motion of the template. Therefore, the assumption of a rigid connection can be made when considering the stiffness of the crane hoist.

However, the influence of resonance of the hoisting system due to the template in the crane is not yet taken into consideration. By the assumption of a rigid connection, only the resonance period of the Thialf is taken into account. From figure F.3 stated in Appendix F it can be obtained that the resonance period of the Thialf is approximately 22 seconds. Wave periods of this range are not considered since they have a low occurrence frequency. In reality there is also resonance of the hoisting system due to the template hanging in the crane that should be taken into account. This is determined by equation 5.2. Resonance of the hoisting system will occur for incoming waves with a peak period equal to the resonance period. Resonance of the structure will result in higher dynamic loading and can eventually lead to failure. This should be avoided, and therefore the operability will be lower in reality. The effect of the resonance period on the operability is determined arbitrarily and is shown in figure 5.18 below. Table 5.7 states the resonance period determined for each foundation concept, determined by equation 5.2. The exact influence of the resonance period on the operability should be determined in a more detailed design stage.

	Mudmat	Suction bucket	Push-in pile	Helical pile
T_0 of developed concepts for sand [s]	7.5	5.5	5	5
T_0 of developed concepts for clay [s]	7.5	4.5	4	4

Table 5.7: Determined resonance period of each foundation concept

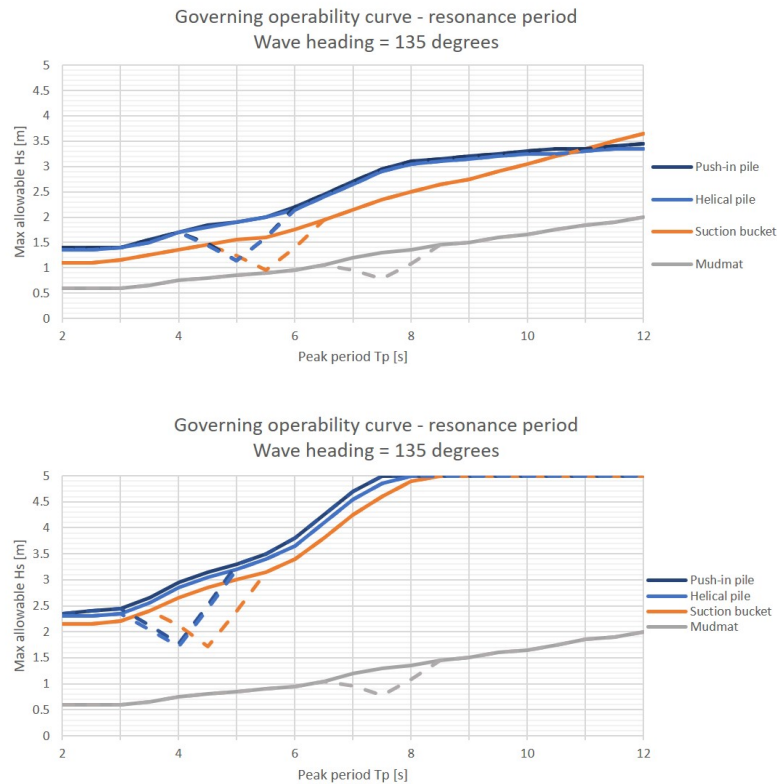


Figure 5.18: Influence of resonance period on the operability curve (arbitrarily chosen)

The horizontal extent of the lifted object is relatively small compared to the wave length

This assumption states that the vertical force acting on the horizontal surface area is equally distributed at each point of the foundation, as shown on the left in figure 5.19. In reality this is not the case, since the horizontal surface area can not be assumed small compared to the wave lengths that correspond to a peak period up to 12 seconds. This assumption does hold when considering very small wave lengths up to approximately 2 seconds. Hence, the average of the forces can be considered equal at each leg. For peak periods ranging between 2 - 12 seconds the vertical force will vary over the full horizontal extent. For a wave length of 45 meter (equal to the horizontal extend of the template) as shown on the right in figure 5.19, the template will be excited to an upward vertical force at the left side of the template. However, there is no force excited at the right side of the template since this part of the template is not submerged. As a consequence, this will result in a rotation of the template. This wave length corresponds to a wave period of 5.4 seconds and is shown in figure 5.19 below.

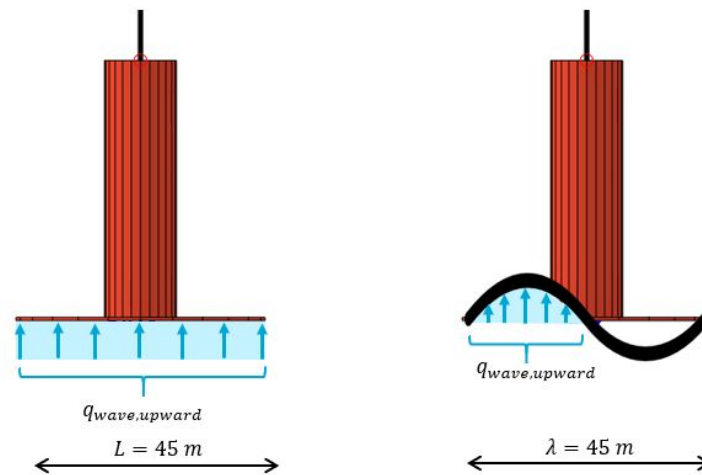


Figure 5.19: Vertical forces acting on the template; left: assumption by DNV; right: wave length of 45 m

The assumption of an equally distributed force over the full horizontal extent will result in an overestimation of the vertical hydrodynamic forces. The forces depicted in on the right in figure 5.19 will induce roll and pitch motions of the template, which is undesirable and can be a limiting criteria when determining the operability. This effect can be of importance when the horizontal extent of the lifted object is not relatively small compared to the wave length. The effect of roll and pitch motions are aggravated if this occurs during the resonance period of the system.

The load case is dominated by the vertical relative motion between the object and water

This assumption neglects the influence of the horizontal forces acting on the template. This is a reasonable assumption for the mudmat foundation concept, since the vertical surface area is small compared to the horizontal surface area. However, the behavior of the foundation concepts that include a suction bucket can significantly be influenced by the horizontal component of the hydrodynamic forces. This effect on the operability of each concept should be determined in a more detailed design stage.

Influence of soil type

Considering the operability results stated in table 6.2, it can be found that the foundation concepts developed for a clay seabed have a much better performance compared to the concepts developed for the sand seabed. The diameter for the clay concepts are much smaller due to the limitation of the embedment ratio that is incorporated. However, the operability determined here only takes the vertical forces acting on the horizontal surface area into account. As stated in the section above, the effect of the horizontal forces acting on the vertical surface area is not considered.

Validity of the results

The DNV simplified method is applied to give conservative estimates of the hydrodynamic forces acting on a structure when lifting through the wave zone. Taking all comments of the previous sections into account, the validity of the applied method to this situation can be questioned. Determining the operability of each foundation concept solely on the hydrodynamic forces acting in vertical direction is too short-sighted to compare it with reality. The hydrodynamic forces acting in horizontal direction can not be neglected since it can be assumed to influence the operability too largely. Additionally, the roll and pitch motions of the template due to the vertical forces are not accounted for. This could also affect the operability of the template in vertical direction. Nonetheless, the hydrodynamic forces that act on the template in vertical direction are considerably valid, and are presumably an overestimation of the vertical forces that will be obtained in reality. This statement is made due to the assumption that the horizontal extent is small compared to the wave length, which assumes that the force is equally distributed over the horizontal surface area. Therefore, the results are a good approximation when considering the influence of a reduction of the horizontal surface area on the operability in vertical direction. The determined operability based on the hydrodynamic forces in vertical direction should be considered as

a part of the total operability. In order to determine the total operability, a follow up study should be performed on the influence of the forces in horizontal direction. Combining these two operability curves will display a better representation of the behavior in reality.

Additionally, neglecting the influence of the resonance of the hoisting system is a questionable assumption, mainly since the resonance period corresponds to a peak period that has a great occurrence frequency. Effects such as slack-sling will presumably not occur due to the stiffness of the crane hoist and the weight of the template hanging in the crane.

A phenomena that is possible to occur for the foundation concepts that contain a suction bucket concept, is the forming of air cushions inside the bucket. This effect is formed by limited evacuation of air through the ventilation hole. The compression and collapse of air cushions when lifting the template through the wave zone are not considered in this simplified method. It is stated by DNV that this effect is likely to contribute to a reduction of the slamming force [18]. Not taking this into account is therefore a more conservative assumption.

Beside the assumptions made when using the DNV simplified method, there are also other aspects that are not taken into account at this stage. Effects of the hydrodynamic loading on the dynamics of the template structure itself are currently not considered since this thesis covers a preliminary design stage. During a more detailed design stage the effects of dynamics of the template structure due to hydrodynamic loading should be considered. This could have a significant effect on any potential damages that occur during the lifting operation.

Concept selection by means of a multi-criteria analysis

A multi-criteria analysis is performed to evaluate each developed foundation concept, and to select the most preferred concept. This is done based on the criteria stated in Table 6.1. A MCA is a frequently used tool to select or rank multiple alternatives based on a set of criteria [16]. The MCA method that is used to rank the foundation concepts is the so-called Weighted Product Model (WPM). The WPM approach is chosen since this method eliminates any units of measure. It consists of the multiplication of all criteria values to get a score. The higher the score, the better. The WPM can be described in a formula as follows:

$$\text{Total score per concept } P(A_k) = \prod_{j=1}^m (a_{Kj})^{w_j}, \text{ for } K = 1, 2, 3, \dots, m \quad (6.1)$$

where:

- j is the index
- m is the number of features
- a_{Kj} is the value of the j -th feature
- w_j is the weight of the j -th feature

6.1. Criteria for the template installation sequence

Each criterion that is considered for this MCA is ranked relative to each other as shown in table E.1 in appendix E. The weight factor of each criteria can be assigned based on this ranking. From table 6.1 below it can be obtained that the installation time and the construction costs are the most important criteria for the MCA at this conceptual level.

Criteria	Weight
Lifting operation	1
Installation time	2
Construction costs	2
Damage risk	1

Table 6.1: The considered criteria with their corresponding weight level

Lifting operation

This criterion considers the lifting operation when lifting the template through the wave zone, as determined in chapter 5. For the score of this criterion, the results of the operability stated in chapter 5 are used. That is the operability that states the amount of time the template can be lifted through the wave zone, expressed in percentage based on 24 hours. These results are stated in table 6.2 and are as follows:

Foundation concept	Lifting operation [%] - sand	Lifting operation [%] - clay
Mudmat	23.0	23.0
Suction bucket	67.2	94.0
Push-in pile	78.0	94.8
Helical pile	78.0	94.8

Table 6.2: Operability of the lifting operation of each developed foundation concept for a sand and clay seabed

Installation time

For this criterion an estimation is made on the installation time for each of the developed concepts. In correspondence with installation experts within Heerema, a basis-of-design level template installation sequence is determined for the foundation concepts developed for a sand seabed. The installation time is determined based on reference projects within Heerema and on assumptions made by experts when considering the push-in pile and helical pile foundations. The estimated installation sequence is stated in appendix D. In order to determine the installation steps and their corresponding time schedule, the installation process of the initial He Dreih template is used as a basis and is expanded for each of the concepts. Table 6.3 below shows the estimated installation time for each of the considered foundation concepts.

Concept	Installation time for sand [hr]	Installation time for clay [hr]
Mudmat	3	3
Suction bucket	6	8
Push-in pile	48	49
Helical pile	44	45

Table 6.3: Estimated installation time of each developed foundation concept

In order to be conservative, a 50 percentile (P50) range is taken into account for the estimated installation time of each template installation sequence. The P50 range takes into account that for half of the installations, the installation time will be lower than the estimated installation time and for the other half the installation time exceeds the estimated time schedule. This results in the following graph, where the error-bars show the P50 range.

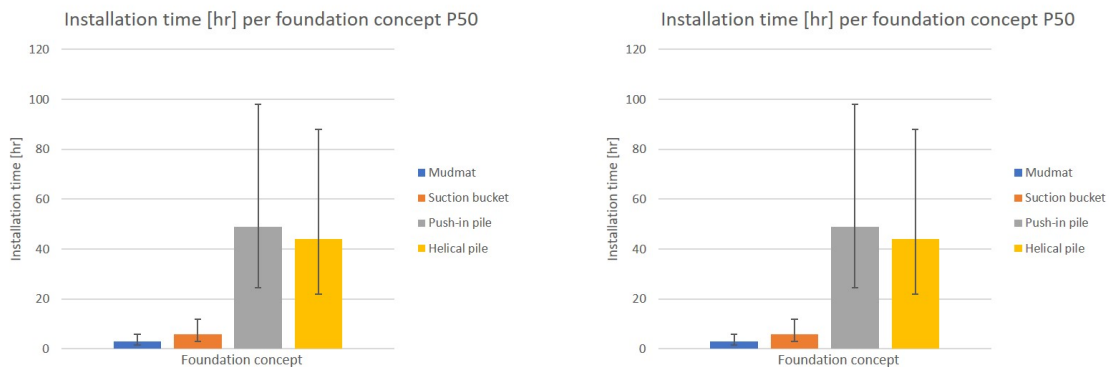


Figure 6.1: Estimated installation time based on a P50 range for concepts developed for sand (left) and for clay (right)

Construction costs

For an estimation of the construction costs of each foundation concept, a breakdown is made of the development process between procurement, engineering and the installation tools that are required. Since these are the three general aspects that sum up to the total structural costs of a foundation concept, each aspect is elaborated separately.

Considering the level of design of this research, it is estimated that class 5 should be considered stated by the AACE [25]. This class has as typical end usage a concept screening, which is of relevance

for this research. The AACE states that an expected accuracy range should be incorporated in a cost estimation and is dependent on the level of design that is considered. Class 5 considers an expected accuracy range of -50% in the most ideal situation, and +100% in the least ideal situation.

Procurement

Procurement is based on the amount of steel that is required for each foundation concept. A breakdown of the steel price is made for three aspects. These are the fabrication of the steel plate, welding of the foundation and the installation of the frame on the barge. The steel prices are dependent on the difficulty of welding and the amount of welding that is required. For example, a mudmat requires a lot more welds than a push-in pile, since a push-in pile is just a steel cylinder. These prices are estimated based on reference prices within Heerema. Hence, they are not the same prices used at Heerema but are in the same order of magnitude. Based on the determined steel price and the density of steel, this can be directly related to the weight of each foundation concept to give an estimate of the procurement costs. The results are stated in table 6.4 below.

Foundation concept	Weight [mT]	Steel price [EUR/mT]	Procurement costs [*10 ⁶ EUR]
<i>Concepts developed for a sand seabed</i>			
Mudmat	800	7400	5.9
Suction bucket	1050	6700	7.0
Push-in pile	1040	6900	7.2
Helical pile	1010	7100	7.2
<i>Concepts developed for a clay seabed</i>			
Mudmat	800	7400	5.9
Suction bucket	1380	6700	9.2
Push-in pile	1020	6900	7.0
Helical pile	1165	7100	8.3

Table 6.4: Estimated procurement costs for the concepts developed for a sand seabed

A more detailed overview of the breakdown of the procurement costs considering the steel price can be found in appendix E.

Engineering

The engineering costs of each foundation concept is assumed to be a certain percentage of the procurement costs. The amount of percentage is dependent on the type of foundation technique. Since the mudmat and suction bucket foundation have been widely used in practice, the engineering phase will take less time compared to the push-in pile and helical pile foundation concepts. The push-in pile and helical pile foundations have never been used in practice. Therefore there is no field experience available and a lot more engineering and model testing is required. The assumed percentage to determine the engineering costs is stated in the table below.

Foundation concept	Percentage [%]	Procurement costs [*10 ⁶ EUR]	Engineering costs [*10 ⁶ EUR]
<i>Concepts developed for a sand seabed</i>			
Mudmat	5	5.9	0.3
Suction bucket	5	7.0	0.4
Push-in pile	8	7.2	0.6
Helical pile	8	7.2	0.6
<i>Concepts developed for a clay seabed</i>			
Mudmat	5	5.9	0.3
Suction bucket	5	9.2	0.5
Push-in pile	8	7.0	0.6
Helical pile	8	8.3	0.7

Table 6.5: Estimated engineering costs

Tooling

Thirdly, the costs of the tooling that are required for installation of the template are considered. These costs are determined based on reference projects or by the experience of cost engineering experts. For the push-in pile and helical pile innovative and costly installation tools are required. For the push-in pile, a hydraulic tool to push the piles into the seabed is needed, and the helical piles require a tool to provide the sufficient torque to install the piles into the seabed. A figure of these tools are shown in figure 2.5 and 2.6. The estimated costs are stated in table 6.6 below.

Foundation concept	Tooling costs [$\cdot 10^6$ EUR]
Mudmat	3
Suction bucket	4
Push-in pile	11
Helical pile	17

Table 6.6: Estimated tooling costs

The table below lists the total costs including the expected accuracy range that should be taken into account. Figure 6.2 show the total costs plotted in a graph, including the expected accuracy range stated by the AACE [25].

Foundation concept	Total costs [$\cdot 10^6$ EUR]	-50% total costs [$\cdot 10^6$ EUR]	+100% total costs [$\cdot 10^6$ EUR]
<i>Concepts developed for a clay seabed</i>			
Mudmat	9	4.5	18
Suction bucket	11	5.5	22
Push-in pile	19	9.5	38
Helical pile	25	12.5	50
<i>Concepts developed for a sand seabed</i>			
Mudmat	9	4.5	18
Suction bucket	11	5.5	22
Push-in pile	19	9.5	38
Helical pile	25	12.5	50

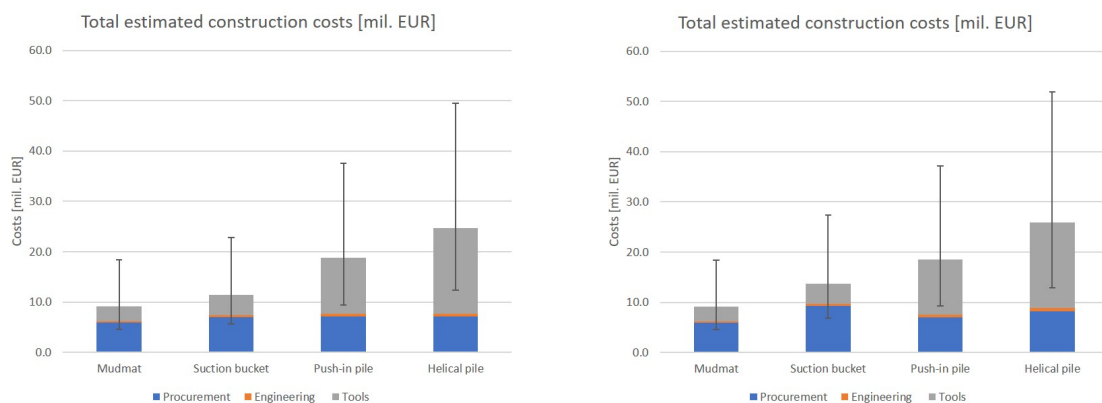


Figure 6.2: Estimated construction costs for concepts developed for sand (left) and for clay (right) including the expected accuracy range

Damage risk

The damage risk is also of importance for the evaluation of each foundation concept. If a foundation concept can easily be damaged, this can have large consequences for the total installation time of the template. However, the damage risk is hard to determine quantitatively at this level of design. Therefore a qualitative value will be assigned to each foundation concept. A minus (-) will be given if damages

are less likely to occur, and a plus (+) will be assigned if damages are prone to occur during installation. This is afterwards converted to a quantitative value between 0 - 1, where 0 is no risk and a 1 is given if damages can not be avoided. The results are shown in table 6.7 below.

Foundation concept	Damage risk
Mudmat	--
Suction bucket	-
Push-in pile	++
Helical pile	++

Table 6.7: Estimated damage risk of each foundation concept

The mudmat and suction bucket foundation concepts are concepts that have gained field experience. Therefore the weak spots of these concepts are known for which more attention can be given to. For the mudmat foundation only settlement on the seabed is required. The suction bucket can obtain damages during penetration, since the soil can always have unexpected characteristics. Considering the push-in pile and helical pile foundation concepts, no field experience is available since these concepts have not been put into practice yet. This results in a lot of uncertainties that can occur during installation. On top of that, complex tools are required for the installation of the piles into the seabed.

6.2. Results

Developed foundation concepts for a sand seabed

Figure 6.5 below show the results of the criteria for each of the considered foundation concept. The top row state the weight of each considered criteria obtained from table 6.1.

Weight	0.17	0.33	0.33	0.17
	Lifting operation [%]	Installation time [hr]	Construction costs [mil EUR]	Damage risk
Mudmat	23%	3	9	0.2
Suction bucket	67%	6	11	0.4
Push-in pile	78%	48	19	0.8
Helical pile	78%	44	25	0.8

Figure 6.3: Results of the considered criteria

However, each considered criteria has a different unit of measure. In order to be able to compare each criteria and to evaluate the results by means of the WPM, the units of measure should be eliminated. This is done by means of normalization on a scale of 0 - 1, where 0 has a negative influence and 1 has a positive influence. Afterwards the weight of each criteria has to be taken into account to determine the total score of each foundation concept. The result is stated in figure 6.6 below.

Weight	0.17	0.33	0.33	0.17	Result
	Lifting operation	Installation time	Construction costs	Damage risk	
Mudmat	● 0.29	● 1.00	● 1.00	● 1.00	0.82
Suction bucket	● 0.86	● 0.42	● 0.81	● 0.50	0.61
Push-in pile	● 1.00	● 0.05	● 0.49	● 0.25	0.24
Helical pile	● 1.00	● 0.06	● 0.37	● 0.25	0.22

Figure 6.4: Results of the MCA by means of the WPM

Developed foundation concepts for a clay seabed

The foundation concepts developed for a clay seabed have different dimensions compared to the concepts developed for a sand seabed. Different dimensions result in a different weight of each concept, hence the construction costs are different. On top of that, the estimated installation time of the suction buckets for clay is different since the length of the skirts are longer for a clay seabed. On top of that, a difference of soil type will also result in a different installation time of the suction buckets. Below the results of the MCA applied to the foundation concepts developed for a clay seabed are stated.

Weight	0.17	0.33	0.33	0.17
	Lifting operation [%]	Installation time [hr]	Construction costs [mil EUR]	Damage risk
Mudmat	23%	3	9	0.2
Suction bucket	94%	8	14	0.4
Push-in pile	95%	49	19	0.8
Helical pile	95%	45	26	0.8

Figure 6.5: Results of the considered criteria for a clay seabed

Weight	0.17	0.33	0.33	0.17	Result
	Lifting operation	Installation time	Construction costs	Damage risk	
Mudmat	● 0.24	● 1.00	● 1.00	● 1.00	0.79
Suction bucket	● 0.99	● 0.38	● 0.67	● 0.50	0.56
Push-in pile	● 1.00	● 0.06	● 0.50	● 0.25	0.25
Helical pile	● 1.00	● 0.07	● 0.36	● 0.25	0.23

Figure 6.6: Results of the MCA for a clay seabed by means of the WPM

From the results it can be obtained that the mudmat foundation concept is the most preferred option for both the sand and clay seabed, based on the considered criteria. It can be obtained that despite its low operability, the mudmat foundation scores best on the other considered criteria. The helical pile and push-in pile are the least preferred options. Although the operability is relatively large, these concepts score low on the other criteria. These concepts are costly and have a high damage risk mainly since they have not been put into practice yet. Therefore extensive research and engineering is required to ensure safe and correct installation. Considering the mudmat and suction bucket foundation concepts, less engineering is required since their weak spots are generally known based on field experience. The push-in pile and helical pile foundation concepts require a lot of time to install, since the piles can only be installed separately. Based on the stated criteria it can be concluded that the operability of the concepts do not play the governing role when determining the most preferred foundation concept for template installation.

6.3. Discussion

It is important to note that currently only one installation sequence of the template is considered. In reality, the template has to be installed multiple times and this is not taken into account. Additionally, the operational costs of the Thialf are not taken into account at this stage. For the overall execution of a project this could become an important aspect, for which the operability can become a dominant role. If the operability is low, the period for waiting on weather (WoW) is respectively long. Since multiple installations need to be executed, a long WoW period can have a large effect on the total duration of the project which can therefore result in large operational costs.

When considering the full monopile installation sequence, this includes the template installation sequence. Therefore an estimation is made on the total duration of the He Dreiht Wind Farm project. This estimation is made for each of the developed foundation concepts, based on the template installation time stated in table 6.3. The operability of each concept is taken into account for determining the waiting on weather period. It is assumed that installation of the monopile to its required penetration depth takes 4 hours. On top of that the assumption is made that the retrieval time of the template is equal to the installation time. It is considered that there are no disruptions and that each monopile installation sequence is equal for each monopile. The operability for lifting the template through the wave zone is also considered to be equal for the template retrieval. Lastly it is considered that the installation of the monopile can be performed at any environmental condition, meaning there is no waiting on weather to be considered. Based on these assumptions, an estimation is made on the duration of the installation of 64 monopiles that are considered for the He Dreiht Wind Farm project. The results are stated in table 6.9 below.

The duration of the project for each foundation concept is determined as follows:

$$T_{project} = WoW_{TP} + T_{TP,installation} + T_{MP,installation} + WoW_{TP} + T_{TP,retrieval} \quad (6.2)$$

where:

$$WoW_{TP} = operability[\%] * 24[hr] \quad (6.3)$$

$$T_{TP,installation} = T_{TP,retrieval} \quad (6.4)$$

The total estimated duration for the installation of 64 monopiles is shown in table 6.9 and figure 6.7 below. The assumption is made that the installation time of each monopile is equal and that the template installation time is as stated in table 6.3. In figure 6.7 also the 50 percentile range is included.

Foundation concept	WoW [hr]	Template installation [hr]	Project duration [days]
Mudmat	18.5	3	123
Suction bucket	7.9	6	85
Push-in pile	5.3	48	295
Helical pile	5.3	44	274

Table 6.8: Estimated duration of the installation of 64 monopiles for a sand seabed

Foundation concept	WoW [hr]	Template installation [hr]	Project duration [days]
Mudmat	18.5	3	123
Suction bucket	1.5	8	61
Push-in pile	1.3	49	273
Helical pile	1.3	45	275

Table 6.9: Estimated duration of the installation of 64 monopiles for a clay seabed

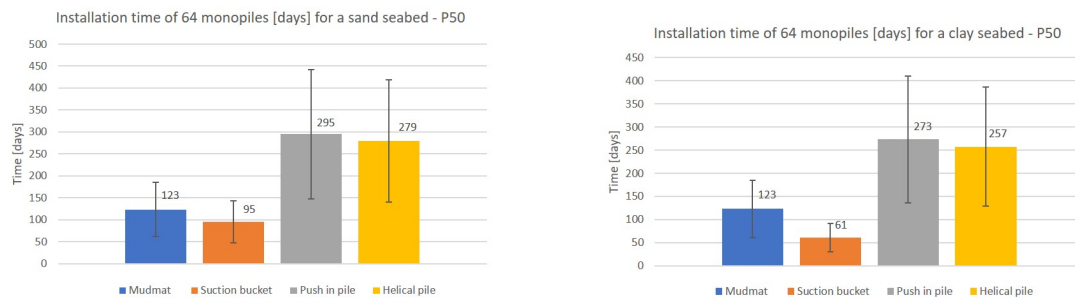


Figure 6.7: Installation time [days] of 64 monopiles for a sand and clay seabed

This shows that when looking at the total project duration, executing the project with the suction bucket foundation concept would take the least time. However, this is not accounted for since this research thesis considers the template installation sequence. Additionally, when considering the total project duration also additional criteria such as logistics and vessel costs have to be considered. On top of that, more attention should be paid to the damage sensitivity of the concepts. Additionally a more detailed estimation of the installation time and its potential risks for downtime should be determined.

Conclusion, discussion and recommendations

7.1. Conclusion

The following design statement was stated for this research thesis:

"Optimization of the installation sequence of the He Dreih Monopile Installation Template by improving the template foundation design."

To improve the template foundation design to optimize the installation sequence, a mudmat, a suction bucket, a push-in pile and a helical pile foundation technique are considered. It is shown that based on the considered foundation techniques, the mudmat foundation concept is the most optimized concept. This is regardless the considered homogeneous sand seabed or clay seabed. Despite the low performance of the operability when lifting the template through the wave zone, the performance is compensated by a quick installation time, low construction costs and a relatively low damage sensitivity of the mudmat foundation technique. Therefore, when considering the criteria stated for the performed MCA concerning the template installation sequence, this concept shows the best overall performance.

The foundation of the template is designed on three critical cases concerning the environmental loads acting on the template. The first case is when lifting the template through the wave zone. This case is considered to determine the hydrodynamic loads acting on the template in vertical direction, and is used for the hydrodynamic analysis. The second case is the template set down on the seabed. For this case it is shown that an additional foundation concept is required for the pile foundation techniques, in order to provide stability during this case. The third is the contingency case. Here the environmental conditions are extreme and monopile installation can not be executed safely. Therefore the template is left alone. However, stability on the seabed should be ensured by the template during these extreme environmental conditions. These two cases are considered for the design of the foundation in order to ensure stability.

Considering the dimensions of each developed concept, the mudmat foundation concept shows the largest horizontal surface area. The minimum required area to ensure stability is 924 m^2 , regardless the type of soil that is considered. This is caused since there is no penetration into the soil, and the stability is only obtained from the horizontal surface area. The suction bucket foundation concept resulted in a horizontal surface area of 390 m^2 for the concept developed for a sand seabed. For a clay seabed this resulted in an area of 117 m^2 . Considering the pile foundations an additional foundation is required in order to ensure stability during the set down case. This is caused since the piles can only be installed after the template is set down on the seabed. A suction bucket foundation is chosen to ensure initial stability during the set down case. This proved to be governing for the horizontal surface area for both pile foundation concepts. For the push-in pile foundation concept, this resulted in a horizontal surface area of 306 m^2 for the concept developed for a sand seabed, and 75 m^2 for a clay seabed. Considering the helical pile foundation concept, the results are 319 m^2 for a sand seabed and 88 m^2 for a clay seabed.

The hydrodynamic analysis is performed to determine the operability when lifting the template through the wave zone. This shows the lowest results for the mudmat foundation concept. Due to its large

horizontal surface area the operability is determined at 23% for both considered soil types. The suction bucket foundation concept showed to have an operability of 67% for the concept developed for a sand seabed. For a clay seabed this resulted in an operability of 94%. The push-in pile and helical pile foundation concepts show approximately the same results. These concepts show an operability of 78% for the concepts developed for a sand seabed, and 95% for the concepts developed for a clay seabed.

The effect of a low performance on operability obtained for the mudmat foundation concept is compensated by a high performance when considering the installation time, construction costs and risk for damages during the template installation sequence. The push-in pile and helical pile foundation concepts show a very low performance considering the installation time, construction costs and risk for damages. During the design of the initial foundation concept the operability was believed to play a governing role for the performance of the template installation sequence. However, it can be concluded that based on the criteria taken into account in the multi-criteria analysis, the construction costs and installation time also play a dominant role in the overall performance of the template installation sequence. The results obtained for each developed concept are summarized in Table 7.1 below.

<i>Weight criteria</i>	0.17	0.33	0.33	0.17
Concepts developed for a sand seabed				
	Operability [%]	Installation time [hr]	Construction costs [mil EUR]	Damage risk
Mudmat	23%	3	9	0.2
Suction bucket	67%	6	11	0.4
Push-in pile	78%	48	19	0.8
Helical pile	78%	44	25	0.8
Concepts developed for a clay seabed				
	Operability [%]	Installation time [hr]	Construction costs [mil EUR]	Damage risk
Mudmat	23%	3	9	0.2
Suction bucket	94%	8	14	0.4
Push-in pile	95%	49	19	0.8
Helical pile	95%	45	26	0.8

Figure 7.1: Summary of the results obtained by the multi-criteria analysis

7.2. Discussion

The discussion considers the research questions stated for this thesis to support the design statement. These are the following:

Research question 1: What is the effect of the critical cases obtained during the template installation sequence in terms of environmental loading?

As stated in the conclusions, there are three cases that can be considered critical during the template installation sequence in terms of environmental loading. The first case is obtained when lifting the template through the wave zone. This case is considered for the hydrodynamic analysis and determines the hydrodynamic loading in vertical direction acting on the foundation. The second case is the template set down case and the third case is the contingency case. Due to the template set down case, an additional foundation concept is required in order to ensure stability for the pile foundation concepts. The environmental loads acting on the template during the set down and contingency case are considered to determine the design of the foundation concepts. Therefore, the critical cases, that are inherently to the environmental conditions that are considered during these cases, can have a large effect on the design of the template. The environmental loads are based on metocean data of the He Dreiht location between March and October, from the past 40 years. In terms of environmental loading, the loads are determined by means of Morison's equation. This results in an overestimation since radiation and diffraction is not taken into account. On the other hand a simplification is made, since only the NMS is considered and the load acting on the supporting frame and foundation are neglected.

Research question 2: What are the effects of the considered seabed characteristics on the design of the template?

The effects of the seabed characteristics on the design of the foundation concepts are significant. This is mainly caused by the embedment ratio limit that is to be used for the concepts that contain a suction bucket foundation. For a sand seabed, the embedment ratio limit states a maximum diameter of 15 m to avoid fluidization. For a clay seabed the diameter is limited to a maximum of 5 m. On top of that, since the capacity of the suction bucket and pile foundations is mainly obtained by their skin resistance, different soil characteristics result in a different capacity of the foundations. The results are only determined for a homogeneous seabed layer. In reality, the seabed layers will be non-homogeneous. This could influence the design of the foundation concepts. Additionally, the embedment ratio limit also resulted in the fact that each developed foundation concept exceeded the weight limit. This limit is dependent on the considered type of seabed characteristics. Therefore adjustments to the supporting frame are required.

Research question 3: What are the advantages and disadvantages of the considered method used for the hydrodynamic analysis?

The DNV simplified method is used since it was believed that the hydrodynamic forces acting in vertical direction play the governing role for the operability during the design of the initial foundation concept. The advantage of this method is that it determines conservative values of the hydrodynamic loading acting in the vertical direction, when lifting through the wave zone. Therefore, an estimation of the difference in vertical loading between each foundation concept can be determined relatively quick. However, the main disadvantage arises when considering the foundation concepts that have a considerably large vertical surface area with respect to the horizontal surface area. This resulted to be the case for the suction bucket, push-in pile and helical pile foundation concepts. In that case, the horizontal forces acting on the foundation can also influence the operability of the foundation concepts. Since the simplified method used in this thesis only considers the hydrodynamic forces in vertical direction, only a part of the total operability is determined when lifting the template through the wave zone. On top of that, the influence of roll and pitch motions on the behavior of the template is not taken into account by the considered method. Additionally, the applied method calculates the operability results without taking influence of resonance into account. Since the determined resonance periods are in the same order of magnitude as the peak periods that occur most frequently, resonance and roll and pitch motions can

have a significant effect on the operability of the foundation concepts.

Research question 4: What are the advantages and disadvantages of the alternative foundation concepts compared to the considered conventional foundation concepts?

The push-in pile and helical pile foundation concepts are new techniques that are currently under development. The conventional techniques are the mudmat and suction bucket foundations. The main advantage of the alternative foundation concepts is the improvement in operability when lifting the template through the wave zone, caused by a smaller horizontal surface area. Since most capacity is obtained by the skin friction of the pile, the diameter can be reduced significantly. However, a large disadvantage is the installation method of both pile foundation techniques. Installing pile foundations in the seabed is a time consuming process. Additionally, field experience has proven that the actual seabed conditions are often different than expected. This results in a lot of uncertainties considering the installation time. On top of that, the pile foundations can only be installed after the template is set down on the seabed, resulting in an additional foundation technique that is required to ensure stability during the set down case.

Research question 5: Which foundation concept is preferred for optimization of the monopile template installation sequence, based on the assumptions and limitations stated throughout this thesis?

Based on the assumptions and limitations stated throughout this thesis and based on the considered foundation concepts, the mudmat foundation concept proved to be the preferred concept for optimization of the template installation sequence. It can be obtained that the operability does not play the governing role when looking at the template installation sequence. The low performance of the operability is compensated by a high performance on installation time, construction costs and risk of damages. However, this is also much dependent on the weight that is assigned to each criteria in the multi-criteria analysis.

7.3. Recommendations

For a more detailed design stage, the environmental loads acting on the template during the set down and contingency case should be determined based on a diffraction analysis. This approach would be less conservative and therefore a better approximation of the environmental loads for the design of the foundation concept can be determined. Additionally, the presence of the supporting frame and foundation should be taken into account when determining the loads acting on the template.

Throughout this research, it is considered that the template is installed with a fixed Noise Mitigation System (NMS). However, it is observed that the presence of the NMS leads to significant environmental loads during template installation. It would be interesting to perform a feasibility study on installing the template construction and NMS separately, and to research how this would effect the design of the foundation concepts.

The hydrodynamic analysis performed throughout this thesis only considers the hydrodynamic forces acting on the foundation in vertical direction. Since the suction bucket, push-in pile and helical pile foundation contain a large vertical surface area with respect to the horizontal area, the horizontal forces can have a significant influence on the operability. Therefore, the influence of the horizontal loading on the operability when lifting the template through the wave zone should be investigated for each foundation concept. On top of that, also the influence of the hydrodynamic forces on pitch and roll motions when lifting the template through the wave zone should be considered. Large pitch and roll motions of the template and crane hoist can affect the operability of the foundation concepts.

The method used for the hydrodynamic analysis neglects the effect of resonance. However, it is obtained that the resonance period of each foundation concepts is in the same range as the peak periods that occur most frequently. Therefore, the influence of resonance on the operability of each foundation technique should be researched. This could have a significant influence on the operability of each developed foundation concept.

This research is focused on the performance of the template installation sequence. However, this is only a part of the total project execution. It is also interesting to determine which foundation concept is preferred when considering the total project duration. In order to do so, an extensive risk assessment should be performed on the uncertainties considering installation and potential damage risks. Also aspects considering logistics should be taken into account. This is not considered throughout this research, but should be considered when looking into the total duration of the project execution.

This research considers the design of a structure that is installed on the seabed temporarily. It is therefore sufficient to use foundation techniques that can be installed and retrieved in a relatively short period. This is not the case for the push-in pile and helical pile foundation concepts. For permanent structures, the installation time on the seabed might play a less dominant roll for the overall performance of a foundation concept. It is recommended to perform a feasibility study on using the push-in pile and helical pile foundation concepts as a foundation for permanent structures, to study its potential.

It is interesting to investigate the application of the push-in pile and helical pile foundation concepts for the execution of projects outside of the operational months. During these months, concepts as a mud-mat and suction bucket might not be a cost effective solution. Since the performance on operability of the push-in pile and helical pile foundation techniques are high, these techniques challenge the status quo when considering the execution of projects outside of the operational months. On top of that, there is less competitiveness from other companies which could make it a more cost-effective solution.

References

- [1] Acteon. *Mudmat foundation - pre piling template*. 2020. URL: <https://acteon.com/products-services/pre-piling-templates/>.
- [2] C. Andrey et al. *Offshore renewable energy and grids*. 2021.
- [3] Selim Altun, Burakahmet Göktepe, and Alper Sezer. "Relationships between shape characteristics and shear strength of sands". In: *Soils and foundations* 51.5 (2011), pp. 857–871.
- [4] American Petroleum Institute API. "Geotechnical and Foundation Design Considerations". In: *API* 1 (2011), p. 120.
- [5] Muhammad Arshad and Brendan C O'Kelly. "Analysis and design of monopile foundations for offshore wind-turbine structures". In: *Marine Georesources & Geotechnology* 34.6 (2016), pp. 503–525.
- [6] Alan James Bond, DW Hight, and RJ Jardine. "Design of Piles in Sand in the UK Sector of the North Sea". In: (1997).
- [7] Zhang Chao et al. "Dynamic amplification factors for a system with multiple-degrees-of-freedom". In: *Earthquake Engineering and Engineering Vibration* 19.2 (2020), pp. 363–375.
- [8] Heerema Marine Contractors. "Functional specification He Dreih Monopile Template". In: (2022).
- [9] A. Bogerd Cost Engineering Consultancy. *Investment cost of offshore wind energy*. URL: https://www.costengineering.eu/images/papers/Wind_Energy.pdf.
- [10] White David and Cassidy Mark. *Offshore Geotechnical Engineering: Mark Randolph and Susan Gourvenec*. 2017.
- [11] Bas van Dijk. "Design of suction foundations". In: *Journal of Zhejiang University-SCIENCE A* 19.8 (2018), pp. 579–599.
- [12] J.A. Focht and L.M. Kraft. "Axial Performance and Capacity of Piles". In: *Planning and Design of Fixed Offshore Platforms* (1986), pp. 763–800.
- [13] Sif Offshore Foundations. *Company Profile*. 2021.
- [14] DNV GL. "DNVGL-RP-C205". In: *Recommended Practice—Environmental Conditions and Environmental Loads* (2017).
- [15] DNV GL. "DNVGL-ST-N001 - Marine operations and marine warranty". In: (2020).
- [16] IGI Global. *What is Multi-Criteria Analysis*. URL: <https://www.igi-global.com/dictionary/multi-criteria-analysis/40115>.
- [17] Datis Export Group. *Troll A Platform*. 2020. URL: <https://datis-inc.com/blog/troll-a-platform/>.
- [18] DNVGL Group et al. *DNVGL-RP-N103 - Modelling and analysis of marine operations*. 2017.
- [19] J Brinch Hansen. "A revised and extended formula for bearing capacity". In: (1970).
- [20] K.W. Hermans. *Future XL monopile foundation design for a 10 MW wind turbine in deep water*. 2016.
- [21] Leo H Holthuijsen. *Waves in oceanic and coastal waters*. Cambridge university press, 2010.
- [22] Guy T Houlby and Byron W Byrne. "Design procedures for installation of suction caissons in clay and other materials". In: *Proceedings of the Institution of Civil Engineers-Geotechnical Engineering* 158.2 (2005), pp. 75–82.
- [23] M Huisman. "Silent foundation concept: helical piles for skirt and pre-piled jacket foundations". In: *ISSPEA 2019* (2019), p. 117.
- [24] American Petroleum Institute. "API RP 2A-WSD standard". In: 22nd (2014).

- [25] AACE International. "Cost Estimate Classification System (SAMPLE)". In: (2020).
- [26] IQIP. *Offshore Product Overview*. 2022.
- [27] ISO ISO. "19901-4, Petroleum and natural gas industries—specific requirements for offshore structures—Part 4". In: *Geotechnical and foundation design considerations* (2016).
- [28] Johan MJ Journée and WW Massie. *Offshore hydromechanics*. Vol. 1. Delft University of Technology Delft, 2001.
- [29] Dan Kallehave et al. "Optimization of monopiles for offshore wind turbines". In: *Philosophical Transactions of the Royal Society A: Mathematical, Physical and Engineering Sciences* 373.2035 (2015), p. 20140100.
- [30] O Kjekstad and T Lunne. "Soil parameters used for design of gravity platforms in the North Sea". In: *Applied Ocean Research* 3.2 (1981), pp. 50–58.
- [31] Leland M Kraft Jr, John A Focht Jr, and Srinath F Amerasinghe. "Friction capacity of piles driven into clay". In: *Journal of the Geotechnical Engineering Division* 107.11 (1981), pp. 1521–1541.
- [32] Margaret Manion. "McGraw-Hill encyclopedia of science and technology". In: *Reference & user services quarterly* 42.2 (2002), p. 178.
- [33] Mark P Mitsch and Samuel P Clemence. "UPLIFT CAPACITY OF HELIX ANCHORS IN SAND." In: *Unknown Host Publication Title*. American Society of Civil Engineers (ASCE), 1985, pp. 26–47.
- [34] Abbas Mohajerani, Dusan Bosnjak, and Damon Bromwich. "Analysis and design methods of screw piles: A review". In: *Soils and Foundations* 56.1 (2016), pp. 115–128.
- [35] Jeom Kee Paik and Anil Kumar Thayamballi. *Ship-shaped offshore installations: design, building, and operation*. Cambridge University Press, 2007.
- [36] Lizer Ramirez, Daniel Fraile, and Guy Brindley. "Offshore wind in Europe: Key trends and statistics 2019". In: (2020).
- [37] M. Randolph and S. Gourvenec. *Offshore Geotechnical Engineering*. Taylor Francis, 2011.
- [38] S Narasimha Rao and YVSN Prasad. "Estimation of uplift capacity of helical anchors in clays". In: *Journal of Geotechnical Engineering* 119.2 (1993), pp. 352–357.
- [39] J Van Der Tempel et al. "Offshore environmental loads and wind turbine design: impact of wind, wave, currents and ice". In: *Wind Energy Systems*. Elsevier, 2011, pp. 463–478.
- [40] Det Norske Veritas. *DNV Classification Notes no. 30.4*. 1992.
- [41] Arnold Verruijt and Stefan van Baars. *Grondmechanica*. VSSD, 2005.
- [42] JH Vugts and K van Zandwijk. *Handbook of Bottom Founded Offshore Structures*. 2001.
- [43] Offshore WIND. *Beyond XXL - Slim Monopiles for Deep-Water Wind Farms*. 2020. URL: <https://www.offshorewind.biz/2020/05/11/beyond-xxl-slim-monopiles-for-deep-water-wind-farms/>.
- [44] R Young. *Soil properties and behaviour, p2*. Vol. 5. Elsevier, 2012.
- [45] TKI Wind Op Zee. *(Inter)national discussion on underwater noise; regulation of underwater noise caused by pile driving in the Netherlands*. 2014.
- [46] Puyang Zhang et al. "Dynamic characteristics analysis of three-bucket jacket foundation lowering through the splash zone". In: *Renewable Energy* 199 (2022), pp. 1116–1132.

List of Figures

1.1	Components of an offshore wind turbine with a monopile foundation [5]	2
1.2	Location of the He Dreiht Wind Farm	3
1.3	Initial template concept design	3
1.4	Monopile installation by means of a template construction	5
1.5	Critical cases during template installation in terms of environmental loads	6
2.1	Left: Gravity Based; Middle: Monopile foundation; Right: Suction bucket [29]	10
2.2	Concrete Gravity Based Structure (Troll A platform) [17]	10
2.3	Mudmat foundation [1]	11
2.4	Jacket structure with a suction bucket foundation [42]	12
2.5	Push-in pile foundation including hydraulic installation tool	13
2.6	Artist impression of the helical pile (left) and torque tool (right)	13
2.7	Non-linear elastic stress-strain relation under linear increased loading	14
2.8	Example of a non-cohesive soil structure (left) and a cohesive soil structure (right)	15
2.9	Left: bearing failure; middle: sliding failure; right: overturning failure [42]	16
2.10	Bearing failure of a shallow foundation under symmetrical vertical loading [42]	17
2.11	Shear failure of a shallow foundation due to overturning loading	18
2.12	Failure modes due to sliding	19
2.13	Envelope of the ultimate capacity under undrained conditions [4]	21
2.14	Envelope of the ultimate capacity under drained conditions [4]	22
2.15	Resistance components of axial capacity in compression (left) and tension (right) [4]	24
2.16	Failure shapes of deep foundation under vertical action for non-cohesive (left) and cohesive soils (right) [42]	27
2.17	Coefficients C1, C2 and C3 as a function of the internal friction ϕ' [4]	28
2.18	Environmental load distribution acting on the template	32
2.19	Relation between motions and waves [28]	33
2.20	JONSWAP and Pierson-Moskovitz wave spectrum	34
2.21	Added mass of a three-dimensional circular disc	38
3.1	Template construction and properties	40
3.2	Template configuration case study showing top view (left) and side view (right)	41
3.3	Wave scatter diagram of the He Dreiht Wind Farm location (based on operational months of 1979-2020)	42
3.4	Wave load directions, horizontal (left) and diagonal (right)	44
3.5	Template simplification	45
4.1	Artist impression on the foundation concepts; from left to right: Mudmat; Suction bucket; Push-in pile; Helical pile (foundation concepts are not to scale)	47
4.2	Lateral (left) and axial (right) foundation reactions due to the loads acting on the template	48
4.3	Mudmat foundation schematic drawing; side view (left) and top view (right)	49
4.4	Suction bucket schematic drawing; side view (left), bottom view (right)	50
4.5	Push-in pile schematic drawing; Side view (left) and top view (right)	52
4.6	Helical pile schematic overview; side view (left), top view (right)	54
4.7	Left: Pile in compression; Right: Pile in tension	55
4.8	Suction bucket dimensions for sand (left) and clay (right)	57
4.9	Weight of the suction bucket foundation [mT]	58
4.10	Soil resistance as a function of the penetration depth	59
4.11	Diameter and pile length dimensions for a sand (left figure) and clay (right figure) seabed	60
4.12	Weight of the push-in pile foundations [mT]	61

4.13 Diameter and pile length dimensions for a sand (left) and clay (right) seabed	62
4.14 Weight of the helical pile foundations [mT]	62
5.1 Crane position of portside (PS) crane	65
5.2 Significant wave height for an undisturbed and shielded incoming unit wave of $H_s = 1m$, with an incoming angle of 135°	66
5.3 Overview of the mudmat foundation concept model during lifting	67
5.4 Hydrodynamic forces in vertical direction acting on the template, for both considered load cases	68
5.5 Load case 1: +1 m below waterline	69
5.6 Load case 1: -1 m below waterline	69
5.7 Heave motion of the crane tip due to the incoming wave	72
5.8 Relative heave motion, velocity and acceleration of the crane tip	73
5.9 Total hydrodynamic force for each foundation concept for load case 1	74
5.10 Total hydrodynamic force for each foundation concept for load case 2	75
5.12 Operability curves based on a DAF limit of 1.3	75
5.13 Governing operability curve for each foundation concept developed for a sand seabed	76
5.15 Operability curves based on a DAF limit of 1.3	76
5.16 Governing operability curve for each foundation concept developed for a clay seabed	77
5.17 RAO of the relative distance between template and crane tip	78
5.18 Influence of resonance period on the operability curve (arbitrarily chosen)	79
5.19 Vertical forces acting on the template; left: assumption by DNV; right: wave length of 45 m	80
6.1 Estimated installation time based on a P50 range for concepts developed for sand (left) and for clay (right)	83
6.2 Estimated construction costs for concepts developed for sand (left) and for clay (right) including the expected accuracy range	85
6.3 Results of the considered criteria	86
6.4 Results of the MCA by means of the WPM	86
6.5 Results of the considered criteria for a clay seabed	87
6.6 Results of the MCA for a clay seabed by means of the WPM	87
6.7 Installation time [days] of 64 monopiles for a sand and clay seabed	88
7.1 Summary of the results obtained by the multi-criteria analysis	90
B.1 Properties of the initial template design	104
E.1 Estimation of the steel price for each concept	109
F.1 Operability of the foundation concepts developed for a sand seabed	110
F.2 Operability of the foundation concepts developed for a clay seabed	110
F.3 Resonance period of the Thialf in heave direction	111
G.1 Characteristic components of the Thialf	112

List of Tables

2.1	Shape, depth and inclination factors [42]	19
2.2	Considered safety factors based on the WSD method [4]	29
3.1	Weight of each template segment	41
3.2	Monopile main properties	42
3.3	Considered environmental conditions during the critical cases	43
3.4	Soil properties considered during this thesis	43
3.5	Environmental conditions and corresponding loads during set down and contingency case	45
4.1	Outer limits of the suction bucket dimensions considering the foundation embedment ratio	58
4.2	Determined dimensions of the suction bucket	58
4.3	Dimensions for initial stability	59
4.4	Determined dimensions of the push-in pile	60
4.5	Dimensions of the push-in pile concepts	61
4.6	Determined dimensions of the helical pile	62
4.7	Dimensions of the helical pile concepts	63
4.8	Foundation dimensions of each concept for a sand seabed	63
4.9	Foundation dimensions of each concept for a clay seabed	63
5.1	Position of Thialf CoG and crane tip w.r.t. global origin	66
5.2	Template CoG position w.r.t. global origin	66
5.3	Foundation dimensions of each concept for a sand seabed	71
5.4	Foundation dimensions of each concept for a clay seabed	71
5.5	Static forces of each developed foundation concept	71
5.6	Operability of each developed foundation concept for both type of seabeds	77
5.7	Determined resonance period of each foundation concept	78
6.1	The considered criteria with their corresponding weight level	82
6.2	Operability of the lifting operation of each developed foundation concept for a sand and clay seabed	83
6.3	Estimated installation time of each developed foundation concept	83
6.4	Estimated procurement costs for the concepts developed for a sand seabed	84
6.5	Estimated engineering costs	84
6.6	Estimated tooling costs	85
6.7	Estimated damage risk of each foundation concept	86
6.8	Estimated duration of the installation of 64 monopiles for a sand seabed	88
6.9	Estimated duration of the installation of 64 monopiles for a clay seabed	88
C.1	Installation sequence of the initial He Dreihrt template	105
E.1	Weighting of each criteria	109

Nomenclature

Abbreviations

AACE	Association for the Advancement of Cost Engineering
CoG	Center of Gravity
DP	Dynamic Positioning
EnBW	Energie Baden-Wurttemberg
NMS	Noise Mitigation System
GBS	Gravity Based Structure
HMC	Heerema Marine Contractors
RNA	Rotor Nacelle Assembly
SSCV	Semi-Submersible Crane Vessel
WoW	Waiting on Weather

Symbols

A	actual foundation area
a	characteristic acceleration
A_{33}	heave added mass of the object
c	cohesive shear strength
c_u	undrained shear strength
D	diameter of the pile
$F(t)$	total force on the object
$f(z)$	unit skin friction
H_c	horizontal foundation capacity
H_{max}	maximum wave height
H_s	significant wave height
K	stiffness of the object
M	mass of the object
q	unit end bearing capacity
Q_c	vertical foundation capacity

T_0	resonance period of the object
T_p	peak period
t	wall thickness
V	displaced water volume of the object
v	flow velocity
z	depth below seafloor
ϕ'	friction angle
γ	effective unit weight of soil
ω	angular frequency
ζ_a	characteristic wave amplitude
physical constants	
g	gravitational acceleration



Vessel overview

Semi-Submersible Crane Vessel (SSCV) Sleipnir

Main data

Construction Year	2019
Lift Capacity	20,000 metric tons

Dimensions

Length	220 m
Width	102 m
Draft	12 - 32 m



Semi-Submersible Crane Vessel (SSCV) Thialf

Main data

Construction Year	1985
Lift Capacity	14,200 metric tons

Dimensions

Length	201.6 m
Width	88.4 m
Depth to work deck	49.5 m
Draft	11.9 - 31.6 m



Deepwater Construction Vessel (SSCV) Balder

Main data

Construction Year 1978
Lift Capacity 6,300 metric tons

Dimensions

Length 154 m
Width 86 m
Width of Deck 105 m

Draft

Draft 14 m and deeper
Draft incl. thrusters 4.5 m under hull



Heavy Lift Vessel Aegir

Main data

Construction Year 2012
Lift Capacity 5,000 metric tons

Dimensions

Length 211 m
Width 46 m

Draft

Operating draft 9 - 11 m
Transit draft 8 m



Anchor Handling Tugs Bylgia and Kolga

Main data

Construction Year 2013
Summer draft 7.37 m

Dimensions

Length 72 m
Width 18 m

Bollard pull

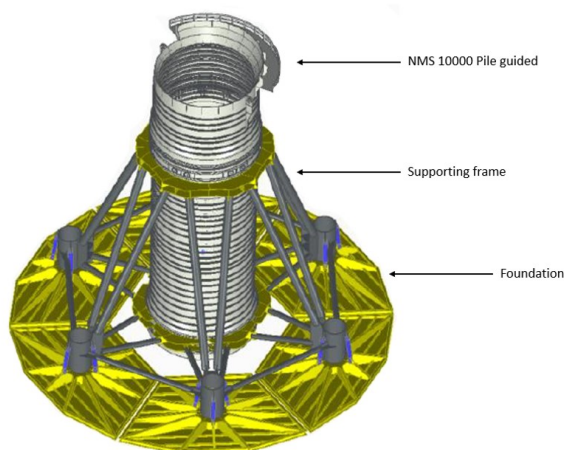
Bylgia 200 t
Kolga 212 t



B

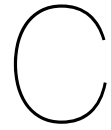
Initial template design properties

This appendix states the properties of the initial designed template. From this the horizontal surface area of the initial mudmat foundation is determined.



Height template	[m]	32
Height NMS + lifting ring with catcher	[m]	47
Diameter (outer) template mudmats	[m]	45
Diameter (inner) template mudmats	[m]	22
Diameter (outer) NMS	[m]	13.6
Weight	[mT]	2400

Figure B.1: Properties of the initial template design



Monopile installation sequence

The table below states the monopile installation sequence of the initial designed template for the He Dreiht Wind Farm. The first phase states the template installation sequence.

1 Template installation

- 1.1 Lift the template from deck to above the wave zone
- 1.2 Lower the template through the wave zone
- 1.3 Template set down on the seabed
- 1.4 Level the template

2 Monopile lowering

- 2.1 Upend the monopile
- 2.2 Lower the monopile tip to 2 meters below the upper centralizer
- 2.3 Lower the monopile to self-weight penetration
- 2.4 Fill the annulus of the NMS with air

3 Monopile driving

- 3.1 Stab the hammer onto the monopile and correct inclination
- 3.2 Start the bubble screen inside the NMS
- 3.3 Drive the monopile to final penetration
- 3.4 Retrieve hammer

4 Template recovery

- 4.1 Lift the template 2 meters free from the seabed
- 4.2 Lift the template until the upper centralizer just below the pile top
- 4.3 Lift the template above the wave zone

5 Contingency procedure

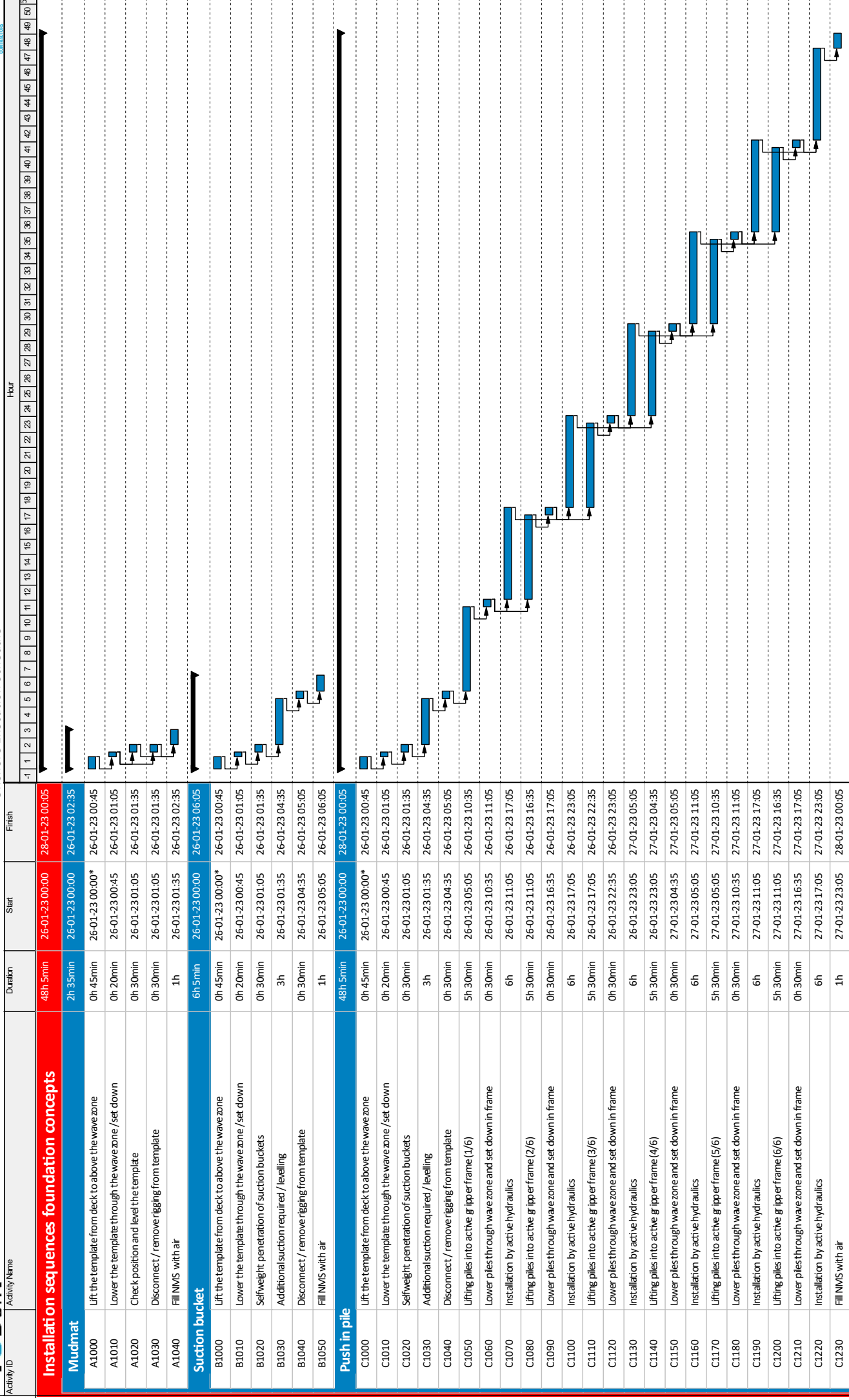
- 5.1 Contingency case - Template only
- 5.2 Contingency case - Template with pile at SWP

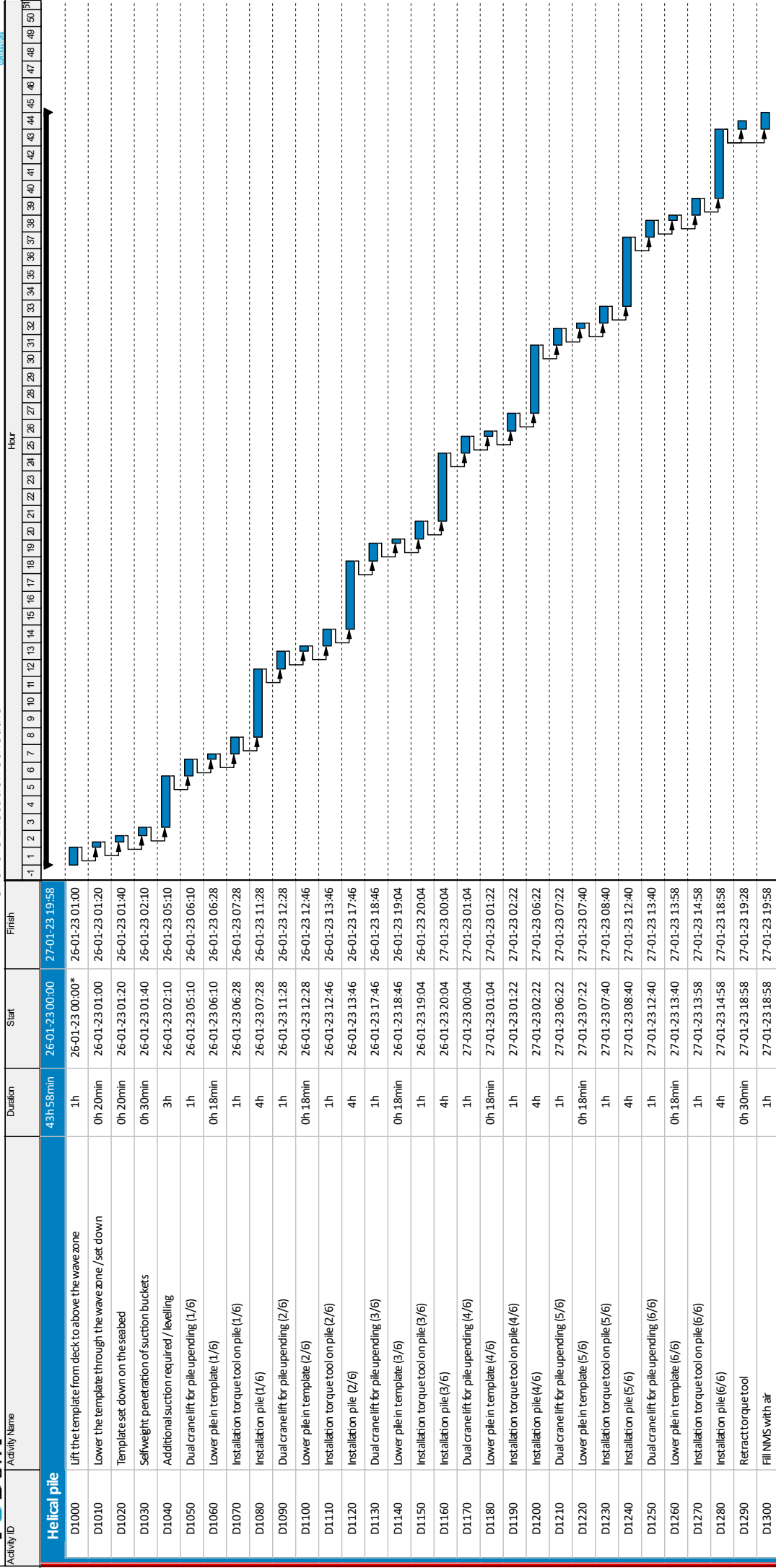
Table C.1: Installation sequence of the initial He Dreiht template



Foundation concept installation sequence - planning

The following two pages shows a planning of the template installation steps of each foundation concept developed for a sand seabed. It states each step that is to be performed with a corresponding time indication. This planning is determined for the level of design that is considered throughout this thesis.







Multi-criteria analysis

The table below shows the weighting matrix of criteria. The weighting of each criterion is determined based on if there is an influence of criterion C_i on criterion C_j .

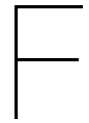
$C_i \downarrow / C_j \rightarrow$	Lifting operation	Installation time	Construction costs	Damage risk	
Lifting operation	1	0	0	0	1
Installation time	0	1	0	1	2
Construction costs	0	0	1	1	2
Damage risk	0	0	0	1	1

Table E.1: Weighting of each criteria

The table shown below states the estimation of the steel price in order to determine the procurement costs for each foundation concept. The procurement costs is the total steel price multiplied by the weight of the foundation concept.

	Sand		Clay		Steel price [EUR/mT]				Total cost foundation [mil. EUR]	
	Weight [mT]	Weight [mT]	Steel plate [EUR/mT]	Welding [EUR/mT]	Installation [EUR/mT]	Total [EUR/mT]	Sand	Clay		
Mudmat	800	800	3700	2200	1500	7400	5.9	5.9		
Suction bucket	1050	1380	3700	1500	1500	6700	7.0	9.2		
Push-in pile	270	130	3700	1300	1500	6900	7.2	6.9		
<i>Suction bucket</i>	770	890	3700	1700	1500	6700				
Helical pile	240	275	3700	1600	1500	7100	7.2	8.3		
<i>Suction bucket</i>	770	890	3700	1900	1500	6700				

Figure E.1: Estimation of the steel price for each concept



Operability

The figures F.1 and F.2 shown below state the operability curve combined with the wave scatter diagram of the He Dreihl wind farm location. From this the operability of each foundation concept is determined.

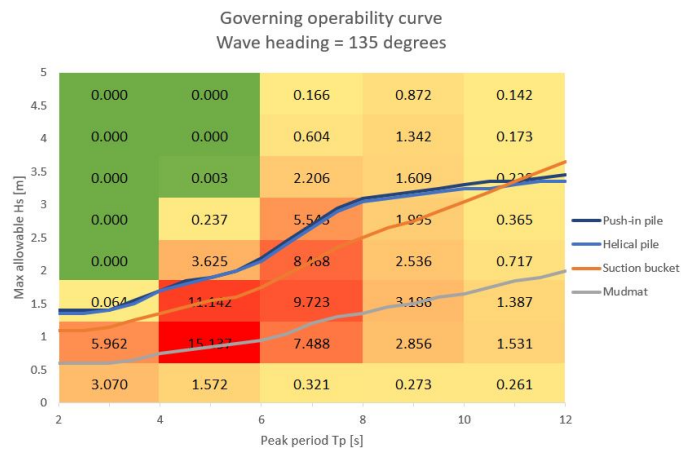


Figure F.1: Operability of the foundation concepts developed for a sand seabed

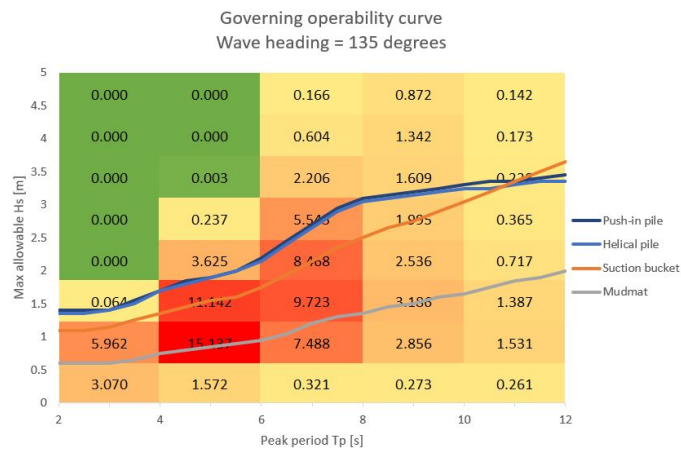


Figure F.2: Operability of the foundation concepts developed for a clay seabed

Resonance period of the Thialf

This figure shows the amplitude [m/m] of the Thialf in heave direction. It can be obtained that the resonance period is around 21-22 seconds.

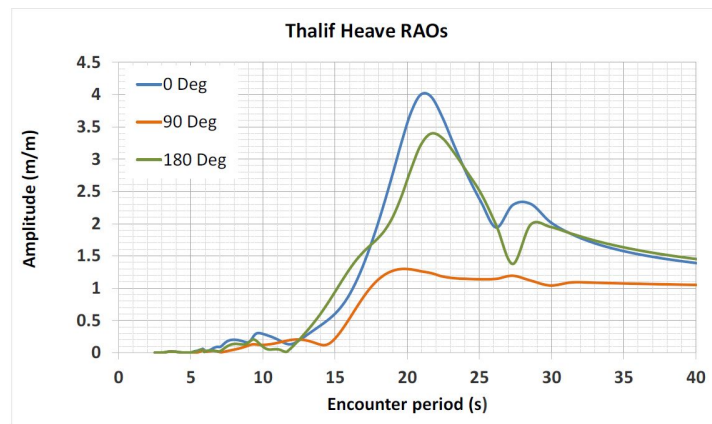


Figure F.3: Resonance period of the Thialf in heave direction

Thialf components overview

Figure G.1 shows the Thialf model from Liftdyn. The important components considering the hydrodynamic analysis are stated. Additionally the global axis reference system and the Center of Gravity (CoG) of the Thialf are stated. For the hydrodynamic analysis the crane boom and crane hoisting system are assumed to be rigid.

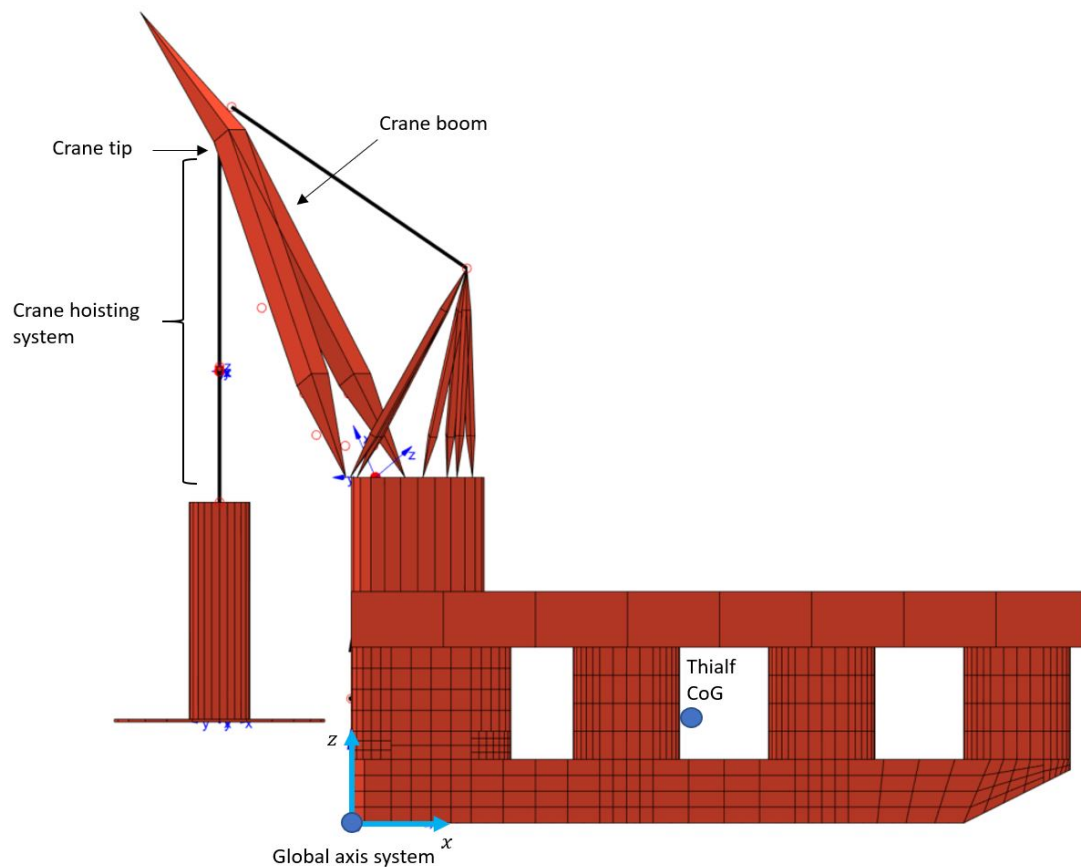


Figure G.1: Characteristic components of the Thialf